

UCLA

UCLA Electronic Theses and Dissertations

Title

Microglial mitochondria: defining the landscape and testing links between organelle remodeling and microglial function

Permalink

<https://escholarship.org/uc/item/8rj0q8vx>

Author

Espinoza, Katherine

Publication Date

2024

Peer reviewed|Thesis/dissertation

UNIVERSITY OF CALIFORNIA

Los Angeles

Microglial mitochondria: defining the landscape and testing links between organelle remodeling
and microglial function

A dissertation submitted in partial satisfaction of the
requirement for the degree Doctor of Philosophy in
Neuroscience

by

Katherine Espinoza

2024

© Copyright by

Katherine Espinoza

2024

ABSTRACT OF DISSERTATION

Microglial mitochondria: defining the landscape and testing links between organelle remodeling
and microglial function

by

Katherine Espinoza

Doctor of Philosophy in Neuroscience

University of California, Los Angeles, 2024

Dr. Lindsay M. De Biase, Chair

Microglia are the resident immune cells of the central nervous system (CNS) and they carry out numerous and diverse functions throughout the lifespan. A central feature of microglia that allows them to carry out such diverse functional roles is phenotypic flexibility. Microglia can rapidly alter their morphology, secretion of signaling factors, and gene expression, in addition to remodeling other cellular attributes. The field has characterized a few microglial cell surface receptors that can instruct microglia about specific cell processes that are needed such as phagocytosis, synapse support, and disease associated response. However, much remains unknown about how microglia integrate information from numerous receptors and coordinately regulate multiple cell properties to rapidly shift into the appropriate cellular phenotype. Mitochondria, generally known for their ATP / energy producing capability, may play a critical role in this process of regulating cell properties and function. This dissertation aims to build on

our current understanding of microglial function and how mitochondria may play critical roles in regulating microglial attributes in the CNS.

In chapter 1, I will outline key microglia functions and supporting evidence that mitochondria can regulate cellular function. Chapter 2 will focus on how mitochondrial properties change and are linked to microglial morphology through the rodent lifespan and during inflammatory insults. Chapter 3 is dedicated to understanding mitochondrial roles during early development of the rodent brain and how mitochondrial morphology remodeling is linked to microglial phagocytic structures. Almost nothing is known about microglial mitochondria in vivo. Hence, the work outlined in this dissertation project provides foundational and essential information about microglial mitochondrial function. This will enable numerous future studies aiming to understand how microglial cellular response is shaped by mitochondrial state in the CNS.

This dissertation of Katherine Espinoza is approved.

Dean Buonomano

Michael Sofroniew

Ajit Divakaruni

Lindsay M. De Biase, Committee Chair

University of California, Los Angeles

2024

This dissertation is dedicated to my parents.

Santiago Espinoza and Rosa Solorio

Table of Contents

ABSTRACT OF DISSERTATION	ii
Table of Contents	v
Acknowledgements	ix
Curriculum Vitae	x
Chapter 1: Introduction	1
1.1 Ontogeny of microglia and other CNS cells	1
1.2 Microglial Functions in the CNS throughout the lifespan	2
1.3 Microglia Cellular State and Heterogeneity	5
1.4 The Microglia “Sensome”	7
1.5 Microglial metabolism – a new frontier for microglial biology.....	10
1.6 Future directions.....	14
References Cited	15
Chapter 2: Dynamic changes in mitochondria support phenotypic flexibility of microglia.....	24
2.1 Abstract	24
2.2 Introduction	25
2.3 Results	26
2.3.1 Regional specialization of microglia is accompanied by regional differences in mitochondrial mass and number.....	26

2.3.2 Mitochondrial number is correlated with morphological complexity of microglia, particularly in the VTA.....	28
2.3.3 Mitochondrial number and mitochondrial motility are not aligned with microglial tissue surveillance.....	30
2.3.4 Mitochondrial distribution is stable during early phases of microglial response to focal injury.....	32
2.3.5 Mitochondrial remodeling is evident at the earliest stages of microglial responses to inflammatory challenge.....	33
2.3.6 Increased mitochondrial mass and mitochondrial elongation are associated with microglial responses to inflammatory challenge.....	37
2.4 Discussion.....	39
2.4.1 The underappreciated complexity of mitochondria.....	39
2.4.2 How does mitochondrial state relate to homeostatic microglial functions?.....	40
2.4.3 Do mitochondria regulate microglial responses to focal injury?.....	43
2.4.4 Do mitochondria regulate microglial responses to CNS challenge?.....	45
2.5 Materials and Methods.....	46
2.6 Tables.....	56
2.7 Figures.....	59
References Cited.....	71
Chapter 3: Structural remodeling of microglial mitochondria across brain region and developmental stage.....	77

3.1 Abstract	77
3.2 Introduction	78
3.3 Results	79
3.4 Discussion	82
3.5 Materials and Methods	85
3.6 Figures	88
References Cited	91
Chapter 4: Conclusion.....	94

Acknowledgements

I would like to begin by thanking my advisor, Dr. Lindsay De Biase for all the scientific mentorship and guidance that made this project possible. I am pleased I had the opportunity to join her lab during the early stages as it provided me with key experience in starting up techniques and new projects in the lab. Her rigorous analysis of experiments also led to generating science that we trust and will contribute new findings to the glial community. I also admire her ability to always come up with insightful questions and have genuine interest in work beyond glial research. This has also broadened my perspective on how to view my work and how it fits in the field of neuroscience.

I would also like to thank the research community that made this possible. I want to thank my lab mates: Ari Schaler, Dr. Fanny Etienne, Dr. Daniel Gray, Megan Chappell and Keionna Newton, Eric Moca, and Keenan Hope. They have all made the lab a wonderfully supportive and collaborative lab environment throughout the years. Their support and camaraderie were key in pushing me forward during my PhD. I'd like to give special thanks to Ari Schaler as the coauthor on the work presented in Chapter 2. I also appreciate Drs. Fanny Etienne and Daniel Gray for sharing their expertise. I also want to thank my undergraduate students Casandra Chamorro, Megan Yu and Arielle Sass for giving me the opportunity to support their scientific journey. I'd like to acknowledge Laura Denardo's lab for contributing to a wonderful lab dynamic and being great lab neighbors. I also want to thank my committee members: Drs. Dean Buonomano, Michael Sofroniew, Ajit Divakaruni and Ye Zhang for their time support, and project guidance.

Additionally, I thank UCLA programs such as NSIDP and Bioscience Programs for providing support throughout my PhD. Also, for providing funding resources such as Cota

Robles and UC President's Pre-Professoriate Fellowship which were instrumental in allowing me to dedicate my time to research and professional development. I'd like to acknowledge additional funding resources such as the Jennifer Buchwald fellowship. I also thank the Physiology Department and Brain Research Institute for their administrative support.

Lastly, I want to thank all my family, friends, and colleagues. They were key in making the PhD a memorable and joyful experience. I learned a lot from them, and this shaped my growth throughout the years. Thank you!

Curriculum Vitae

Education

- 2013-2017 Bachelor of Science, Neuroscience University of California, Riverside
2018-2024 Doctoral Candidate, Neuroscience University of California, Los Angeles

Selected Research Experience

- 2017-2018 Laboratory Assistant I – Khaleel Razak
University of California, Riverside Department of Psychology and Neuroscience
- 2015-2017 Undergraduate Researcher – Iryna Ethell
University of California, Riverside Department of Biomedical Sciences
- 2016 HHMI EXROP Fellow – Matthew Warman
Boston Children's Hospital

Publications

E.N. Moca, D. Lecca, K.T. Hope, F. Etienne, A.W. Schaler, K. Espinoza, M.S. Chappell, D.T. Gray, D. Tweedie, S. Sidhu, L. Masukawa, H. Sito, R. Mathew, D.R. Saban, N.H. Greig and L.M. De Biase, Microglia Drive Pockets of Neuroinflammation in Middle Age, *Journal of Neuroscience* (2022)

S.M. Reinhard, M. Abundez-Toledo, K. Espinoza, K.A. Razak, Effects of developmental noise exposure on inhibitory cell densities and perineuronal nets in A1 and AAF of mice, *Hearing Research* (2019)

S.M Reinhard, M. Rais, S. Afroz; Y. Hanania, K. Pendi, K. Espinoza, R. Rosenthal, D.K. Binder, I.M. Ethell, K.A. Razak, Reduced perineuronal net expression in Fmr1 KO mice auditory cortex and amygdala is linked to impaired fear -associated memory, *Neurobiology of Learning and Memory* (2019)

J. Caetano-Lopes, S.G. Lessard, S. Hann, K. Espinoza, K.S. Kang, K.E. Lim, D.J. Horan, H.R. Noonan, D. Hu, R. Baron, A.G. Robling, M.L. Warman, *Clcn7^{F318L/+}* as a new mouse model of Albers-Schönberg disease, *Bone* (2017)

Awards, Certificates and Fellowships

2022 - 2023 UC President's Pre-Professoriate Fellowship – Graduate Division, UCLA

2020 Entering Mentoring Training Program, UCLA – Certificate

2019 Jennifer S. Buchwald Graduate Fellowship – Physiology Department, UCLA

2018 – 2022 Cota Robles Fellowship – Bioscience Programs

2016 Howard Hughes Medical Institute (HHMI) Exceptional Research Opportunities Program Scholar – Fellowship

Chapter 1: Introduction

1.1 Ontogeny of microglia and other CNS cells

The central nervous system (CNS) is comprised of highly specialized cell types. CNS cell types conserved across vertebrate species include neurons, glial cells, and ependymal cells, which are important in homeostasis of cerebrospinal fluid. Glial cells include oligodendrocytes, astrocytes, and tissue resident macrophages, known as microglia in the parenchyma, and CNS border associated macrophages, located in the meningeal space and choroid plexus. Neurons are electrically diverse and drive information transfer and storage in the CNS. Neurons rely on non-neuronal cells to enable numerous aspects of neuronal function. For example, oligodendrocytes, generated from oligodendrocyte precursor cells myelinate axons and provide insulation as well as support during remyelination after injury (1,2). Astrocytes, the most abundant glial cell, are important in regulating glutamate and ion concentrations necessary for neuronal function and neuron's ability to communicate with other cells in the CNS (1,3)

A type of resident immune cells of the brain are microglia. These cells make up roughly 5% of CNS cells yet they are highly dynamic cells. Historically recognized functional roles for these cells include phagocytosis of pathogens and responses to inflammatory insults and disease (4). Newly discovered functional roles include support of synaptic function, modification of neuronal survival and aid in regulation of cytokines and other signaling factors in context of disease (4–6). Microglia are known to be highly motile in their resting state and continuously survey and monitor the local environment through cell process extensions and protrusions (7–9). Such dynamics may allow microglia to communicate with other cells in the brain parenchyma via direct contact and sampling of their microenvironment. As the resident immune cell of the brain, microglia have been considered to perform limited functions associated with monitoring of

the brain parenchyma and debris clearance, but as more research uncovers additional microglial functions, targeting and further understanding these cells in many physiological contexts is increasingly relevant.

For a full understanding of how microglia may be supporting CNS function, it is critical to appreciate that they have distinct developmental origins from other cells in the brain. Neurons, oligodendrocytes, and astrocytes originate from neural progenitor cells arising from the neural tube (2,10). Studies in rodents and humans confirm that microglia originate from the embryonic yolk sac as primitive macrophages progenitors. These cells are distinct from other types of tissue resident macrophages and circulating monocytes derived from bone marrow progenitors (11–14). After yolk sac derived progenitors have invaded the developing nervous system, microglial cells emerge in brain pial surface around embryonic day 8.5 in rodents (11–15). In human development, microglia are identified in early stages of gestation, from 4.5 weeks, by characteristic expression of Iba1, CD68, CD45 and MHC-II, which are genes important in microglial function (11). Their differentiation and survival is controlled by colony stimulating factor 1(CSF-1) and the CSF1 receptor (12). Microglia are additionally able to maintain their adult pool via proliferation in situ (15,16).

1.2 Microglial Functions in the CNS throughout the lifespan

As microglia emergence into the rodent and human developing brain precedes neurogenesis and gliogenesis of astrocytes and oligodendrocyte lineage cells, microglia may have specialized roles in the progression of neuronal and glial maturation (13,17). To maintain homeostasis in the brain parenchyma, there may be several signaling factors orchestrating neurogenesis and other cellular processes (18–20). Microglia in embryonic stages and early post-

natal development differ greatly from microglia in adulthood (15,21). In embryonic stages, microglia express genes involved in neural migration and cytokine secretion (22), suggesting key roles for microglia in neuronal positioning and maturation. During embryogenesis microglia may also “fine tune” the expression of soluble factors needed for wiring of neuronal circuitry (17,23). For example, in early forebrain circuitry formation, microglia are critical in the outgrowth of dopaminergic axons and positioning of interneurons (20,23). Microglia also modulate adult neurogenesis in hippocampal circuitry and other cellular processes such as oligodendrogenesis (24). Hence, mounting evidence indicates that microglia play key supportive roles during embryonic development.

Recent work demonstrates microglia may continue to regulate key aspects of circuit development during postnatal periods. As previously described, microglia themselves move through multiple phases of maturation from embryogenesis into adulthood (22). Distinct microglial subtypes are also thought to exist in early postnatal development. For example, to protect cholinergic innervations in the ventral striatum in early post-natal development, microglia in this region establish a distinct molecular signature and morphology associated with a more phagocytic, reactive function (25). Microglia also play key roles in surveilling the environment and in synaptic pruning in early postnatal development in regions such as the hippocampus and retinogeniculate circuitry (26,27).

In adulthood, microglia show prominent expression of genes related to signaling pathways establishing microglia maturation and surveillance (22). Microglia continue to regulate processes such as synaptic pruning in adulthood but at a reduced rate (28). During adulthood, microglia also contribute to experience dependent modifications that occur in the visual system, suggesting they impact synaptic plasticity (6). Microglia are also capable of secreting factors

such as bone-derived neurotrophic factor that affect synaptic plasticity in hippocampus and motor cortex in post developmental stages (29). Microglia modulation of synaptic activity and behavior can also occur via release of soluble factors which stimulate other glial cells such as astrocytes and indirectly affect neuronal activity (30). Supporting appropriate levels of synaptic may be a key function of microglia that is likely perturbed during aging and disease.

In context of aging, the CNS undergoes many changes in synaptic number and plasticity which may contribute to increased susceptibility to disease (31). Hallmarks of aging include changes in intracellular signaling, genomic instability and, in humans loss of regional integrity (32,33). The microglial cellular changes observed in aged rodents and human are quite heterogeneous which may hint that some microglial responses in aging are detrimental and others adaptive (31,34,35). For example, in middle aged and aged brains microglia show distinct morphological and gene expression changes, suggesting different functional responses at each phase of aging (36–40). Other aging studies have shown that hippocampal neurogenesis is reliant on signaling from neural precursor cells to chemokine receptors, suggesting microglia may be involved in maintaining neurogenesis during aging (41).

Along with supportive functions, microglia can also become dysregulated in aging and contribute to pathological changes during aging. Microglia exhibit increased inflammatory profiles in response to lipopolysaccharide challenge in an aging rodents compared to young adulthood (42). This suggests a different susceptibility to an inflammatory challenge in the aging context. Microglia may also engage in excessive synaptic engulfment and, yet, can also show deficiencies in phagocytosis of pathological aggregates (28,43). Such evidence suggests that changes in microglial function during aging makes key contributing to neuronal decline and death observed in the aging brain (31). Moreover, microglial cellular changes during aging can

vary across individuals and may contribute to why some individuals are more susceptible to the development of disease.

Diseases such as Alzheimer's disease (AD) and Parkinson's disease share aging as a common risk factor. These diseases are characterized by neuropathological hallmarks such as neuron death, synapse loss and amyloid plaques and neurofibrillary tangles (38,44). In AD, pathological processing of amyloid precursor protein contributes to plaques in the brain and increase in inflammation which can lead to impaired synaptic function (44,45). In human tissue, an age associated increase in dystrophic microglia is found and observed to a greater degree in patients with AD and dementia with lewy bodies (46). Previous transcriptomic studies in the context of AD, showed microglial subclusters are characterized by altered transcription of genes involved in calcium activation, response to injury and motility pathways (35). Microglia can actively engulf amyloid beta fibrils, which may be protective but they also secrete inflammatory cytokines which contribute to disease progression (45). This highlights how microglial degradative capacity could be beneficial under physiological conditions but may lead to aberrant behavior under pathological conditions(47). Together, these studies illustrate why studying microglia under disease conditions may lead to further understanding of disease progression and how to reduce disease risk.

1.3 Microglia Cellular State and Heterogeneity

The previous section highlighted that microglia have many distinct functional roles across the vertebrate lifespan. How these observed microglial morphological, and molecular signature differences are linked to these functional roles is quite complex. Before delving into the various cellular states and differences observed across microglia, it is important to explore

why such differences are relevant to brain health. What is the purpose of understanding and defining such heterogeneity and how does this relate to maintaining CNS health? As neurodegeneration research progresses, it has become increasingly important to explore how various regions and cell types are affected by such changes in the brain. We understand that specific regions and cell types become more susceptible to effects of disease and age, and to the complexity of treatment in many conditions (48). Microglia, as functionally diverse immune cells, undergo a range of changes in response to disease. Defining their various states is critical in furthering understanding of susceptibility to disease.

Historically, microglial functional states were categorized as one of two distinct phenotypes – a pro-inflammatory “M1” state or a tissue repair “M2” state. These two distinct cellular states emerged from primary monocyte studies and are largely based on study of microglial responses to purified isolated stimuli delivered *in vitro* (49). Over the progression of glial research, these M1 and M2 phenotypes are not thought to accurately reflect microglial or macrophage biology and are an oversimplification of complex morphological and genetic variability. In physiological conditions microglia exhibit numerous nuanced differences in a region and age dependent manner (49,50). Microglial morphology and molecular profile are found to be dynamic resulting in many possible states across physiological and disease conditions (51). Examples of a few redefined categorizations include proliferative associated microglia, disease associated and activated associated microglia, all of which are linked to different physiological states including postnatal development and disease (51). In summary, microglia undergo many diverse context-dependent states in mice and humans (15).

Indeed, microglia exhibit heterogeneity in cell density, cellular and subcellular structures, capacity for self-renewal, patterns of gene expression, and metabolism (22,36,52). This

heterogeneity can be observed across brain regions, lifespan, and sex. Regional heterogeneity has been described in both rodent and human studies. Studies of human microglia show that multiple phenotypic signatures such as cell abundance and cell markers depend on the brain region in which the cells reside (36,53). These region-specific signatures may be driven by environmental cues (4,54,55). Several studies have shown that microglia in the mesolimbic system have different maturation timepoints as well as cell density and morphological differences compared to cortical microglia (54,56). Other brain regions such as the cerebellum have microglia that are more sparsely distributed and less branched. These cerebellar microglia also exhibit different cell process motility compared to cortical microglia, and can interact with Purkinje neurons (57). In hippocampus, cortex and striatum microglia have varying fractalkine expression (58). Expression of mitochondrial genes and lysosomal genes also differ across nuclei in the basal ganglia compared to cortex, suggesting microglia are fine tuned to their localization (54).

1.4 The Microglia “Sensome”

The ability of microglia to sense the local environment and periphery and integrate signals from other cell types is essential for them to provide homeostatic support of surrounding tissue and to modulate neuronal activity. Potential mechanisms aiding in this function include more than 1000 microglial signaling receptors, known as the microglial “sensome” (55,59). These signaling molecules have been identified and demonstrated to change in microglia across different contexts and across the rodent lifespan. These various “sensome” pathways include receptors involved in immune response, phagocytosis, and cell metabolism (55). Some well described pathways by which microglia sense the local environment include fractalkine signaling, complement pathway signaling, growth factor signaling and purinergic signaling. Multiple studies suggest that neurons use the fractalkine pathway to regulate microglial function.

Neuronally derived fractalkine (or CX3CL1) can signal to microglial fractalkine receptor (or CX3CR1) to regulate microglial release of inflammatory factors (60). Fractalkine signaling may also enable microglia to recognize neuronal hyperactivity (61,62). Other evidence shows that fractalkine signaling mediates microglial regulation of synaptic rewiring during sensory deprivation such as whisker lesioning (63). Finally, loss of this signaling pathway via CX3CR1 knockout in microglia leads to downregulation of immune-related genes, simplified microglial morphology, and acceleration of key aspects of microglial aging (37,64).

Beyond the fractalkine pathway, microglia also interact with their environment via immune signaling molecules that are part of the classical complement pathway (CCP). This innate immune pathway is involved in host defense and involves tagging pathogens with complement proteins. These proteins can be recognized by cells that express complement receptors, initiating phagocytosis and pathogen lysis (65). Surprisingly these signaling factors are highly abundant in the brain even in the absence of infection. During development these proteins are involved in tagging of excess synapses or dying cells that need to be removed (61,66,67). The signaling cascade is initiated by C1q binding to synapses or apoptotic cells, then followed by deposition of complement factor C3 leading to recognition by the microglial C3 receptor (Itgam/CD11b) and subsequent phagocytosis (66). Studies in which C3R and C1q are deficient show that microglia contribute to elimination of excess synapses during development (27,68). Additionally, the complement pathway factors are also upregulated in contexts of disease. C1q and C3 are upregulated in Huntington's disease and AD and are implicated in microglial-based synapse removal during pre-symptomatic phases of disease (65,66,69–71). Along with complement pathway, another class of immune molecules function as “don't eat me” signals which can tag cells to prevent phagocytosis (72). This type of signal includes CD47, a member

of the Ig superfamily (73). Depletion of CD47 during development increased engulfment of synapses by microglia (74,75). These examples highlight how these canonical pathways are employed in other contexts beyond innate immunity, playing an important role in microglial interactions with multiple CNS elements.

Purinergic signaling is another prominent mechanism by which microglia interact with other cells in the CNS and sense the local microenvironment. ATP induces robust membrane chemotaxis in microglia during a response to injury in the brain parenchyma (6,8,76,77). This extension of cell processes toward sites of injury depends on microglial expression of purinergic receptors (77) and indicates that purinergic signaling may be a key mechanism by which microglia can monitor activity and integrity of nearby neurons (78). Purinergic receptors such as P2RY12, have also been shown to be involved in microglial contact of neuronal somas and microglial dampening of excessive neuronal activity (61). In the hippocampus, microglial P2X4 receptors have also been implicated in microglial interactions with mossy fiber tracts with potential roles in modulating presynaptic plasticity (79). Such mechanisms of microglia interaction with other cells in the parenchyma have been the focus of many studies trying to understand how microglia regulate their functions and respond to the local environment. While this sensitive idea has been the focus of a few key studies, there is still a lot to be understood about how microglia integrate these external signaling factors to generate specific microglial functions. Additionally, the heterogeneity observed in microglial genes and morphology presents an added layer of complexity, where some signaling factors may be playing different roles across regions. New mechanisms need to be explored to understand microglial function in the CNS and how these cells can integrate information from their local environment.

1.5 Microglial metabolism – a new frontier for microglial biology

To understand how cellular metabolism and energetics could be critical in microglial functions, cellular metabolism as a source of meeting cellular energy demand must be defined. Cellular metabolism is comprised of chemical reactions that serve to convert nutrients to energy or lead to synthesis of larger biomolecules. These complex reactions can lead to a set of functions that trigger cell renewal or cellular degradation. This process is essential for cellular fitness and requires processing of nutrients to aid in energy generation in mitochondria and use of metabolites to synthesize cellular structures (80–82). Cellular metabolism processes include oxidative phosphorylation (OXPHOS), tricyclic acid cycle (TCA cycle), glycolysis, the pentose phosphate pathway, amino acid metabolism, and fatty acid oxidation. In cells, such as macrophages, which share similar functions and ontogeny microglia, cell metabolic reprogramming is critical in regulating their functions and orchestrating dynamic changes in the functional states. Cellular metabolic reprogramming means the switch from one energy source to another. Tissue resident macrophages exhibit prominent energy plasticity and can completely rewire their cellular metabolism to induce a polarization into proinflammatory or anti-inflammatory phenotypes (80–82). The pro-inflammatory “M1” phenotype is associated with an enhanced glycolytic burst to support energy production and the anti-inflammatory “M2” phenotype is linked to oxidative phosphorylation and fatty acid oxidation for sustained energy (80–82). These M1/M2 phenotypes were identified *in vitro* and have provided useful insight into how metabolic changes *precede* and induce changes in cellular function. However, macrophages *in vivo* have diverse gene expression profiles and more complex changes in metabolic pathways to determine their activation phenotype and magnitude of response following various tissue challenges (81,83).

Although microglia are the immune cells of the CNS, our understanding of microglial cell metabolism is very limited. Most studies of cell metabolism in the CNS have been centered around disease models and their impact on neuronal health. Yet, recent findings in the microglial field indicate that elucidating metabolic function in these cells will be important for a full understanding of microglial roles in CNS health and disease. Microglia share many properties with macrophages in other organs and both cells acting as the professional phagocytes in their tissues of residence. The evidence that metabolic reprogramming plays a critical role in regulating dynamic changes in macrophage function raises the possibility that metabolic reprogramming is similarly critical in regulating microglial function. One key study supporting this idea shows that microglia are metabolically flexible and can use multiple metabolites as a source of energy even under conditions of hypoxia or lack of glucose (7). Microglia have also been identified to undergo changes in cellular energetics in aging rodents and during an inflammatory insults in mice and humans (55,84). Microglia can also reprogram their metabolic state in a context of high fat diet where metabolites for energy demand are modified (85). Additionally, the metabolite lactate has been identified as a regulator of microglial function in the context of microglial-synapse interactions (86). Finally, changes in cell metabolism appear to play a role in microglia reaching a state of tolerance and failing to respond to protein aggregates in AD (87). Together, these studies suggest that cell metabolism could play a central role in regulation of microglial properties and function.

As previously described, cell metabolism is viewed as a response in microglia to a pathological environment. To comprehend other components of cell metabolism, we turn to mitochondrial function. How are cell metabolism and mitochondria linked? Mitochondria serve cell metabolism as energy producing hubs, biosynthesis centers, and waste management hubs

(88). While supporting global cell metabolism, mitochondrial physiology is another source of metabolism by which cellular function may be altered. Historically, mitochondria were viewed simplistically as producing ATP necessary for numerous aspects of cell function. However, growing evidence shows they are highly dynamic organelles that have much more complex functions that allow cells to adapt to their local environment. For example, they are essential in directing cellular stress responses through mitochondrial regulation of nuclear transcription (89,90). Mitochondria are also important in regulating cellular fate decisions such as cell death or survival. Mitochondrial signaling is achieved via transport of metabolites, buffering of calcium, and physical contact with other organelles and subcellular compartments (89). In the context of immune response, mitochondria contain structural and molecular components that are linked to their bacterial origin and can serve as damage associated molecular patterns (DAMPs) that can be released to regulate cellular function (90–92). Moreover, mitochondrial function is not static but is constantly changing. These organelles can undergo complex morphological changes and alter their distribution within a cell. Dynamics that drive mitochondrial changes in number are fission, or the division of single mitochondrion into two mitochondria, and fusion, the joining of mitochondrial membranes of distinct mitochondria (93–96). In addition, to their complex morphology, mitochondria have complex motility and can interact with the cytoskeleton to transport to locations of high energy demand, or locations where there is a need for regulation of calcium homeostasis, and reactive oxygen species biogenesis (97). Within the context of macrophage function, modification of mitochondrial state can govern polarization of macrophage phenotypes (90) and macrophage responses to inflammation (81), indicating that this organelle is likely to play a central role in regulating the attributes of tissue resident macrophages.

In the CNS mitochondria have been studied primarily in neurons and are critical organelles for axon branching, calcium regulation in conjunction with endoplasmic reticulum, neurogenesis and neuronal repair (98). Mitochondria in neurons are also very dynamic and can divide and fuse to establish distribution in the neuron periphery. They have been shown to play critical roles in shaping neuronal activity and health (93,98,99). A recent study using proteomics approaches also revealed that mitochondria take on specialized roles across distinct neuron populations. For example, in cerebellar Purkinje neurons, they were tuned to interact with endoplasmic reticulum, whereas in cerebellar granule cells, they were tuned to engage in calcium buffering (100). Astrocytes and mitochondria research has been emerging and studies show mitochondria in astrocytes are equipped to aid in fatty acid beta oxidation (100), revealing a surprising degree of “fine tuning” of mitochondria for different functions across distinct CNS cell types. Other studies of mitochondria in astrocytes have demonstrated that mitochondria drive maturation in astrocyte development and astrocyte atrophy in aging (101,102). This emerging examination of mitochondrial function in non-neuronal CNS cells demonstrates the key links between mitochondrial molecular and structural specialization and differences in cellular function.

Despite increasing investigations of mitochondria in diverse cell types of the CNS, not much is known about mitochondrial function in microglia. Interest in metabolic reprogramming of microglia is gaining attention, but how manipulation of mitochondrial state affects microglial function is unclear. Additionally, whether there is a specialized “tuning” of microglial mitochondria for specific functions, as was seen in other CNS cells, has not been determined. Some studies have shown that microglia can release mitochondrial components or transfer mitochondria to neurons, with key impacts on neuronal health (103,104). Other studies have

suggested a role for mitochondria in regulating microglial responses to inflammatory conditions and in giving rise to sex differences in immune activation (105,106). Recent evidence also suggests that perturbation of mitochondrial function can alter microglial responses to sensory deprivation, as well as synaptic interactions and phagocytic responses in anxiety-like conditions and models of AD (103,107) (108). Together, these pioneering studies suggest that more knowledge about microglial mitochondria is needed for a greater understanding of the fundamental biology of these cells under physiological and disease conditions.

1.6 Future directions

Current microglial mitochondria studies suggest the tantalizing possibility that this organelle plays a key role in microglial ability to integrate signals from the local environment and alter cellular properties to interact appropriately with other cells and structures in the CNS. However, it is not fully understood if these organelles can regulate and promote changes in microglial structural and molecular profiles. Mitochondria are highly complex organelles that interact with broader cell metabolism in intricate ways. Identifying which components of the organelle may be most critical for regulating key aspects of microglial function and how they may influence microglial phenotype may open new avenues for therapeutic targeting of microglial function. Current therapeutic approaches tend to be narrowly focused, such as manipulating part of the complement or fractalkine pathway. There are few methods by which we can induce coordinated remodeling of numerous microglial attributes in any given context. Targeting microglia through manipulating their mitochondria may have this capability. A deeper understanding of this organelle could reshape how we think about microglia and their interactions with the CNS.

The following chapters aim to map, for the first time, key mitochondrial features in microglia across multiple conditions in which microglia experience structural and molecular changes. Identifying correlations between these dynamic cells and state of these organelles can advance our understanding of the mitochondrial landscape determines overall cell phenotype and function. We also aim to carry out targeted manipulation of the microglial mitochondrial network to reveal the molecular properties of microglia that are most potently regulated by this organelle. The work provides a novel and extensive analysis of mitochondria across microglial functions and can be a foundation for understanding how mitochondria may regulate microglial function in physiological and disease conditions.

References Cited

1. Jäkel S, Dimou L. Glial Cells and Their Function in the Adult Brain: A Journey through the History of Their Ablation. *Front Cell Neurosci* [Internet]. 2017 Feb 13 [cited 2024 Apr 19];11. Available from: <https://www.frontiersin.org/articles/10.3389/fncel.2017.00024>
2. Kuhn S, Gritti L, Crooks D, Dombrowski Y. Oligodendrocytes in Development, Myelin Generation and Beyond. *Cells*. 2019 Nov 12;8(11):1424.
3. Lee HG, Wheeler MA, Quintana FJ. Function and therapeutic value of astrocytes in neurological diseases. *Nat Rev Drug Discov*. 2022 May;21(5):339–58.
4. De Biase LM, Bonci A. Region-Specific Phenotypes of Microglia: The Role of Local Regulatory Cues. *Neuroscientist*. 2019 Aug 1;25(4):314–33.
5. Colonna M, Butovsky O. Microglia Function in the Central Nervous System During Health and Neurodegeneration. *Annu Rev Immunol*. 2017 Apr 26;35:441–68.
6. Tremblay MÈ, Stevens B, Sierra A, Wake H, Bessis A, Nimmerjahn A. The Role of Microglia in the Healthy Brain. *J Neurosci*. 2011 Nov 9;31(45):16064–9.
7. Bernier LP, York EM, Kamyabi A, Choi HB, Weilinger NL, MacVicar BA. Microglial metabolic flexibility supports immune surveillance of the brain parenchyma. *Nat Commun*. 2020 Mar 25;11(1):1559.
8. Davalos D, Grutzendler J, Yang G, Kim JV, Zuo Y, Jung S, et al. ATP mediates rapid microglial response to local brain injury in vivo. *Nat Neurosci*. 2005 Jun;8(6):752–8.

9. Nimmerjahn A, Kirchhoff F, Helmchen F. Resting Microglial Cells Are Highly Dynamic Surveillants of Brain Parenchyma in Vivo. *Science*. 2005 May 27;308(5726):1314–8.
10. de Graaf-Peters VB, Hadders-Algra M. Ontogeny of the human central nervous system: What is happening when? *Early Human Development*. 2006 Apr 1;82(4):257–66.
11. Ginhoux F, Lim S, Hoeffel G, Low D, Huber T. Origin and differentiation of microglia. *Front Cell Neurosci* [Internet]. 2013 Apr 17 [cited 2024 Apr 19];7. Available from: <https://www.frontiersin.org/articles/10.3389/fncel.2013.00045>
12. Ginhoux F, Greter M, Leboeuf M, Nandi S, See P, Gokhan S, et al. Fate Mapping Analysis Reveals That Adult Microglia Derive from Primitive Macrophages. *Science*. 2010 Nov 5;330(6005):841–5.
13. Mendes MS, Majewska AK. An overview of microglia ontogeny and maturation in the homeostatic and pathological brain. *Eur J Neurosci*. 2021 Jun;53(11):3525–47.
14. Sharma K, Bisht K, Eyo UB. A Comparative Biology of Microglia Across Species. *Front Cell Dev Biol* [Internet]. 2021 Apr 1 [cited 2024 Apr 19];9. Available from: <https://www.frontiersin.org/articles/10.3389/fcell.2021.652748>
15. Prinz M, Masuda T, Wheeler MA, Quintana FJ. Microglia and Central Nervous System–Associated Macrophages—From Origin to Disease Modulation. *Annu Rev Immunol*. 2021 Apr 26;39:251–77.
16. Waisman A, Ginhoux F, Greter M, Bruttger J. Homeostasis of Microglia in the Adult Brain: Review of Novel Microglia Depletion Systems. *Trends in Immunology*. 2015 Oct 1;36(10):625–36.
17. Hattori Y. The multifaceted roles of embryonic microglia in the developing brain. *Front Cell Neurosci* [Internet]. 2023 May 12 [cited 2024 Apr 19];17. Available from: <https://www.frontiersin.org/articles/10.3389/fncel.2023.988952>
18. Arnò B, Grassivaro F, Rossi C, Bergamaschi A, Castiglioni V, Furlan R, et al. Neural progenitor cells orchestrate microglia migration and positioning into the developing cortex. *Nat Commun*. 2014 Nov 26;5(1):5611.
19. Smolders SMT, Swinnen N, Kessels S, Arnauts K, Smolders S, Le Bras B, et al. Age-specific function of $\alpha 5\beta 1$ integrin in microglial migration during early colonization of the developing mouse cortex. *Glia*. 2017;65(7):1072–88.
20. Hattori Y, Naito Y, Tsugawa Y, Nonaka S, Wake H, Nagasawa T, et al. Transient microglial absence assists postmigratory cortical neurons in proper differentiation. *Nat Commun*. 2020 Apr 2;11(1):1631.

21. Swinnen N, Smolders S, Avila A, Notelaers K, Paesen R, Ameloot M, et al. Complex invasion pattern of the cerebral cortex by microglial cells during development of the mouse embryo. *Glia*. 2013;61(2):150–63.
22. Matcovitch-Natan O, Winter DR, Giladi A, Vargas Aguilar S, Spinrad A, Sarrazin S, et al. Microglia development follows a stepwise program to regulate brain homeostasis. *Science*. 2016 Aug 19;353(6301):aad8670.
23. Squarzoni P, Oller G, Hoeffel G, Pont-Lezica L, Rostaing P, Low D, et al. Microglia Modulate Wiring of the Embryonic Forebrain. *Cell Reports*. 2014 Sep 11;8(5):1271–9.
24. Butovsky O, Ziv Y, Schwartz A, Landa G, Talpalar AE, Pluchino S, et al. Microglia activated by IL-4 or IFN- γ differentially induce neurogenesis and oligodendrogenesis from adult stem/progenitor cells. *Molecular and Cellular Neuroscience*. 2006 Jan 1;31(1):149–60.
25. Stratoulis V, Ruiz R, Kanatani S, Osman AM, Keane L, Armengol JA, et al. ARG1-expressing microglia show a distinct molecular signature and modulate postnatal development and function of the mouse brain. *Nat Neurosci*. 2023 Jun;26(6):1008–20.
26. Paolicelli RC, Bolasco G, Pagani F, Maggi L, Scianni M, Panzanelli P, et al. Synaptic Pruning by Microglia Is Necessary for Normal Brain Development. *Science*. 2011 Sep 9;333(6048):1456–8.
27. Schafer DP, Lehrman EK, Kautzman AG, Koyama R, Mardinly AR, Yamasaki R, et al. Microglia Sculpt Postnatal Neural Circuits in an Activity and Complement-Dependent Manner. *Neuron*. 2012 May 24;74(4):691–705.
28. Deczkowska A, Matcovitch-Natan O, Tsitsou-Kampeli A, Ben-Hamo S, Dvir-Szternfeld R, Spinrad A, et al. Mef2C restrains microglial inflammatory response and is lost in brain ageing in an IFN-I-dependent manner. *Nat Commun*. 2017 Sep 28;8(1):717.
29. Parkhurst CN, Yang G, Ninan I, Savas JN, Yates JR, Lafaille JJ, et al. Microglia Promote Learning-Dependent Synapse Formation through Brain-Derived Neurotrophic Factor. *Cell*. 2013 Dec 19;155(7):1596–609.
30. Liddelow SA, Guttenplan KA, Clarke LE, Bennett FC, Bohlen CJ, Schirmer L, et al. Neurotoxic reactive astrocytes are induced by activated microglia. *Nature*. 2017 Jan;541(7638):481–7.
31. Morrison JH, Baxter MG. The ageing cortical synapse: hallmarks and implications for cognitive decline. *Nat Rev Neurosci*. 2012 Apr;13(4):240–50.
32. López-Otín C, Blasco MA, Partridge L, Serrano M, Kroemer G. The Hallmarks of Aging. *Cell*. 2013 Jun 6;153(6):1194–217.

33. Damoiseaux JS. Effects of aging on functional and structural brain connectivity. *NeuroImage*. 2017 Oct 15;160:32–40.
34. Angelova DM, Brown DR. Microglia and the aging brain: are senescent microglia the key to neurodegeneration? *Journal of Neurochemistry*. 2019;151(6):676–88.
35. Prater KE, Green KJ, Mamde S, Sun W, Cochoit A, Smith CL, et al. Human microglia show unique transcriptional changes in Alzheimer’s disease. *Nat Aging*. 2023 Jul;3(7):894–907.
36. Grabert K, Michoel T, Karavolos MH, Clohisey S, Baillie JK, Stevens MP, et al. Microglial brain region–dependent diversity and selective regional sensitivities to aging. *Nat Neurosci*. 2016 Mar;19(3):504–16.
37. Moca EN, Lecca D, Hope KT, Etienne F, Schaler AW, Espinoza K, et al. Microglia Drive Pockets of Neuroinflammation in Middle Age. *J Neurosci*. 2022 May 11;42(19):3896–918.
38. Spittau B. Aging Microglia—Phenotypes, Functions and Implications for Age-Related Neurodegenerative Diseases. *Front Aging Neurosci* [Internet]. 2017 Jun 14 [cited 2024 Apr 19];9. Available from: <https://www.frontiersin.org/articles/10.3389/fnagi.2017.00194>
39. Streit WJ, Xue QS. Microglia in dementia with Lewy bodies. *Brain, Behavior, and Immunity*. 2016 Jul 1;55:191–201.
40. Yoo HJ, Kwon MS. Aged Microglia in Neurodegenerative Diseases: Microglia Lifespan and Culture Methods. *Front Aging Neurosci* [Internet]. 2022 Jan 5 [cited 2024 Apr 19];13. Available from: <https://www.frontiersin.org/articles/10.3389/fnagi.2021.766267>
41. Vukovic J, Colditz MJ, Blackmore DG, Ruitenber MJ, Bartlett PF. Microglia modulate hippocampal neural precursor activity in response to exercise and aging. *J Neurosci*. 2012 May 9;32(19):6435–43.
42. Sierra A, Beccari S, Diaz-Aparicio I, Encinas JM, Comeau S, Tremblay MÈ. Surveillance, Phagocytosis, and Inflammation: How Never-Resting Microglia Influence Adult Hippocampal Neurogenesis. *Neural Plasticity*. 2014 Mar 19;2014:e610343.
43. Deczkowska A, Amit I, Schwartz M. Microglial immune checkpoint mechanisms. *Nat Neurosci*. 2018 Jun;21(6):779–86.
44. Serrano-Pozo A, Frosch MP, Masliah E, Hyman BT. Neuropathological Alterations in Alzheimer Disease. *Cold Spring Harb Perspect Med*. 2011 Sep 1;1(1):a006189.
45. Javanmehr N, Saleki K, Alijanizadeh P, Rezaei N. Microglia dynamics in aging-related neurobehavioral and neuroinflammatory diseases. *Journal of Neuroinflammation*. 2022 Nov 17;19(1):273.

46. Shahidehpour RK, Higdon RE, Crawford NG, Neltner JH, Ighodaro ET, Patel E, et al. Dystrophic microglia are associated with neurodegenerative disease and not healthy aging in the human brain. *Neurobiology of Aging*. 2021 Mar 1;99:19–27.
47. Hemonnot AL, Hua J, Ulmann L, Hirbec H. Microglia in Alzheimer Disease: Well-Known Targets and New Opportunities. *Front Aging Neurosci*. 2019 Aug 30;11:233.
48. Young AL, Marinescu RV, Oxtoby NP, Bocchetta M, Yong K, Firth NC, et al. Uncovering the heterogeneity and temporal complexity of neurodegenerative diseases with Subtype and Stage Inference. *Nat Commun*. 2018 Oct 15;9:4273.
49. Ransohoff RM. A polarizing question: do M1 and M2 microglia exist? *Nat Neurosci*. 2016 Aug;19(8):987–91.
50. Wang J, He W, Zhang J. A richer and more diverse future for microglia phenotypes. *Heliyon*. 2023 Mar 21;9(4):e14713.
51. Paolicelli RC, Sierra A, Stevens B, Tremblay ME, Aguzzi A, Ajami B, et al. Microglia states and nomenclature: A field at its crossroads. *Neuron*. 2022 Nov 2;110(21):3458–83.
52. Gosselin D, Skola D, Coufal NG, Holtman IR, Schlachetzki JCM, Sajti E, et al. An environment-dependent transcriptional network specifies human microglia identity. *Science*. 2017 Jun 23;356(6344):eaal3222.
53. Böttcher C, Schlickeiser S, Sneeboer MAM, Kunkel D, Knop A, Paza E, et al. Human microglia regional heterogeneity and phenotypes determined by multiplexed single-cell mass cytometry. *Nat Neurosci*. 2019 Jan;22(1):78–90.
54. De Biase LM, Schuebel KE, Fusfeld ZH, Jair K, Hawes IA, Cimbrotto R, et al. Local Cues Establish and Maintain Region-Specific Phenotypes of Basal Ganglia Microglia. *Neuron*. 2017 Jul 19;95(2):341–356.e6.
55. Hickman SE, Kingery ND, Ohsumi TK, Borowsky ML, Wang L chong, Means TK, et al. The microglial sensome revealed by direct RNA sequencing. *Nat Neurosci*. 2013 Dec;16(12):1896–905.
56. Hope KT, Hawes IA, Moca EN, Bonci A, De Biase LM. Maturation of the microglial population varies across mesolimbic nuclei. *Eur J Neurosci*. 2020 Oct;52(7):3689–709.
57. Stowell RD, Wong EL, Batchelor HN, Mendes MS, Lamantia CE, Whitelaw BS, et al. Cerebellar microglia are dynamically unique and survey Purkinje neurons in vivo. *Developmental Neurobiology*. 2018;78(6):627–44.
58. Tarozzo G, Bortolazzi S, Crochemore C, Chen SC, Lira AS, Abrams JS, et al. Fractalkine protein localization and gene expression in mouse brain. *J Neurosci Res*. 2003 Jul 1;73(1):81–8.

59. Healy LM, Zia S, Plemel JR. Towards a definition of microglia heterogeneity. *Commun Biol.* 2022 Oct 20;5(1):1–6.
60. Zhao J, Li Q, Ouyang X, Wang F, Li Q, Xu Z, et al. The effect of CX3CL1/ CX3CR1 signal axis on microglia in central nervous system diseases. *Journal of Neurorestoratology.* 2023 Mar 1;11(1):100042.
61. Cserép C, Pósfai B, Lénárt N, Fekete R, László ZI, Lele Z, et al. Microglia monitor and protect neuronal function through specialized somatic purinergic junctions. *Science.* 2020 Jan 31;367(6477):528–37.
62. Umpierre AD, Wu LJ. How Microglia Sense and Regulate Neuronal Activity. *Glia.* 2021 Jul;69(7):1637–53.
63. Gunner G, Cheadle L, Johnson KM, Ayata P, Badimon A, Mondo E, et al. Sensory lesioning induces microglial synapse elimination via ADAM10 and fractalkine signaling. *Nat Neurosci.* 2019 Jul;22(7):1075–88.
64. Gyoneva S, Hosur R, Gosselin D, Zhang B, Ouyang Z, Cotleur AC, et al. Cx3cr1-deficient microglia exhibit a premature aging transcriptome. *Life Sci Alliance.* 2019 Nov 27;2(6):e201900453.
65. Gomez-Arboledas A, Acharya MM, Tenner AJ. The Role of Complement in Synaptic Pruning and Neurodegeneration. *Immunotargets Ther.* 2021 Sep 24;10:373–86.
66. Dejanovic B, Wu T, Tsai MC, Graykowski D, Gandham VD, Rose CM, et al. Complement C1q-dependent excitatory and inhibitory synapse elimination by astrocytes and microglia in Alzheimer’s disease mouse models. *Nat Aging.* 2022 Sep;2(9):837–50.
67. Stevens B, Johnson MB. The complement cascade repurposed in the brain. *Nat Rev Immunol.* 2021 Oct;21(10):624–5.
68. Stevens B, Allen NJ, Vazquez LE, Howell GR, Christopherson KS, Nouri N, et al. The classical complement cascade mediates CNS synapse elimination. *Cell.* 2007 Dec 14;131(6):1164–78.
69. Loeffler DA, Camp DM, Bennett DA. Plaque complement activation and cognitive loss in Alzheimer’s disease. *J Neuroinflammation.* 2008 Mar 11;5(1):9.
70. Wilton DK, Mastro K, Heller MD, Gergits FW, Willing CR, Fahey JB, et al. Microglia and complement mediate early corticostriatal synapse loss and cognitive dysfunction in Huntington’s disease. *Nat Med.* 2023 Nov;29(11):2866–84.
71. Zabel MK, Kirsch WM. From development to dysfunction: Microglia and the complement cascade in CNS homeostasis. *Ageing Res Rev.* 2013 Jun;12(3):749–56.
72. Grimsley¹ C, Ravichandran² KS. Cues for apoptotic cell engulfment: eat-me, don’t eat-me and come-get-me signals. *Trends in Cell Biology.* 2003 Dec 1;13(12):648–56.

73. Okazawa H, Motegi S ichiro, Ohyama N, Ohnishi H, Tomizawa T, Kaneko Y, et al. Negative Regulation of Phagocytosis in Macrophages by the CD47-SHPS-1 System1. *The Journal of Immunology*. 2005 Feb 15;174(4):2004–11.
74. Lehrman EK, Wilton DK, Litvina EY, Welsh CA, Chang ST, Frouin A, et al. CD47 protects synapses from excess microglia-mediated pruning during development. *Neuron*. 2018 Oct 10;100(1):120-134.e6.
75. Jiang D, Burger CA, Akhanov V, Liang JH, Mackin RD, Albrecht NE, et al. Neuronal signal-regulatory protein alpha drives microglial phagocytosis by limiting microglial interaction with CD47 in the retina. *Immunity*. 2022 Dec 13;55(12):2318-2335.e7.
76. Honda S, Sasaki Y, Ohsawa K, Imai Y, Nakamura Y, Inoue K, et al. Extracellular ATP or ADP induce chemotaxis of cultured microglia through Gi/o-coupled P2Y receptors. *J Neurosci*. 2001 Mar 15;21(6):1975–82.
77. Ohsawa K, Irino Y, Nakamura Y, Akazawa C, Inoue K, Kohsaka S. Involvement of P2X4 and P2Y12 receptors in ATP-induced microglial chemotaxis. *Glia*. 2007;55(6):604–16.
78. York EM, Bernier LP, MacVicar BA. Microglial modulation of neuronal activity in the healthy brain. *Dev Neurobiol*. 2018 Jun;78(6):593–603.
79. George J, Cunha RA, Mulle C, Amédée T. Microglia-derived purines modulate mossy fibre synaptic transmission and plasticity through P2X4 and A1 receptors. *Eur J Neurosci*. 2016 May;43(10):1366–78.
80. Wculek SK, Dunphy G, Heras-Murillo I, Mastrangelo A, Sancho D. Metabolism of tissue macrophages in homeostasis and pathology. *Cell Mol Immunol*. 2022 Mar;19(3):384–408.
81. Kolliniati O, Ieronymaki E, Vergadi E, Tsatsanis C. Metabolic Regulation of Macrophage Activation. *J Innate Immun*. 2021 Jul 9;14(1):51–68.
82. Sun JX, Xu XH, Jin L. Effects of Metabolism on Macrophage Polarization Under Different Disease Backgrounds. *Front Immunol [Internet]*. 2022 Jul 14 [cited 2024 Apr 23];13. Available from: <https://www.frontiersin.org/journals/immunology/articles/10.3389/fimmu.2022.880286/full>
83. Gautier EL, Shay T, Miller J, Greter M, Jakubzick C, Ivanov S, et al. Gene-expression profiles and transcriptional regulatory pathways that underlie the identity and diversity of mouse tissue macrophages. *Nat Immunol*. 2012 Nov;13(11):1118–28.
84. Sabogal-Guáqueta AM, Marmolejo-Garza A, Trombetta-Lima M, Oun A, Hunneman J, Chen T, et al. Species-specific metabolic reprogramming in human and mouse microglia during inflammatory pathway induction. *Nat Commun*. 2023 Oct 13;14(1):6454.

85. Drougard A, Ma EH, Wegert V, Sheldon R, Panzeri I, Vatsa N, et al. A rapid microglial metabolic response controls metabolism and improves memory. *eLife* [Internet]. 2023 Jun 5 [cited 2024 Apr 23];12. Available from: <https://elifesciences.org/reviewed-preprints/87120>
86. Monsorno K, Buckinx A, Paolicelli RC. Microglial metabolic flexibility: emerging roles for lactate. *Trends in Endocrinology & Metabolism*. 2022 Mar 1;33(3):186–95.
87. Baik SH, Kang S, Lee W, Choi H, Chung S, Kim JI, et al. A Breakdown in Metabolic Reprogramming Causes Microglia Dysfunction in Alzheimer’s Disease. *Cell Metabolism*. 2019 Sep 3;30(3):493-507.e6.
88. Spinelli JB, Haigis MC. The Multifaceted Contributions of Mitochondria to Cellular Metabolism. *Nat Cell Biol*. 2018 Jul;20(7):745–54.
89. Shen K, Pender CL, Bar-Ziv R, Zhang H, Wickham K, Willey E, et al. Mitochondria as Cellular and Organismal Signaling Hubs. *Annual Review of Cell and Developmental Biology*. 2022 Oct 6;38(Volume 38, 2022):179–218.
90. Weinberg SE, Sena LA, Chandel NS. Mitochondria in the Regulation of Innate and Adaptive Immunity. *Immunity*. 2015 Mar 17;42(3):406–17.
91. West AP, Shadel GS. Mitochondrial DNA in innate immune responses and inflammatory pathology. *Nat Rev Immunol*. 2017 Jun;17(6):363–75.
92. Missiroli S, Genovese I, Perrone M, Vezzani B, Vitto VAM, Giorgi C. The Role of Mitochondria in Inflammation: From Cancer to Neurodegenerative Disorders. *Journal of Clinical Medicine*. 2020 Mar;9(3):740.
93. Chiurazzi M, Di Maro M, Cozzolino M, Colantuoni A. Mitochondrial Dynamics and Microglia as New Targets in Metabolism Regulation. *Int J Mol Sci*. 2020 May 13;21(10):3450.
94. Fenton AR, Jongens TA, Holzbaur ELF. Mitochondrial dynamics: Shaping and remodeling an organelle network. *Curr Opin Cell Biol*. 2021 Feb;68:28–36.
95. Friedman JR, Nunnari J. Mitochondrial form and function. *Nature*. 2014 Jan;505(7483):335–43.
96. Ozcan U. Mitofusins: Mighty Regulators of Metabolism. *Cell*. 2013 Sep 26;155(1):17–8.
97. Boldogh IR, Pon LA. Mitochondria on the move. *Trends Cell Biol*. 2007 Oct;17(10):502–10.
98. Rangaraju V, Lewis TL, Hirabayashi Y, Bergami M, Motori E, Cartoni R, et al. Pleiotropic Mitochondria: The Influence of Mitochondria on Neuronal Development and Disease. *J Neurosci*. 2019 Oct 16;39(42):8200–8.

99. Dietrich MO, Liu ZW, Horvath TL. Mitochondrial Dynamics Controlled by Mitofusins Regulate Agrp Neuronal Activity and Diet-Induced Obesity. *Cell*. 2013 Sep 26;155(1):188–99.
100. Fecher C, Trovò L, Müller SA, Snaidero N, Wettmarshausen J, Heink S, et al. Cell-type-specific profiling of brain mitochondria reveals functional and molecular diversity. *Nat Neurosci*. 2019 Oct;22(10):1731–42.
101. Zehnder T, Petrelli F, Romanos J, De Oliveira Figueiredo EC, Lewis TL, Déglon N, et al. Mitochondrial biogenesis in developing astrocytes regulates astrocyte maturation and synapse formation. *Cell Rep*. 2021 Apr 13;35(2):108952.
102. Popov A, Brazhe N, Morozova K, Yashin K, Bychkov M, Nosova O, et al. Mitochondrial malfunction and atrophy of astrocytes in the aged human cerebral cortex. *Nat Commun*. 2023 Dec 16;14(1):8380.
103. Yasumoto Y, Stoiljkovic M, Kim JD, Sestan-Pesa M, Gao XB, Diano S, et al. Ucp2-dependent microglia-neuronal coupling controls ventral hippocampal circuit function and anxiety-like behavior. *Mol Psychiatry*. 2021 Jul;26(7):2740–52.
104. Joshi AU, Minhas PS, Liddel SA, Haileselassie B, Andreasson KI, Dorn GW, et al. Fragmented mitochondria released from microglia trigger A1 astrocytic response and propagate inflammatory neurodegeneration. *Nat Neurosci*. 2019 Oct;22(10):1635–48.
105. Nair S, Sobotka KS, Joshi P, Gressens P, Fleiss B, Thornton C, et al. Lipopolysaccharide-induced alteration of mitochondrial morphology induces a metabolic shift in microglia modulating the inflammatory response in vitro and in vivo. *Glia*. 2019;67(6):1047–61.
106. Bordt EA, Moya HA, Jo YC, Ravichandran CT, Bankowski IM, Ceasrine AM, et al. Gonadal hormones impart male-biased behavioral vulnerabilities to immune activation via microglial mitochondrial function. *Brain Behav Immun*. 2024 Jan;115:680–95.
107. Maes ME, Colombo G, Schoot Uiterkamp FE, Sternberg F, Venturino A, Pohl EE, et al. Mitochondrial network adaptations of microglia reveal sex-specific stress response after injury and UCP2 knockout. *iScience*. 2023 Oct 20;26(10):107780.
108. Fairley LH, Lai KO, Wong JH, Chong WJ, Vincent AS, D’Agostino G, et al. Mitochondrial control of microglial phagocytosis by the translocator protein and hexokinase 2 in Alzheimer’s disease. *Proc Natl Acad Sci U S A*. 2023 Feb 21;120(8):e2209177120.

Chapter 2: Dynamic changes in mitochondria support phenotypic flexibility of microglia

2.1 Abstract

The ability of microglia to sense the environment and alter their cellular phenotype according to local neuron and tissue needs is a hallmark feature of these cells. Numerous receptors that comprise the microglial “sensors” have been identified, but how microglia interpret combined signaling from diverse receptors and adjust multiple cellular attributes in a coordinated fashion is not well understood. Mitochondria are increasingly recognized as essential signaling hubs, and these organelles can regulate coordinated remodeling of cell attributes in immune cells, including macrophages. Given these findings, surprisingly little is known about microglial mitochondria *in vivo* and how the state of these organelles may impact microglial attributes and functions. Here, we generated novel transgenic crosses for high resolution analysis of microglial mitochondria in both fixed tissue and acute brain sections. Fixed tissue analysis indicated that mitochondrial abundance was tightly linked to microglial morphological complexity and that regional differences in microglial phenotype were accompanied by regional differences in mitochondrial mass and number. Surprisingly, multiphoton imaging revealed that mitochondrial abundance was not correlated with microglial cell process remodeling or rapid cell process extension toward focal sites of tissue injury. FACS- and qPCR-based analyses revealed remodeling of microglial mitochondrial state within hours of systemic LPS injections. Moreover, microglial expression of inflammation-, trophic-, and phagocytosis-relevant genes was strongly correlated with expression levels of numerous mitochondrial-relevant genes. Overall, this study provides foundational information about microglial mitochondria and their relationship to differences in cell phenotype that occur across brain region, and during pathological insults. Moreover, these data demonstrate mitochondria support microglial phenotypic flexibility.

2.2 Introduction

An essential and defining characteristic of microglia is their ability to rapidly remodel their attributes and shift into different functional states (1–3). During embryonic and early postnatal development, microglia undergo extensive morphological and transcriptomic changes as they support different phases of CNS maturation (4–9). In adulthood, microglia exhibit prominent regional differences in cell density, morphology, motility, and phagocytic behaviors to optimally support local neuron function and tissue homeostasis (10–15). Finally, microglia show dramatic alteration of numerous cell attributes as they respond to CNS challenges. This includes unique patterns of change in cell properties in response to everything from chronic stress, to high fat diet, to pollution exposure, to aging, to brain injury, and to disease (16–22). The ability of microglia to remodel their properties and acquire distinct cellular functional states plays a critical role in shaping neuronal health in all these contexts.

Clearly a critical ingredient in microglial capacity to rapidly alter cellular phenotype rests on their ability to sense the local environment. Microglia possess an impressive repertoire of cell surface receptors that detect everything from ATP to pathogens to trophic factors (23–25). They also continually extend and retract their cell processes into the surrounding tissue (26–28), enabling dynamic and highly localized sensing of the surrounding environment. The field has elucidated how multiple cell surface receptors and associated intracellular signaling pathways can regulate key microglial properties and functions. These include P2RY12, TLR4, TGFBR2, CX3CR1, CR3 (ITGAM), and CSFR1, among many others. Yet, there are major gaps in our understanding of how microglia “interpret” simultaneous streams of information coming from distinct signaling axes and convert this into coordinated remodeling of multiple cell attributes to achieve the needed cellular phenotype in any given context.

Recent findings suggest that mitochondria may play an essential role in regulating coordinated changes in cell attributes. Mitochondria influence intracellular signaling by buffering calcium, by providing metabolites needed for protein post-translational modifications, by interacting physically with other organelles, and by signaling to the nucleus to impact gene expression (29–32). Research in macrophages supports this view of mitochondria as signaling hubs, demonstrating that mitochondria regulate macrophage responses to pathology and shifts into distinct inflammatory states (33–39). Little is known about mitochondria in microglia *in vivo*. However, regional differences in microglial phenotype are accompanied by prominent differences in expression of mitochondrial-relevant genes (40), and the state of mitochondria appears to be linked to microglial responses to early life immune challenge, brain injury, and protein aggregates in neurodegenerative disease (41–44). Given these intriguing observations, it is surprising how little is known about potential mitochondrial regulation of microglial attributes and phenotypic changes. In this study, we use novel transgenic crosses and multidisciplinary approaches to define for the first time the mitochondrial landscape within microglia *in vivo* and explore the relationship of these organelles to microglial phenotypic remodeling across brain regions, and in response to inflammatory insult.

2.3 Results

2.3.1 Regional specialization of microglia is accompanied by regional differences in mitochondrial mass and number

Mitochondria impact cellular function in numerous ways beyond simply producing ATP. Moreover, mitochondrial abundance, morphology, and molecular composition vary dramatically across cell types and these organelles appear to be “tuned” to carry out cell specific functions (45). Yet, little is known about microglial mitochondria *in vivo*. To enable visualization of

microglial mitochondria *in vivo*, we crossed mice that express inducible cre recombinase in microglia (*CX3CRI^{CreER/+}*) with mice that express a mitochondrial-targeted GFP (*mitoGFP*) in Cre-dependent fashion (Fig. 1A)(46,47). In fixed tissue from young adult (2mo) double transgenic *CX3CRI^{CreER/+};mitoGFP* mice (*MG-mitoGFP* mice), numerous GFP⁺ structures could be observed throughout the somas and cell processes of microglia (Fig. 1B and Fig. S1A,B) in multiple brain regions. Consistent with reports of tamoxifen-independent recombination when using *CX3CRI^{CreER/+}* and reporter lines with minimal distance between loxP sites(48,49), significant recombination was observed in *MG-mitoGFP* mice without administration of tamoxifen. Quantification in fixed tissue from nucleus accumbens (NAc) and ventral tegmental area (VTA), two brain regions where microglia display distinct cellular phenotypes, revealed that roughly 60-85% of IBA1⁺ microglia contained GFP-tagged mitochondria in both brain regions (Fig. S1A - C). Moreover, GFP-labeled structures were not observed outside of IBA1⁺ cells. Using flow cytometry to measure the percentage of GFP⁺ microglia in midbrain (containing VTA) and striatum (containing NAc), similarly indicated that approximately 80% of microglia were GFP⁺ even in the absence of tamoxifen injection (Fig. S1D- F). Flow cytometry also confirmed that other CNS cells were not GFP⁺ (Fig. S1G), validating cellular specificity of the mitochondrial reporter. Finally, to verify that GFP-tagged structures are mitochondria, we used tetramethylrhodamine (TMRM), a mitochondrial membrane potential indicator, to label mitochondria in acute brain sections from *MG-mitoGFP* mice and found that GFP⁺ structures were consistently colocalized with TMRM (Fig. S1H-I). Together these results indicate that *MG-mitoGFP* mice accurately reveal the *in vivo* distribution of microglial mitochondria.

To explore the relationship between mitochondrial networks and baseline structure of microglia in young adult mice, we carried out high resolution confocal imaging and 3D reconstruction of both microglia and their mitochondria in the NAc and VTA (Fig. 1B and Fig. S2A), where microglia show prominent differences in cell density, branching complexity, and gene expression (40). Consistent with previous findings, microglial tissue coverage in the NAc exceeded that observed in VTA (40) (Fig. 1C). Aspect ratio and sphericity of individual mitochondria, which are measures of mitochondrial networks, were also consistent across NAc and VTA microglia (Fig. S2B, D). However, despite showing reduced tissue coverage, VTA microglia exhibited a greater number of mitochondria relative to cell volume, as well as a greater total mitochondrial volume relative to cell volume (mitochondrial mass). (Fig. 1D, E). Together these observations indicate that key mitochondrial metrics vary across brain regions where microglia show distinct cellular phenotypes.

2.3.2 Mitochondrial number is correlated with morphological complexity of microglia, particularly in the VTA

Microglia continually survey the surrounding brain tissue and their capacity to carry out this function is influenced by cell branching and morphological complexity. To explore how mitochondrial networks relate to microglial branching structure, we crossed *MG-mitoGFP* mice to *Ai14* reporter mice to drive cytosolic expression of TdTomato (TdTom) in microglia along with GFP tagging of microglial mitochondria (Fig. 1A)(46,47,50). In fixed tissue from young adult (2mo) triple transgenic *MG-mitoGFP;Ai14* mice, microglia that expressed only mitoGFP, microglia that expressed only TdTom, and microglia that were positive for both mitoEGFP and TdTom could be observed (Fig. S1E). In the absence of tamoxifen injection, incidence of mitoGFP+TdTom+ cells were low enough to allow rigorous and unequivocal reconstruction of

the branching patterns of individual microglial cells, as well as their mitochondrial networks (Fig. 1F). Consistent with previous findings(40), VTA microglia exhibited lower total process length and fewer branch points than NAc microglia in young adult *MG-mitoGFP;Ai14* mice (Fig. 1G,I). The maximum number of intersections in Sholl analysis was also lower in VTA compared to NAc microglia (Fig. 1H). Sholl analysis also revealed that the subcellular distribution of mitochondria within microglia follows branching complexity of the cell (Fig. S2F, G). For example, number of microglial intersections reach a maximum around 20-25 μm from the cell soma in both the NAc and the VTA. Similarly, we see that mitochondrial distribution follows a similar trend, with peak mitochondrial number is occurring around 20 μm from the cell soma in both the NAc and the VTA (Fig. S2F, G).

Using linear regression to further probe links between morphological and mitochondrial features of microglia revealed several general trends. First, there were more significant or nearly significant associations between total *number* of mitochondria and morphological features of microglia than there were associations between total *volume* of mitochondria and morphological features of microglia (Fig. 1J,K,L). Second, there were a greater number of significant and nearly significant correlations between mitochondrial and morphological features of microglia within the VTA than in the NAc (Fig. 1J,K,L). Some observed relationships seem to make intuitive sense; for example, greater cell process length was significantly correlated with increased total volume of mitochondria in NAc and was nearly significant in VTA (Fig. 1L, and Fig. S2I). In other words, a greater amount of cell process requires a greater number of mitochondria. Some observed relationships were more surprising, however. For example, both the total number of branch points and maximum number of Sholl intersections were positively correlated with total mitochondrial number in VTA microglia. Hence, for VTA microglia, it is not simply the amount

of total cell process, but also the architecture of cell processes that are related to mitochondria within the cell (Fig. 1J, K,L). Together these analyses suggest that remodeling of microglial morphological structure is likely to require or be accompanied by remodeling of mitochondrial networks within these cells.

2.3.3 Mitochondrial number and mitochondrial motility are not aligned with microglial tissue surveillance

In addition to morphological structure, the dynamics of microglial cell process extension and retraction shapes their overall capacity to survey the local brain parenchyma(26,27).

Continual morphological remodeling of microglia is assumed to be an energy intensive process.

However, the relationship between microglial cell process motility and mitochondrial abundance and distribution has not been explored previously. To gain initial insight into the relationship

between these organelles and microglial motility, we performed two-photon imaging in acute brain sections prepared from young adult (2-3mo) *MG-mitoGFP;Ai14* mice. In

mitoGFP+TdT⁺ microglia, we carried out simultaneous imaging of both microglial cell processes (TdT) and mitochondria within these cells (GFP) and could observe motility of

both (Fig. 2A-C). A combination of modified 3DMorph code, FIJI plugins, and Imaris were used to reconstruct cells and organelles and track motility of both over time. Microglia were imaged at

least 60mm below the surface of the brain section and microglial motility (total process

remodeling, normalized to cell area) was not correlated with time elapsed since preparation of brain sections (Fig. 2D). Moreover, motility was not substantially different between cells with

fewer or greater number of Sholl intersections (Fig. S3F), suggesting that observed dynamics are not primarily driven by responses to brain slice preparation. Finally, the positive correlation we

observed between total mitochondrial volume and Sholl intersections in fixed tissue was preserved in acute brain sections (Fig. S3D).

Microglial motility was similar across NAc and VTA microglia (Fig. S3G), implying that tissue surveillance will be less complete over a given time interval in the VTA, as VTA microglia are less branched and have lower tissue coverage compared to NAc microglia (Fig. 1C, G-I). Although VTA microglia showed greater mitochondrial mass and mitochondrial # compared to NAc microglia, there was no correlation between total mitochondrial volume and microglial motility in the VTA (Fig. 2E). In the NAc, there was a negative correlation such that microglia with lower total mitochondrial volume showed greater cell process motility (Fig. 2E). These observations suggest that there is a more robust relationship between mitochondrial abundance and underlying cell morphology than with dynamic remodeling of that morphology. However, mitochondria are not exceedingly abundant within microglia, raising the question of whether there will be differences in local cell process motility depending on distance to the nearest mitochondrion.

Mitochondria themselves are highly motile organelles and their trafficking and localization can impact key cellular functions such as synaptic plasticity in neurons (51,52). Microglial mitochondria exhibited numerous forms of motility that included “jitter,” more concerted directional movement, and occasional examples of fission and fusion (Fig. 2F). 3D reconstruction of mitochondria in Imaris and tracking across time revealed that mitochondrial network motility (total displacement normalized to total mitochondrial volume) was similar in NAc and VTA microglia (Fig. 2G). Average displacement of mitochondrial movement was also similar in NAc and VTA microglia (Fig. 2H-I). Linear regression analyses indicated that there was no significant relationship between average and total mitochondrial motility and cell process

remodeling of microglia in either the NAc or the VTA (Fig. 2J-K). This finding further reinforces the idea that mitochondrial abundance, distribution, and motility are not linked in any direct fashion to baseline microglial tissue surveillance. Nonetheless, additional future analysis will be needed to explore whether there are highly localized changes in cell process extension or retraction in the presence of a mitochondrial trafficking or fission/fusion event.

Although there was no significant relationship between time post sectioning and microglial tissue surveillance, there were trends toward a relationship between time post sectioning and mitochondrial motility in both the NAc and the VTA (Fig. S3E). This observation suggests that alterations in the functional state of mitochondria may occur prior to any changes in microglial surveillance capacity. Intriguingly, potential associations were in opposite directions across brain region such that mitochondrial motility appeared to increase in NAc with greater time post-sectioning, and mitochondrial motility appeared to decrease with greater time post-sectioning. This observation raises the possibility that there are regional differences in microglial responses to brain sectioning and that divergent mitochondrial remodeling may play a role in regulating such regional differences in microglial response to brain sectioning.

2.3.4 Mitochondrial distribution is stable during early phases of microglial response to focal injury

The results described above suggest that mitochondrial abundance and mitochondrial motility are not strongly tied to baseline microglial tissue surveillance. In addition to homeostatic tissue surveillance, microglia exhibit rapid and robust cell process extension toward focal sites of CNS injury in an ATP dependent manner (26,53). To begin defining mitochondrial dynamics in the context of microglial responses to acute injury, we imaged microglial processes and mitochondrial dynamics in response to focal laser lesion. Consistent with numerous studies in the

field, microglia in acute brain sections from *MG-mitoGFP;Ai14* mice extended cell processes toward the site of focal laser lesion, contacting the lesion within 10-15min (Fig. 3A-E).

Surprisingly, these rapidly extending cell processes did not contain any mitochondria and no mitochondria were trafficked into these lesion-responsive processes even 70min post-lesion (Fig. 3A-E). Moreover, there did not appear to be obvious changes in somatic mitochondria or redistribution of mitochondria in processes on the non-lesion side of the cell. These findings suggest that energy needed for this rapid injury-induced morphological remodeling does not require mitochondria to be precisely at the site of cell process extension and/or energy needed for this remodeling is generated from glycolysis. Future experiments using *in vivo* imaging will be needed to explore whether mitochondrial distribution within injury responsive microglia emerges during time periods several hours post-lesion. Future experiments can also define whether changes in mitochondrial membrane potential, calcium buffering, or production of reactive oxygen species occur during rapid microglial responses to injury.

2.3.5 Mitochondrial remodeling is evident at the earliest stages of microglial responses to inflammatory challenge

In addition to tissue injury, microglia exhibit rapid responses to pathogens and inflammatory signals related to infection (54,55). To further explore the role of mitochondria in microglial responses to pathological challenges, we used intraperitoneal (i.p.) injections of lipopolysaccharide (LPS), a component of the cell wall of gram-negative bacteria, which is widely used to model systemic inflammatory responses that accompany infection. Microglia responds to this challenge with prominent changes in morphology and gene expression that emerge within hours of LPS injection and continue to evolve for several days afterwards. *In vitro* studies indicate that mitochondrial fragmentation and metabolic shifts from oxidative

phosphorylation to glycolysis occur within microglia following LPS exposure (56–59) and, in macrophages, mitochondrial alterations play an essential role in enabling and regulating changes in macrophage attributes as they respond to inflammatory challenges(60,61).

To explore early and late responses of microglia and their mitochondria to inflammatory challenge, young adult (3-4mo) *MG-MitoEGFP* mice were given i.p. injections of saline or LPS and microglial gene- and protein- expression were analyzed 4hr or 24hr post injection via FACS and downstream qPCR (Fig. 4A). Microglia from both striatum (STR, containing NAc) and midbrain (MB, containing VTA) were collected to enable comparison of microglial responses across brain regions. Within 4hr of LPS challenge, both STR and MB microglia exhibited prominent up-regulation of pro-inflammatory factors (*Il1b*, *Tnfa*), and downregulation of homeostatic microglial genes (*Tgfb1*, *P2ry12*, *Cx3cr1*), consistent with numerous studies showing robust microglial responses to this type of pro-inflammatory challenge (8,62–64). Upregulation of genes associated with microglial phagocytic function (*Cd45*, *Itgam*) was evident by 24hr post injection (Fig. 4B). Overall, STR and MB microglia responded similarly to LPS challenge at the gene expression level, with only *Cd45* and *Cd68* exhibiting significant differences across region in patterns of gene regulation.

Microglial expression of mitochondrial-function related genes was also altered at both 4hr and 24hr post injection (Fig. 4B). Within 4hr of LPS challenge, genes related to mitochondrial ROS handling (*Sod2*, *Cat*) and mitochondrial fission (*Dnm1l*) were significantly altered, with genes related to mitochondrial biogenesis (*Nrf1*, *Ppargc1a*), approaching significance. Some of these gene expression changes were maintained into 24hr post injection (*Sod2*, *Dnm1l*), while others appeared more restricted to the 4hr time point (*Cat*, *Nrf1*). At 24hr post injection, prominent upregulation of electron transport chain component genes *Ndufa12*

(Complex I), *Cox4i1* (Complex IV), and *Atp5d* (Complex V) emerged. Genes related to mitochondrial calcium handling (*Vdac1*, *Micu1*) were also significantly altered. Again, most gene expression changes were similar across STR and MB, with only *Micu1* displaying significant regional differences in expression pattern (Fig. 4B). Together these data indicate that numerous facets of mitochondrial function are remodeled during microglial responses to inflammatory challenge and that such mitochondrial remodeling begins at the earliest stages of shifts in microglial properties. These observations argue against the idea that mitochondrial changes only emerge after changes in microglial cellular function to support the energetic demands of a new cellular state.

Consistent with the idea that mitochondrial state is intimately linked to microglial functional state during responses to inflammatory challenge, Principal Component Analysis (PCA) based solely on expression patterns of mitochondrial function-relevant genes can explain 64.7% of sample variation with the first 2 components and 81% of variation with the first 3 components (Fig. S4A). Moreover, 24hr post injection samples cluster away from Saline samples (Fig. 4C) and 4hr post injection samples are interspersed among Saline samples or skewed toward the 24hr samples.

To further probe the relationship between mitochondrial state and key features of microglial responses to LPS challenge, we used linear regression analyses to examine correlation between individual microglial-state and mitochondrial-state genes (Fig. 4D). As STR and MB microglia exhibited similar patterns of gene expression changes following LPS challenge, samples from both regions were combined for these analyses. At 4hr post LPS, both microglial pro-inflammatory genes *Il1b* and *Tnfa* showed significant correlation with mitochondrial biogenesis genes (*Nrf1*, *Tfam*), mitochondrial fusion and fission genes (*Mnfl*, *Dnm1l*) and the

ROS handling gene *Sod2*. *Cd45*, which is also critically linked to microglial responses to pathological insults, did not show much correlation with mitochondrial-function genes in saline treated animals but exhibited numerous significant correlations at 4hr and 24hr post LPS (Fig. 4D). Expression of homeostatic microglial gene *Cx3cr1* showed significant correlation with numerous mitochondrial-function genes that were lost at 4hr. Many of these correlations were regained with even higher significance at 24hr post LPS. Homeostatic microglial gene *P2ry12* was significantly correlated with expression of electron transport chain genes (*Cox4i1*, *Ndufa12*, *Sdha*) and mitochondrial biogenesis genes (*Nrf1*, *Tfam*, *Ppargc1a*) in saline treated animals. At 4hr post LPS injection, these associations were lost and *P2ry12* instead showed significant correlation with calcium handling gene *Vdac1* and ROS handling genes (*Sod2*, *Cat*, *Gpx1*)(Fig. 4D). Collectively, these findings indicate that multiple facets of microglial function beyond just their production of pro-inflammatory factors are tightly associated with the status of microglial mitochondrial state.

The numerous significant correlations between microglial-functional state genes and mitochondrial function genes were somewhat surprising. As an initial means to probe whether such correlations would be observed between microglial functional state genes and any cellular organelle, we also examined linear regression analyses between *Cd68*, a key microglial lysosome gene, and markers of microglial function (Fig. S4B). No significant correlations were observed between expression of *Cd68* and expression of microglial pro-inflammatory factors *Tnfa* and *Il1b*. Significant correlations were observed between *Cd68* and homeostatic microglial genes *Cx3cr1* and *Tgfb1*, but these were not modulated by LPS treatment. Only *Cd45* and *P2ry12* showed correlations that were gained and lost, respectively, as a function of LPS treatment. This analysis provides initial hints that mitochondria, as organelles, are more tightly linked to

remodeling of microglia function during inflammatory challenge compared to other organelles such as lysosomes.

The qPCR-based analyses presented thus far show high sensitivity for detection of early changes in cell and organelle state following LPS challenge. However, not all transcript level changes are maintained at the protein level. As an initial approach for detecting changes in microglial mitochondria at the protein and functional level, we analyzed data recorded during FACS isolation of microglia. The intensity of GFP, driven by mitoEGFP and reflecting mitochondrial mass, showed large, significant increases at 24hr post injection in both the STR and MB, with hints of emerging increases at 4hrs post injection (Fig. 4E, 4F). In contrast, the intensity of TMRM, a dye that accumulates in mitochondria in a mitochondrial membrane potential dependent manner, decreased significantly at 24hr post LPS (Fig. 4E, 4F). These changes in mitochondrial mass and mitochondrial membrane potential were accompanied by significant protein-level increases in CD45 by 24hr in STR microglia. Similar trends in CD45 levels that did not reach significance were observed in MB microglia. They were also accompanied by significant increases in forward scatter, a measure of cell size. Protein level expression of CX3CR1 and P2RY12 differed across region but not across treatment (Fig S4C). This data confirm that there are changes in mitochondrial state at the protein and functional level that are associated with changes in microglial protein-level expression.

2.3.6 Increased mitochondrial mass and mitochondrial elongation are associated with microglial responses to inflammatory challenge

To investigate how LPS challenge impacts microglial mitochondrial morphology and cellular distribution, we used immunostaining, confocal imaging, and 3D reconstruction in Imaris to analyze NAc and VTA microglial mitochondria in fixed tissue from 3-4mo *MG-*

MitoEGFP mice (Fig. 5A, Fig. S5A). These experiments focused on 24hr post-LPS, as FACS analyses indicated that functional and protein-level changes in microglia and their mitochondria were most evident at this time point (Fig. 4). 3D reconstruction of both microglia and their mitochondria revealed significant increases in mitochondrial mass at 24hr post LPS injection (Fig. 5B), consistent with FACS-based analyses. No significant changes in mitochondrial number were detected (Fig. 5C) and, instead, microglial mitochondria showed significant elongation, as detected by increases in aspect ratio, a measure of the mitochondria's longest axis divided by its shortest axis (Fig. 5D). These observations suggest that increases in mitochondrial mass may be due to mitochondrial biogenesis, coupled with mitochondrial fusion. This would be consistent with qPCR-based increases in mitochondrial biogenesis factors *Nrf1* and *Tfam*, as well as the observation of tight correlation between mitochondrial fission/fusion factors (*Mfn1* and *Dnm1l*) and rapid pro-inflammatory responses of microglia to LPS challenge (Fig. 4B,D). In addition, elongation of mitochondria has been associated with increased capacity of those mitochondria for oxidative phosphorylation (65,66), which would be consistent with the qPCR-based observation of robust increases in electron transport chain components (*Ndufa12*, *Atp5d*, *Cox4i1*, *Sdha*) at 24hrs post LPS (Fig. 4B).

Collectively, these findings indicate that microglial mitochondria undergo extensive functional and structural remodeling as microglia are responding to LPS challenge. Moreover, multiple aspects of mitochondrial state are tightly correlated with key changes in microglial attributes during this response to LPS challenge. Finally, remodeling of mitochondria was detected at very early stages of microglial responses to LPS challenge, supporting the possibility that these organelles play an enabling and regulatory role in shaping microglial responses to this challenge.

2.4 Discussion

2.4.1 The underappreciated complexity of mitochondria.

Mitochondrial energy production is highly efficient, generating 32 molecules of ATP for every molecule of glucose, compared to the 2 molecules of ATP per glucose generated by glycolysis. Mitochondria are also highly dynamic, showing distinct structure and capacity for ATP production depending on subcellular location (45,46,67). Although all cells contain mitochondria and all cells rely on ATP for ongoing function, there is growing appreciation that not all cells “utilize” their mitochondria primarily for generating ATP. Indeed, mitochondria play key roles in generating metabolites and reactive oxygen species (ROS) needed for post-translational protein modifications. They participate in calcium buffering and lipid metabolism and interact with and regulate other organelles such as endoplasmic reticulum, lysosomes, and lipid droplets. Mitochondria can also signal to the nucleus and impact gene expression. Accordingly, the mitochondrial field has moved well beyond viewing this organelle as an energy producer, and instead supports a model in which this organelle is a critical signaling and regulatory hub within the cell (29–32,68).

Multiple studies indicate that mitochondria *regulate* changes in cell function, rather than simply adjusting ATP output “posthoc” to meet energetic needs of a new functional state. For example, in neurons, mitochondria can regulate emergence of synaptic plasticity (45,67) and, in astrocytes, mitochondria can regulate morphological and functional maturation of the cell (67,69). Mitochondria can also regulate the inflammatory state of macrophages and capacity of these cells to rapidly adjust their cellular phenotype in response to various challenges (34–39,68). Given evidence that mitochondrial dysfunction is implicated in developmental delays, epilepsy, migraine, psychiatric disorders, aging, and risk for neurodegeneration (70,71), a better

understanding of how mitochondria impact the function of specific CNS cell types should be a priority for the field. However, because mitochondrial structure and molecular composition vary widely across distinct cell types (45), findings about the functional roles of these organelles cannot be generalized and mitochondria need to be studied with cellular specificity.

Our study is one of the first to provide detailed information about microglial mitochondria *in vivo* and the relationship between these organelles and dynamic changes in microglial function and cellular phenotype. Our findings support the idea that mitochondrial morphology is distinct across CNS cell types. In astrocytes, mitochondria are extremely abundant and make up about 80% of the astrocyte volume in young adult mice (69). This is quite different from what we observed in microglia, where mitochondria occupy about 8% of cellular volume. Qualitatively, our experiments using TMRM incubation in acute brain sections suggest that microglial mitochondria are less hyperpolarized than mitochondria of surrounding cells (Fig. S1H). Our findings also support the idea that individual mitochondria vary depending on subcellular location. We often observed very elongated mitochondria in microglial cell processes and more complex, network-like mitochondria in cell somas. TMRM intensity of cell process mitochondria also appeared lower than that of somatic microglial mitochondria (Fig. S1H). Finally, motility of mitochondria also differed depending on cellular compartment, with cell process mitochondria being more likely to exhibit concerted trafficking in one direction or the other.

2.4.2 How does mitochondrial state relate to homeostatic microglial functions?

Previous studies have suggested that mitochondrial function in microglia changes in the context of disease, stress, and immune activation (41,42,56,72,73). Almost nothing is known, however, about how these organelles impact physiological functions of microglia. Through

rigorous 3D reconstruction of mitochondria and cellular branching within individual microglia, we found key relationships between mitochondrial abundance and microglial morphology in young adult mice. Intriguingly, mitochondrial abundance was correlated with both total process length as well as branching complexity of microglia. Hence, even if microglia have fewer mitochondria than other CNS cells, our data suggest that these organelles are likely to be involved anytime that microglial branching structure needs to be altered. Our FACS-based analyses of key microglial genes and a panel of mitochondrial relevant genes also indicated that mitochondrial status is linked to cell surface expression of key microglial receptors. In young adult mice, expression of *P2ry12*, *Cx3cr1*, and *Tgfb1* were significantly correlated with expression levels of multiple mitochondrial genes involved in oxidative phosphorylation, calcium handling, and ROS handling.

Regional specialization of cellular phenotype is also a key feature of homeostatic microglia (10,14,15,40,74). We found previously that differences in cellular phenotype of VTA microglia, compared to microglia in other basal ganglia nuclei, were accompanied by differences in expression of mitochondrial-relevant genes (40). This observation suggests that mitochondrial state may play a central role in regulating regional differences in microglial cellular phenotype. In this study, we confirm that regional differences in microglial phenotype are indeed accompanied by regional differences in mitochondria within these cells. Lower tissue coverage of VTA microglia was accompanied by elevated mitochondrial mass and mitochondrial number compared to NAc microglia. Whole cell reconstruction confirmed that VTA microglia have lower total process length, number of branch points, and number of Sholl intersections compared to NAc microglia. Yet, the VTA microglia showed a greater number of significant and nearly significant correlations between number of mitochondria and cellular morphological features.

Finally, our FACS analysis indicated that midbrain microglia (containing VTA) from young adult mice had more depolarized mitochondrial membrane potential (lower TMRM intensity) compared to striatum microglia (containing NAc). Together, these observations indicate that differences in mitochondrial status are tightly linked to regional differences in microglial phenotype that are observed under physiological conditions.

One of the most surprising findings of our study relates to microglial cell process motility. Since the discovery of *in vivo* microglial tissue surveillance in 2005 (26,27), the dynamic behaviors of these cells have captivated the field. This continual morphological remodeling is assumed to be an energy intensive process. However, we did not find a strong correlation between microglial cell process remodeling and abundance of mitochondria within VTA microglia. Moreover, abundance of mitochondria was negatively correlated with microglial motility in the NAc, which seems highly counter intuitive if these organelles are providing a primary energy source for cell process remodeling. Future studies will need to investigate highly localized relationships between microglial filopodia and distance to nearest mitochondria and examine whether mitochondrial membrane potential or other features of mitochondrial state are linked to microglial motility.

In this study, we also provide the first analysis of mitochondrial motility within microglia. Mitochondria can alter their distribution within the cell, as well as undergo fission and fusion (52,75). Work in peripheral macrophages demonstrates that such mitochondrial structural remodeling can regulate key cellular functions (34–39). We found that microglial mitochondria exhibit most of the same forms of dynamic remodeling described in other cell types. In both NAc and VTA microglia, we observed mitochondria that appeared to “jitter” in place, mitochondria that underwent elongation or shortening, mitochondria that underwent directional trafficking and,

occasionally, mitochondria that underwent fission or fusion. Some of these dynamic changes in mitochondria were extremely rapid and may not be fully captured when simultaneously acquiring full stacks of individual microglia. Future studies can focus on imaging of mitochondria in an *in vivo* condition to define the features of their motility more fully. It is also worth noting that we occasionally observed mitochondrial movement that was driven by retraction of a microglial cell process that appeared to “pull” a mitochondrion along “passively,” creating another type of mitochondrial motility that is not likely to be observed in more stationary CNS cells. Our study explored how mitochondrial dynamics relate to microglial cell process remodeling, providing the first analysis of this type. At the level of individual cells, we did not observe any correlation between mitochondrial displacement and cell process motility, suggesting that mitochondrial trafficking to specific subcellular locations is not required for baseline microglial tissue surveillance. Future studies can determine whether there are relationships between specific types of mitochondrial remodeling (e.g. fission or fusion) and highly localized microglial cell process motility.

2.4.3 Do mitochondria regulate microglial responses to focal injury?

The discovery of microglial tissue surveillance was accompanied by the discovery of extremely rapid injury responses of microglia (26,27). Following focal tissue injury, nearby microglia extend multiple cell processes toward the lesion and undergo chemotaxis and encapsulate the damaged tissue within 10-15min. This process is dependent on microglial response to extracellular ATP and endogenous release of ATP through lysosomal exocytosis. This leads to long range signaling to increase microglia process migration to site of injury (27,76).

The status of mitochondria during this prominent and rapid morphological remodeling of microglia has not been directly examined. If perhaps endogenous ATP is required for long range response and chemotaxis, mitochondria localization may be important in regulating this response. Through simultaneous multiphoton imaging of microglial mitochondria and microglial cell processes, much to our surprise, we found that mitochondria are relatively stable within the cell, even as microglial processes are rapidly extended toward laser lesions. This finding implies that mitochondrial localization to site of energy demand is not critical. ATP or other metabolites may be reaching the site of injury without the need for mitochondrial trafficking. This may be occurring through mitochondrial interaction with other organelles. Few studies exist demonstrating how ATP may be transported from mitochondria to cell surface, but some studies indicate this process of ATP transport could be via dynamin or kinesin proteins (77). This observation may indicate mitochondria localization and local release of ATP is not necessary for microglia response. Another plausible explanation is that microglia aren't utilizing ATP to fuel this membrane remodeling response and chemotaxis during injury response. Previous study demonstrated microglia can still extend their processes toward a focal injury when oxidative phosphorylation is inhibited via oxygen removal (72). The same study demonstrates similar lesion response is observed in the absence of glycolysis via glucose depletion. This alludes to microglial not requiring ATP production for acute injury response. Future studies can examine longer time points post-lesion in and *in vivo* context to determine whether structural remodeling of mitochondria or substantial mitochondrial trafficking occurs. Future studies can also investigate whether there are other aspects of mitochondrial function such mitochondrial capacity to produce ROS or buffer calcium that are linked microglial cell process extension toward lesions. These findings also hint that mitochondria localization is not a relevant

mechanism for long range ATP release which was previously assumed. Based on this evidence, mitochondria may not be as important for this process as previously understood and could be participating in other microglial responses.

2.4.4 Do mitochondria regulate microglial responses to CNS challenge?

Microglia also exhibit rapid responses to inflammatory insults (78,79). Systemically injected LPS does not cross the blood brain barrier, but does elicit robust pro-inflammatory responses in peripheral immune cells that then impact the brain (80–82). Protein-level increases in inflammatory cytokines such as TNF α and IL1 β can be detected within the blood by 20min post-injection and are subsequently detected within the brain tissue at 1-4hrs post-injection. Once these inflammatory signals enter the brain, microglia rapidly alter gene expression, showing upregulation of *Tnfa* and *Il1b* (among other inflammatory factor) transcripts by 2-4 hours post-injection (78). Microglial responses to this insult continue to evolve with changes in cell morphology, protein-level expression of cell surface receptors, and cell proliferation becoming detectable at 24-48hrs post injection.

We found that increases in microglial *Tnfa* and *Il1b* mRNA detected at 4hrs post injection were accompanied by transcript-level changes in expression of multiple mitochondrial-relevant genes. Moreover, expression levels of *Tnfa*, *Il1b*, and *Cd45* in individual samples were significantly correlated with expression levels of mitochondrial-relevant genes at this 4hr time point. These included genes involved in mitochondrial fission and fusion, calcium handling, and ROS handling, in addition to genes involved in mitochondrial biogenesis and oxidative phosphorylation. These findings support the possibility that mitochondrial signaling functions influence key microglial attributes and suggest that these organelles are doing more than simply altering energy production to support a newly emerging cellular phenotype. Substantial changes

in mitochondrial status continued to be evident in the later phases of microglial responses to inflammatory insult, with significant increases in mitochondrial mass and mitochondrial elongation at 24hrs post LPS injection. Moreover, in principle component analysis, microglia could be clustered solely based on their mitochondrial relevant genes. Together these data argue that capacity of microglia to remodel their mitochondria will have major implications for how effectively these cells respond to inflammatory challenges. Any mitochondrial dysfunction within these cells could exacerbate or hamper their ability to respond to insults.

2.5 Materials and Methods

Transgenic Animal Models

C57Bl6 WT mice were obtained from the NIA Aged Rodent Colony and housed in the UCLA vivarium for at least one month before experiments.

CX3CR1^{CreER/+} mice were originally obtained from Jackson Labs (stock #025524) and subsequently maintained in our colony (1).

Rosa26-lsl-mito-EGFP mice (*mitoEGFP* mice) were obtained from Dr. Jeremy Nathans (Johns Hopkins University) and are available at Jackson Labs (stock #021429). These mice enable cre-dependent expression of GFP that is fused to an N-terminal signal derived from mouse cytochrome c oxidase, subunit VIIIa, enabling specific localization to mitochondria (2).

Ai14 td tomato reporter mice were obtained from Jackson Labs (stock #007914) and subsequently maintained in our colony (3).

Mice used for experiments were heterozygous for all transgenes. In all experiments balanced numbers of male and female mice were used. Mice were housed in normal light/dark cycle and

had ad libitum access to food and water. All experiments were performed in strict accordance with protocols approved by the Animal Care and Use Committees at UCLA.

Lipopolysaccharide Injections

CX3CR1^{CreER/+}; mitoEGFP mice 3 to 5 months of age (mos) received single intraperitoneal injections of 1mg/kg of Lipopolysaccharide (LPS) (Millipore Sigma, strain O55:B5, L2880-25MG) or saline. All injections were performed around ~10am and mice were euthanized for immunohistochemistry or flow cytometry at 4 h or 24 h post-injection.

Tissue collection and immunohistochemistry

CX3CR1^{CreER/+}; mitoEGFP (postnatal day 60, 12-13mo, and 16-18mo) or *CX3CR1^{CreER/+}; mitoEGFP ; Ai14* (postnatal day 60) mice were deeply anesthetized via isoflurane inhalation and transcardially perfused with 1M phosphate buffered saline (PBS; pH 7.4) followed by ice-cold 4% paraformaldehyde (PFA) in 1M PBS. Brain tissue was isolated and postfixed PFS for ~4 h at 4°C and then stored in 1 M PBS with 0.1% sodium azide until sectioning. Coronal brain sections were prepared using a vibratome at 60 mm thickness. For immunostaining, free-floating brain sections were washed with 1M PBS (5 min) and then permeabilized and blocked in a solution of 2% bovine serum albumin (BSA) and 3% normal donkey serum (NDS) and 0.01% of Triton-X for 2 h with rotation at room temperature. Sections were then incubated overnight with primary antibodies prepared in 2% bovine serum albumin (BSA) and 3% normal donkey serum (NDS) at 4°C with rotation. Sections from aged mice were incubated in TrueBlack lipofuscin autofluorescence quencher, (5%; Biotium cat: 23007) for 60 s followed by a 3x5 min rinse in 1M PBS prior to incubation with primary antibodies. Following primary antibody incubation, sections were washed 3x with 1M PBS and then incubated with secondary antibodies prepared in

2% bovine serum albumin (BSA) and 3% normal donkey serum (NDS) at room temperature for 2 h with rotation. This was followed by washes in 1M PBS (3x) with second wash containing 1:4000 dilution of DAPI in 1 M PBS. Sections were mounted using Aqua-Poly/Mount (Polysciences cat: 18606) and cover slipped (coverslips of #1.5 thickness). Primary antibodies used include rabbit anti- Iba1 (1:800; Wako, catalog #019-19741), rat anti-CD68 (1:200; clone FA11, AbD Serotec, catalog #MCA1957), chicken anti-TH (1:500; Aves, catalog #TYH). Secondary antibody combinations include rabbit AlexaFluor-647, chicken AlexaFluor-594, rat AlexaFluor-594, or chicken AlexaFluor-405 (used at 1:1000; all raised in donkey; Jackson ImmunoResearch Laboratories). For each set of analyses, three brain sections containing nucleus accumbens (NAc) and three brain sections containing ventral tegmental area (VTA) were chosen from each mouse. Brain sections were selected based on well-defined anatomical parameters and were matched for anterior-posterior location.

Image acquisition and analysis

Fixed tissue slides were imaged using a Zeiss LSM880 confocal microscope or a Zeiss LSM700 confocal microscope. Within the NAc, images were acquired at the boundary between core and shell (identified anatomically) and include both subregions. In the VTA, images captured were medial to the medial lemniscus. For quantification of MitoEGFP recombination within microglia, stacks of confocal images (z stacks) with a z interval of 1 μm were taken using a 20x objective and imported into ImageJ software for analysis. Maximum intensity projections were counted manually for the % of microglia exhibiting MitoEGFP expression.

For 3D reconstruction of microglia and mitochondria, confocal z stacks were acquired with a 63x objective and z interval of 0.3 μm and imported into Imaris (Bit plane) software for analysis. The

surface reconstruction module was used for quantification of mitochondrial and microglial volumes. For all image analyses, two or three images from separate brain sections were analyzed per mouse to obtain an average value for that mouse. Three to 7 mice were analyzed per brain region, per age and per condition. Sample sizes were selected to be in the upper range of published immunohistochemistry experiments. The filament tracer module was used for in depth analysis of microglial morphology, with 3 to 4 microglia from separate mice reconstructed per brain region. Surfaces were also created for mitochondria from filament-traced microglia to enable linear regression analyses.

Acute brain slice preparation

Acute slices were prepared for ex-vivo two-photon microscopy. *CX3CR1^{CreER/+}; mitoEGFP* or *CX3CR1^{CreER/+}; mitoEGFP; Ai14* mice at 1.5 to 2.5 months were anesthetized with isoflurane and perfused transcardially with 10 ml of oxygenated, ice-cold N-methyl-D-glucamine (NMDG)-based solution containing the following (in mM): 92 NMDG, 20 HEPES, 30 NaHCO₃, 1.2 NaH₂PO₄, 2.5 KCl, 5 sodium ascorbate, 3 sodium pyruvate, 2 thiourea, 10 MgSO₄, and 0.5 CaCl₂, 10 glucose, pH 7.4 (310 mOsm). Brains were then rapidly dissected free and horizontal midbrain sections (230 μm thick) and coronal forebrain sections (300 μm thick) were prepared using a vibratome in ice cold NMDG-based cutting solution bubbled continuously with 95% O₂/5% CO₂. Following sectioning, sections were transferred to a holding chamber containing NMDG solution at 34 °C for 5 min and then transferred to artificial cerebrospinal fluid aCSF solution at room temperature for 30 min recovery containing the following (in mM): 125 NaCl, 2.5 KCl, 1.25 NaH₂PO₄ 2H₂O, 1 MgCl₂ 6H₂O, 26 NaHCO₃, 11 Glucose and 2.4 CaCl₂ 2H₂O and bubbled continuously with 95% O₂/5% CO₂.

Ex vivo two photon imaging

Acute brain slices from NAc and VTA were imaged using a Leica Stellaris 8 Dive, multiphoton microscope equipped with a Coherent Chameleon Ultra II laser and a Leica 25x/1.00 NA W motCORR objective. During video acquisition, acute brain slices were continuously perfused with aCSF bubbled with 95% O₂/5% CO₂. Videos were acquired at least 60 μm below the surface of the slice and video acquisition was carried out 1-3 hours after sectioning. For analysis of microglial mitochondria only (*CX3CR1^{CreER/+}; mitoEGFP* mice) an excitation wavelength of 930 nm was used and EGFP was detected via a non-descanned detector (464 - 542nm). For analysis of microglial mitochondria and microglial cell process motility (*CX3CR1^{CreER/+}; mitoEGFP ; Ai14* mice) excitation wavelength of 930 nm was again employed, to maximize MitoEGFP signal and minimize TdTom signal bleaching. MitoEGFP and TdTom signals were detected via two non descanned detectors (detector 1: 463 – 537nm, detector 2: 558 - 668nm). Stacks of images encompassing entire microglial cells (z-step interval 1 μm) were acquired at 0.02Hz (for mitochondrial motility only) and .008Hz (mitochondrial motility + microglial cell process motility).

Focal Laser Lesion

Acute brain slices from NAc were prepared as described above and were imaged using a Leica Stellaris 8 Dive. The *CX3CR1^{CreER/+}; mitoEGFP; Ai14* mice at ages 1.5 month were used. During video acquisition, acute brain slices were continuously perfused with aCSF bubbled with 95% O₂/5% CO₂. To induce a focal laser lesion, exposure to high power illumination of 750nm for 10 seconds was applied 60 μm below the surface in space surrounded by 4-5 cells. To achieve focal lesion, the zoom setting was set to max zoom available on the Leica Stellaris. Sections were

imaged, zooming out of ROI to encompass 4-5 cells in the stack. Timepoints imaged post lesion included 10, 20, 50, 70 minutes. The excitation wavelength of 930 nm was again employed, to maximize MitoEGFP signal and minimize TdTom signal bleaching. MitoEGFP and TdTom signals were detected via two non descanned detectors (detector 1: 464 – 538nm, detector 2: 558 - 668nm).

Microglial Surveillance and Mitochondrial Properties Analysis

To analyze microglial motility, 3Dmorph, a previously published automated analysis pipeline by York et al., was adapted to analyze microglial motility (4). For microglial motility the Td Tomato channel was used. Movies corresponding to each cell underwent preprocessing through ImageJ using previously published methodology. The video underwent background subtraction, rolling ball radius 50, and applied a median filter. Then we performed z-stack projections of all movies and performed drift correction using the MultiStackReg ImageJ plugin. An ROI around the cell of interest was created based off a max projection of time for each cell and the signal outside of ROI was removed. The td tomato sparse labeling made it a clear method to isolate cells. The adapted 3D morph script was applied to the final 2D movie and collected pixels added/subtracted, total pixels changed, and microglial area change. To calculate microglial motility, the total number of pixels changed was collected and normalized to the total number of pixels in the cells (cell area), giving a quantification of motility normalized to cell size. All data was collected from the same elapsed time from all movies. To gain an understanding of the cell complexity, we used the Simple Neurite Tracer plugin in image j by Arshadi et al (5). Typically used for neuronal morphology but the sholl analysis plugin was used for microglial morphology. The same preprocessing as described previously was used, additionally for the sholl analysis the

first and last frame of the frame of the movie were used and then the output values were averaged to obtain information of cell complexity.

To analyze mitochondrial motility, the isolated MitoEGFP channel movie was used. The 3D movie was motion corrected and the ROI created based on the Td tomato signal was applied to the EGFP channel to isolate mitochondria for corresponding cell. The video was analyzed using Imaris (Bit plane) Software. The surface reconstruction module was used to create surfaces for mitochondrial network across time frames. Editing of each surface track was performed to ensure the surface was accurately visualized across time. The measurements used were Displacement Length and Volume. A sum of these measures was taken per frame and subsequently averaged across the time intervals to achieve net displacement (the displacement was also divided by the time interval to achieve change over time) or total average volume.

Tissue Dissociation and flow cytometry

2-4mo, 12-13mo, and 16-18mo WT and *CX3CR1^{CreER/+}; mitoEGFP* mice were deeply anesthetized with isoflurane and transcardially perfused with 10 ml of chilled 1M PBS. The brain was rapidly removed, cut coronally with a razor blade using anatomical landmarks and midbrain and striatum were dissected free. Samples were thoroughly minced with razor blade on a chilled glass surface and transferred to 1.7mL tubes containing 1 mL Hibernate A Low-Fluorescence (Transnetyx Tissue, Half100). Samples were then mechanically dissociated using gentle sequential trituration with fire-polished glass pipettes of decreasing diameter. Cell suspensions were pelleted via centrifugation and resuspended in 1M PBS + Debris Removal Solution (Miltenyi, 130-109-398). Debris removal was carried out according to manufacturer's instructions. Following debris removal, samples were resuspended in small volumes of 1M PBS

and incubated with primary antibodies on ice for 20min. Tetramethylrhodamine (TMRM) (Biotium, 70017) was used in some experiments to assess mitochondrial membrane potential. For these experiments, samples incubated with TMRM 50nM for 20 min at room temperature, prior to the antibodies step. Following incubation, samples were washed with 1xPBS and filtered through a 35mm filter (Falcon, 352235) prior to sorting.

Throughout the experiment, samples were kept at 4°C on ice. Samples were sorted using a FACS Aria I cell sorter (BD Biosciences). The population of cells containing microglia could be readily identified based on forward scattering (FSC) and side scattering (SSC) properties. A gating strategy based on FSC and SSC width and height was used to select single cells and reduce dead cells and doublets. Microglial cells within this population were then identified and sorted based on combinations of microglial antibodies. Antibody combinations used included anti-CD45 (1:400; Biolegend, 147703), anti-P2RY12 (1:500; Biolegend, 848005), and anti-CX3CR1 (1:800; Biolegend, 149023). Gated Microglia were FACS sorted into 1.7mL tubes containing 50µl Pico Pure RNA extraction buffer and, following the sort, samples were incubated at 42°C for 30 min, and stored in RNase-free tubes at -80°C until further processing.

RNA Extraction and qPCR

Total RNA was extracted from sorted cells using Pico Pure RNA isolation kit (Arcturus Bioscience) according to the manufacturer's instructions. Single strand cDNAs were synthesized using Superscript III first-strand cDNA synthesis kit (Invitrogen, 18080051), according to the manufacturer's protocol. Samples were subjected to PreAmplification-RT-PCR method based on previously published approaches. TaqMan PreAmp Master Mix Kit was used for cDNA preamplification (Cat# 4391128; Applied Biosystems, Life Technologies), using pooled primer mixes of 20x dilution of TaqMan Gene Expression Assay and 80 nM of custom-designed primer

sets. cDNAs were pre-amplified in an ABI 9700 Thermal Cycler using the program: 95°C hold for 10 min, 14 cycles of 90°C denaturation for 15 s, and 60°C annealing and extension for 4 min. Pre-amplification PCR products were immediately diluted five times with molecular biology grade water and stored at -20°C, or immediately processed for RT-PCR.

For qPCR analysis of gene expression, single plex qPCR assays were performed on technical duplicates using TaqMan probes for each gene target or for endogenous control gene (*Gapdh*). TaqMan Advanced Fast PCR Master Mix was used (catalog #4444963; Invitrogen). To avoid amplification of any genomic DNA contamination, primers and probes that amplify across target gene exon–exon junctions were selected when possible. qPCRs reactions were run in a QuantStudio5 using the program: 95°C hold for 20 s, followed by 40 cycles of 95°C denaturation for 3 s, and 60°C annealing and extension for 30 s. Calculations of relative expression from Ct data were conducted according to User Bulletin #23898 for ABI Prism 7900 Sequence Detection System. For each target gene, the average Ct value for the endogenous control (*Gapdh*) was subtracted from the average Ct value for the TaqMan Probe per target gene, to obtain DCt. The relative expression was then plotted as 2^{-DCt} . All TaqMan Assays and custom primers/probes that were used are detailed in Table S2.

Statistics

Data analysis was performed in OriginPro and R. Heatmaps were generated in R using the ComplexHeatmap package (Gu Z, Eils R, Schlesner M, 2016). PCAs were generated in R using the ggplot2 package (Wickham H, 2016). Linear regression analysis for LPS experiments were performed in R, all other linear regression analysis was performed in OriginPro. All graphed values are shown as mean \pm SEM. Statistical details of experiments (statistical tests used, exact value of n, what n represents) can be found in Results and the figure legends. In general,

statistical significance was assessed using one- or two-way ANOVA. Post hoc comparisons were conducted using Student's t test with Bonferroni correction for multiple comparisons. Data are sufficiently normal and variance within groups is sufficiently similar for use of parametric tests. 2 tailed paired t tests were used to compare trends across two different regions within individual mice.

2.6 Tables

Table 1: LPS Relative Gene Expression ANOVA Values

Gene	Treatment		Region	
	F Value	P Value	F Value	P Value
Tgfβ1	3.64818	0.03638	0.74976	0.39245
P2RY12	13.3998	0.0001	0.68065	0.41495
CSF1R	1.13966	0.34319	1.2454	0.27996
CX3CR1	9.42003	0.000533	0.04288	0.83715
CD68	4.11485	0.02483	5.06765	0.03076
CD45	8.86009	0.00077	7.37401	0.01021
Itgam	14.09506	0.000246	1.07928	0.31341
Tnfα	10.23143	0.000317	0.01671	0.8979
Il1β	8.41188	0.00104	0.01627	0.89925
Micu1	5.40554	0.009	5.57555	0.02391
Cat	7.43629	0.00204	0.11711	0.73424
Ppargc1α	2.99706	0.06289	0.15601	0.69526
NRF1	4.43215	0.01924	0.04594	0.83152
Mfn1	0.77771	0.46724	1.3191	0.25854
Dnm1l	4.8918	0.01338	0.31082	0.58072
Sod2	7.41671	0.00206	1.70341	0.20036
TFAM	2.1335	0.13357	1.72655	0.1974
Vdac1	12.4427	0.0001	0.06818	0.79554
GPX1	20.79043	0.0001	1.01441	0.32076
Ndufa12	15.1893	0.0001	0.31724	0.57686
ATP5d	36.99749	0.0001	2.90216	0.09733
Cox4i1	12.11631	0.0001	1.69829	0.20102
Sdha	1.8012	0.18007	0.00647	0.93633

Table 2: LPS Microglila- and Mitochondrial- Function Gene Correlation Values

Genes		CD45			I11β			Tnfα		
		Saline	LPS 4hr	LPS 24hr	Saline	LPS 4hr	LPS 24hr	Saline	LPS 4hr	LPS 24hr
ATP5d	p-value	0.2431858	0.0544093	0.4226752	0.6550352	0.2619578	0.0681475	0.4538506	0.7377642	0.0730097
	R^2 value	0.334	0.524	0.233	0.131	0.322	0.501	0.218	0.098	0.493
Cox4i1	p-value	0.1157809	0.0200081	0.0089488	0.1621148	0.3430984	0.1556162	0.1129764	0.8579773	0.2953556
	R^2 value	0.44	0.612	0.669	0.395	0.274	0.401	0.443	-0.053	0.301
Nudfa12	p-value	0.2422906	0.0023099	0.0016876	0.7186133	0.0419423	0.0504706	0.6492974	0.147684	0.0209055
	R^2 value	0.335	0.743	0.758	0.106	0.549	0.531	0.133	0.408	0.609
Sdha	p-value	0.4506172	0.0002841	0.0015804	0.6588615	0.0742326	0.8758134	0.9581158	0.301592	0.8461645
	R^2 value	0.22	0.825	0.761	0.13	0.492	0.046	0.015	0.298	0.057
NRF1	p-value	0.2594073	0.0008422	0.0039255	0.8527168	0.0089877	0.7600689	0.6917504	0.0056703	0.8328571
	R^2 value	0.323	0.787	0.717	0.055	0.668	-0.09	0.116	0.696	-0.062
TFAM	p-value	0.8741632	0.0042509	0.0063256	0.8032079	0.0059393	0.421008	0.499075	0.0145262	0.6036614
	R^2 value	0.047	0.712	0.69	-0.073	0.694	0.234	-0.197	0.636	0.152
Ppargc1α	p-value	0.5181317	0.0075507	0.1257478	0.219981	0.5074005	0.3096561	0.2397959	0.5631025	0.4755014
	R^2 value	-0.189	0.679	0.429	-0.35	0.194	0.293	-0.336	0.169	0.208
Dnm1l	p-value	0.2554548	0.0272075	1.86E-05	0.9034075	0.0019867	0.1032794	0.573546	0.000308	0.0231476
	R^2 value	0.326	0.587	0.891	-0.036	0.75	0.454	0.165	0.822	0.601
Mfn1	p-value	0.2980079	0.0002391	0.0006036	0.4648597	0.0068494	0.6674759	0.7037022	0.0399632	0.5657062
	R^2 value	0.3	0.83	0.799	-0.213	0.685	0.126	0.112	0.554	0.168
Micu1	p-value	0.6373837	0.0064953	0.2003369	0.1832933	0.099527	0.2235978	0.8299544	0.623895	0.1106621
	R^2 value	0.138	0.688	0.364	0.378	0.458	-0.347	0.063	0.144	-0.445
Vdac1	p-value	0.1323871	0.0062577	0.0263148	0.7683734	0.7220228	0.1794296	0.2024062	0.4086266	0.2362481
	R^2 value	0.422	0.691	0.59	0.087	0.105	0.381	0.363	-0.24	0.339
Sod2	p-value	0.0957826	0.6567594	0.7912816	0.3322633	0.0005101	0.0499464	0.0938519	0.0004696	0.0089933
	R^2 value	0.463	0.13	0.078	0.28	0.805	0.533	0.465	0.808	0.668
Cat	p-value	0.0177587	0.0684149	0.1540199	0.1125453	0.3154697	0.2732579	0.0745688	0.0508409	0.1469016
	R^2 value	0.621	0.5	0.402	0.443	-0.289	-0.315	0.491	-0.531	-0.409
GPX1	p-value	0.040339	0.1163189	0.0001139	0.0704377	0.1470684	0.3076912	0.2903972	0.1047061	0.1809629
	R^2 value	0.553	0.439	0.851	0.497	-0.408	0.294	0.304	-0.452	0.379

Genes		CX3CR1			P2RY12			Tgfb1		
		Saline	LPS 4hr	LPS 24hr	Saline	LPS 4hr	LPS 24hr	Saline	LPS 4hr	LPS 24hr
ATP5d	p-value	0.4105072	0.5076753	0.9340878	0.4767329	0.5131708	0.1157519	0.1829803	0.0174485	0.4313798
	R^2 value	0.239	0.193	0.024	0.207	0.191	-0.44	0.378	0.622	-0.229
Cox4i1	p-value	0.0027175	0.0597268	0.0015382	0.0456197	0.0476818	0.5645317	0.0001213	0.0113298	0.1298754
	R^2 value	0.736	0.515	0.762	0.541	0.537	0.169	0.849	0.653	0.425
Nudfa12	p-value	0.0083784	0.6233487	0.0760113	0.0064932	0.3667395	0.3712984	0.0065535	0.0021063	0.8690594
	R^2 value	0.673	0.144	0.489	0.688	0.261	-0.259	0.688	0.748	0.049
Sdha	p-value	0.0045489	0.3823356	0.0002015	0.0004891	0.2504645	0.0633899	0.005378	0.0104132	0.0023195
	R^2 value	0.709	0.253	0.835	0.807	0.329	0.508	0.699	0.659	0.743
NRF1	p-value	0.0265094	0.6163058	7.19E-05	0.0087298	0.8161447	0.0461778	0.0118585	0.021657	0.0080349
	R^2 value	0.59	-0.147	0.863	0.67	-0.068	0.54	0.65	0.606	0.675
TFAM	p-value	0.1562879	0.5305749	2.73E-06	0.018423	0.7672837	0.1035876	0.1338793	0.0137286	0.0070852
	R^2 value	0.4	-0.183	0.922	0.618	-0.087	0.453	0.421	0.64	0.683
Ppargc1α	p-value	0.3053673	0.3310936	0.0319639	0.0373679	0.1710568	0.1515281	0.3764281	0.0484005	0.0543969
	R^2 value	0.295	0.281	0.574	0.56	0.387	0.404	0.256	0.536	0.524
Dnm1l	p-value	0.1151069	0.0757443	0.0352228	0.1295656	0.1699541	0.6665682	0.1668795	0.0977203	0.6641191
	R^2 value	0.44	-0.489	0.565	0.425	-0.388	-0.126	0.391	0.46	0.127
Mfn1	p-value	0.246613	0.7796219	6.76E-05	0.2649602	0.9730763	0.093375	0.3744659	0.0252031	0.0127115
	R^2 value	0.332	-0.082	0.864	0.32	-0.01	0.466	0.257	0.594	0.645
Micu1	p-value	0.0067055	0.1522964	0.0003608	0.0020538	0.0937312	4.12E-05	0.0029979	0.0041401	9.65E-05
	R^2 value	0.686	0.404	0.817	0.749	0.465	0.875	0.731	0.714	0.855
Vdac1	p-value	0.8189758	0.0205451	0.137403	0.9751623	0.0213546	0.8524203	0.4276314	0.0445127	0.503071
	R^2 value	0.067	0.61	0.418	0.009	0.607	0.055	0.231	0.544	0.195
Sod2	p-value	0.2286088	0.0308238	0.1397987	0.410051	0.0499883	0.0297473	0.0470761	0.2166658	0.0578621
	R^2 value	0.344	-0.577	-0.415	0.239	-0.532	-0.58	0.538	0.352	-0.518
Cat	p-value	0.0264531	8.66E-07	5.16E-05	0.0843675	1.86E-06	8.73E-06	0.0028319	0.0781646	2.00E-06
	R^2 value	0.59	0.936	0.87	0.477	0.927	0.905	0.733	0.486	0.926
GPX1	p-value	0.0021052	0.0003713	0.006925	0.0462797	0.0001095	0.9955963	0.0070403	0.1577771	0.272069
	R^2 value	0.748	0.816	0.684	0.54	0.852	-0.002	0.683	0.399	0.315

Supplementary Table 2: Primers and probes used for qPCR experiments. Related to Figures 4 and S4

Gene	TaqMan Assay ID or custom probe	Forward Primer	Reverse Primer
Aldh1l1	Mm03048957_m1		
ATP5d	Mm00502864_m1		
Cat	Mm00437992_m1		
Cd45 (Ptprc)	Mm01293577_m1		
Cd68	Mm03047343_m1		
Cox4i1	Mm01250094_m1		
Csrf1	Mm01266652_m1		
Cx3cr1	Mm00438354_m1		
Dnm1l	Mm01342903_m1		
Gapdh	MGB - CTCATGACCACAGTCCA - VIC	GACAACCTTTGGCATTGTGGAA	CACAGTCTTCTGGGTGGCAGTGA
Gpx1	Mm04207457_g1		
Il1 β	Mm00434228_m1		
Itgam	Mm00434455_m1		
Mfn1	Mm00612599_m1		
Micu1	Mm00522783_m1		
Nrf1	Mm01135606_m1		
Nudfa12	Mm01240336_m1		
Olig1	Mm00497537_s1		
Olig2	Mm01210556_m1		
P2ry12	Mm00446026_m1		
Ppargc1 α	Mm01208835_m1		
Ppp1r1b	Mm00454892_m1		
Sdha	Mm01352366_m1		
Slc1a2	Mm01275814_m1		
Slc32a1	Mm00494138_m1		
Sod2	Mm01313000_m1		
Tfam	Mm01148667_m1		
Tgf β 1	Mm01178820_m1		
Tnf α	Mm00443258_m1		
Vdac1	Mm00834272_m1		

2.7 Figures

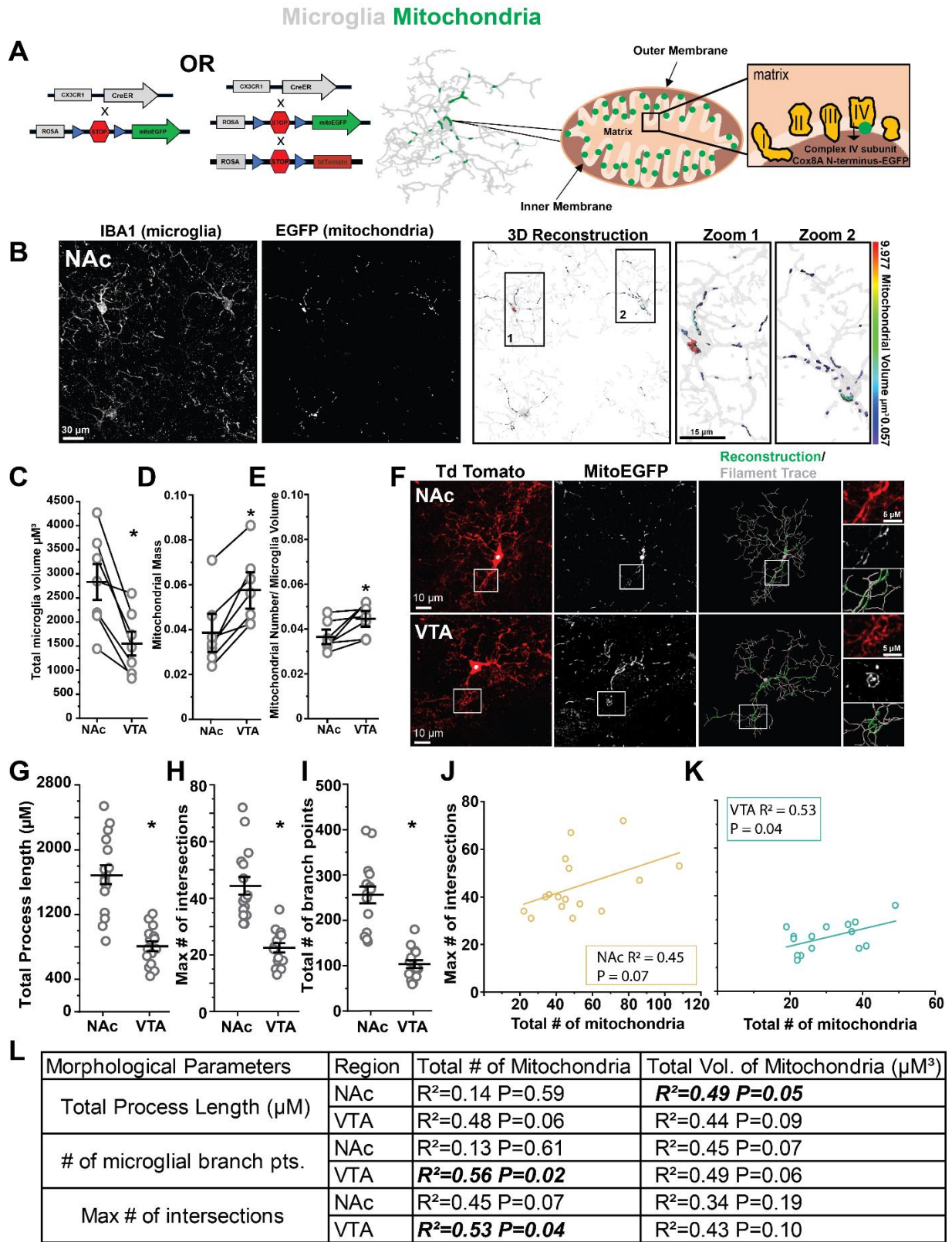


FIGURE 1: Regional specialization of microglia is accompanied by regional differences in mitochondrial mass and number. (A) Schematic showing the mouse lines crossed and the GFP specificity to *cox8a* on complex IV of mitochondria in microglia. (B) Representative high-magnification images at P60 of NAc microglia (*Iba1*) and mitochondria (EGFP); 3D reconstructions of mitochondria (colored according to volume) and zoomed in panels (1 and 2) on bottom left depicting colocalized surfaces. (C) Quantification of microglia volume across NAc and VTA paired t-test $p > 0.014$ microglial volume. (D-E) Quantification of mitochondrial parameters at P60 across regions (NAc, VTA). Within a given age, data points that come from the same mouse are identified by the connecting line. C-D. NAc vs VTA P60 $p = 0.0012$ paired t-test for mitochondrial mass and $p = 0.0267$ for mitochondrial number normalized to microglial volume. (F) Example of microglial cells in NAc and VTA expressing cytosolic TdTom and mitochondrial targeted EGFP (*CX3CR1-CreER;Ai14;mitoEGFP* mice) that was reconstructed using filament-tracing in Imaris. (G-I) Plots of various morphological parameters across individual microglia from NAc and VTA. E-G. NAc vs VTA P60 Two-sample t-test $p < 0.0001$ for total process length, Two-sample t-test $p < 0.0001$ for max number of intersections, Two-sample t-test $p < 0.0001$ for number of branch points. (J-K) Linear regression plots for showing relationships between mitochondrial number and individual microglial morphological parameters such as max # of intersections for both regions (NAc cells $N = 16$ and VTA cells $N = 15$). J,K. NAc $R^2 = 0.45$ $p = 0.07$ VTA $R^2 = 0.53$ $p = 0.04$ for max inters. vs total number of mitochondria. (L) Table showing all correlations.

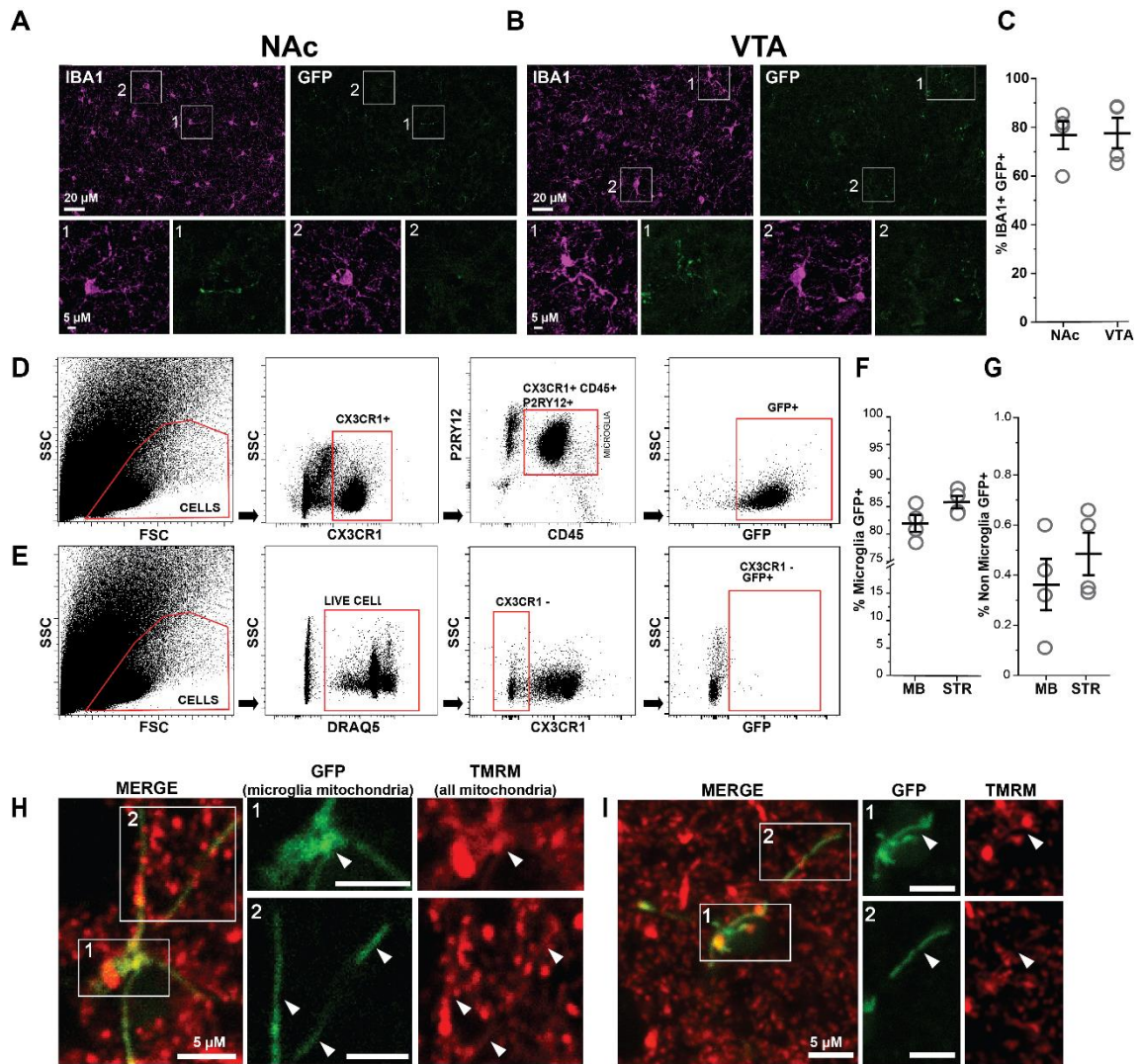


FIGURE S1: Validation of *CX3CR1-CreER; flox-stop mitoEGFP* (*MG-MitoEGFP*) mice. (A) 20x confocal images of native EGFP signal and Iba1 (magenta) staining in *CX3CR1-CreER; flox-stop mitoEGFP* (*MG-MitoEGFP*) mice showing that all EGFP labeled mitochondria are within Iba1+. Box 1 and 2 examples of IBA1+ GFP+ positive cells and IBA1+GFP- cells. (B) Showing native EGFP signal in VTA. (C) Quantification of percentage of microglia showing recombination and expression of EGFP in mitochondria in nucleus accumbens (NAc) and ventral tegmental area (VTA). (D) FACS-based analysis in midbrain (MB) and striatum (STR) of percentage of microglia showing recombination. Sequential gating strategy shown, CX3CR1+P2RY12+CD45+ putative microglia isolated and GFP+ gate shown. (E) Gating strategy for live cells (DRAQ5+), non-microglia (CX3CR1-) and GFP+ shown. (F-G) Percentage of microglia (CX3CR1+P2RY12+CD45+) and non-microglial cells (CX3CR1- Draq5+) showing expression of GFP in MB and STR. (H-I) Live imaging of acute brain sections from *MG-MitoEGFP* mice incubated with mitochondrial membrane potential indicator dye TMRM. Examples 1 and 2 show co-labeling of GFP and TMRM. Zoom 1 shows cell body colocalization and zoom 2 shows colocalization in the processes.

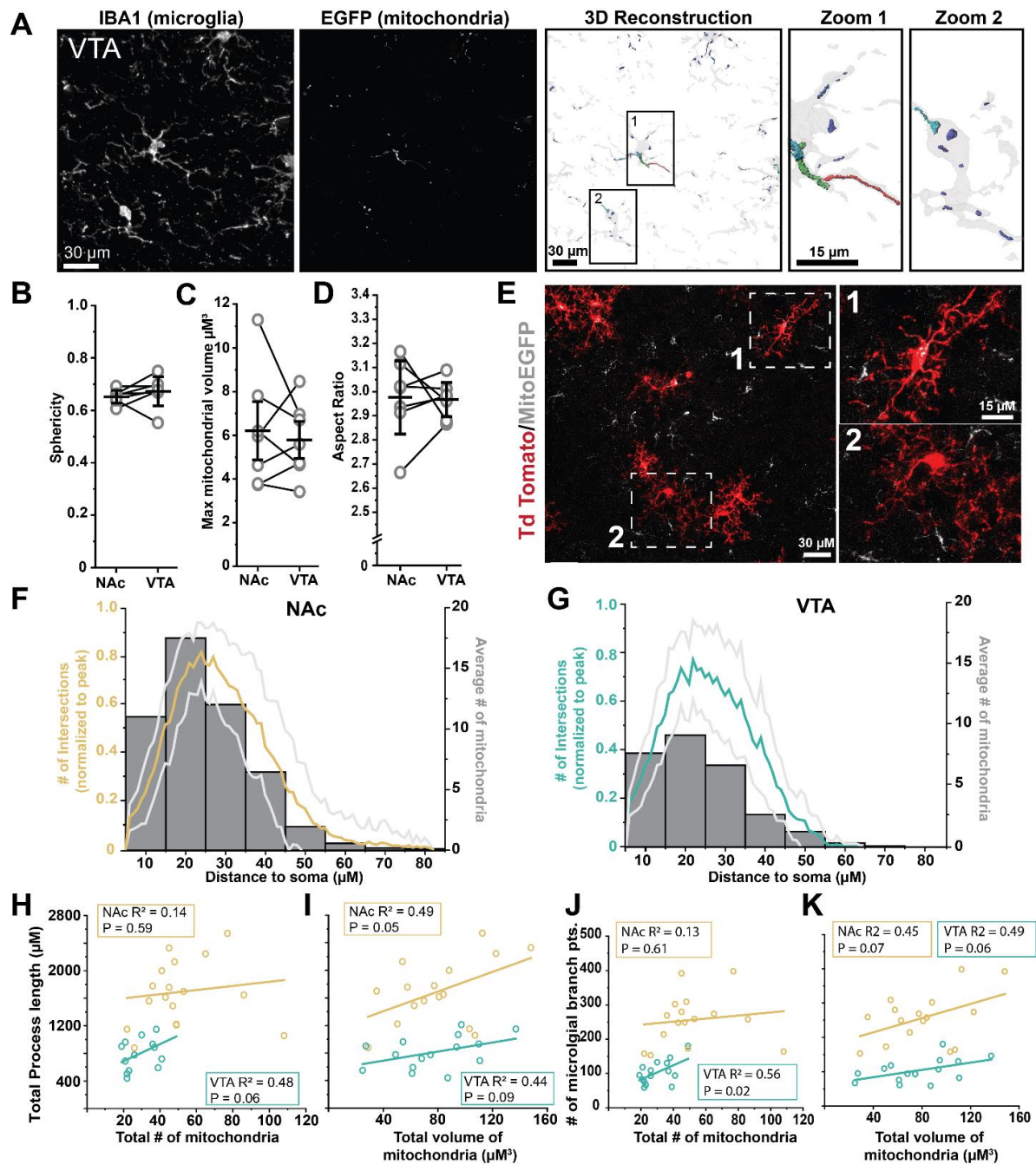


FIGURE S2: Mitochondrial morphology network changes are heterogeneous in microglia (continuation Fig.1) (A) Representative high-magnification images at P60 of NAc microglia (Iba1) and mitochondria (EGFP); 3D reconstructions of mitochondria (colored according to volume) and zoomed in panels (1 and 2) on bottom left depicting colocalized surfaces. (B-D) Quantification of mitochondrial parameters at P60 across regions (NAc, VTA). Within a given age, data points that come from the same mouse are identified by the connecting line. B-D. NAc vs VTA P60 $p=0.346$, n.s paired t-test for sphericity and $p=0.640$, n.s for max mitochondria volume normalized to microglial volume, paired t-test $p=0.894$ aspect ratio = long axis divided by short axis. (E) Representative 20x image of TdTomato and mitoEGFP sparse labeling. (F-G) Sholl analysis of individual reconstructed microglia; normalized to peak and averaged across regions (NAc N=16 and VTA N=15). (H-K) Linear regression plots for showing relationships between microglial process length and mitochondrial morphological parameters for both regions (NAc N=16 and VTA N=15). H-I. linear regression NAc $R^2 = 0.49$ $p=0.05$ for total process length vs total volume of mitochondria, NAc $R^2 = 0.14$ $p=0.59$ VTA $R^2 = 0.48$ $p=0.06$ for total process length vs total number of mitochondria. J-K. NAc

R2 = 0.13 p=0.61 VTA=0.56 p=0.02 for number of mg branch pts vs total number of mitochondria, K. NAc R2 = 0.45 p=0.07 VTA R2 = 0.49 p=0.06 for number of mg branch pts vs total volume of mitochondria.

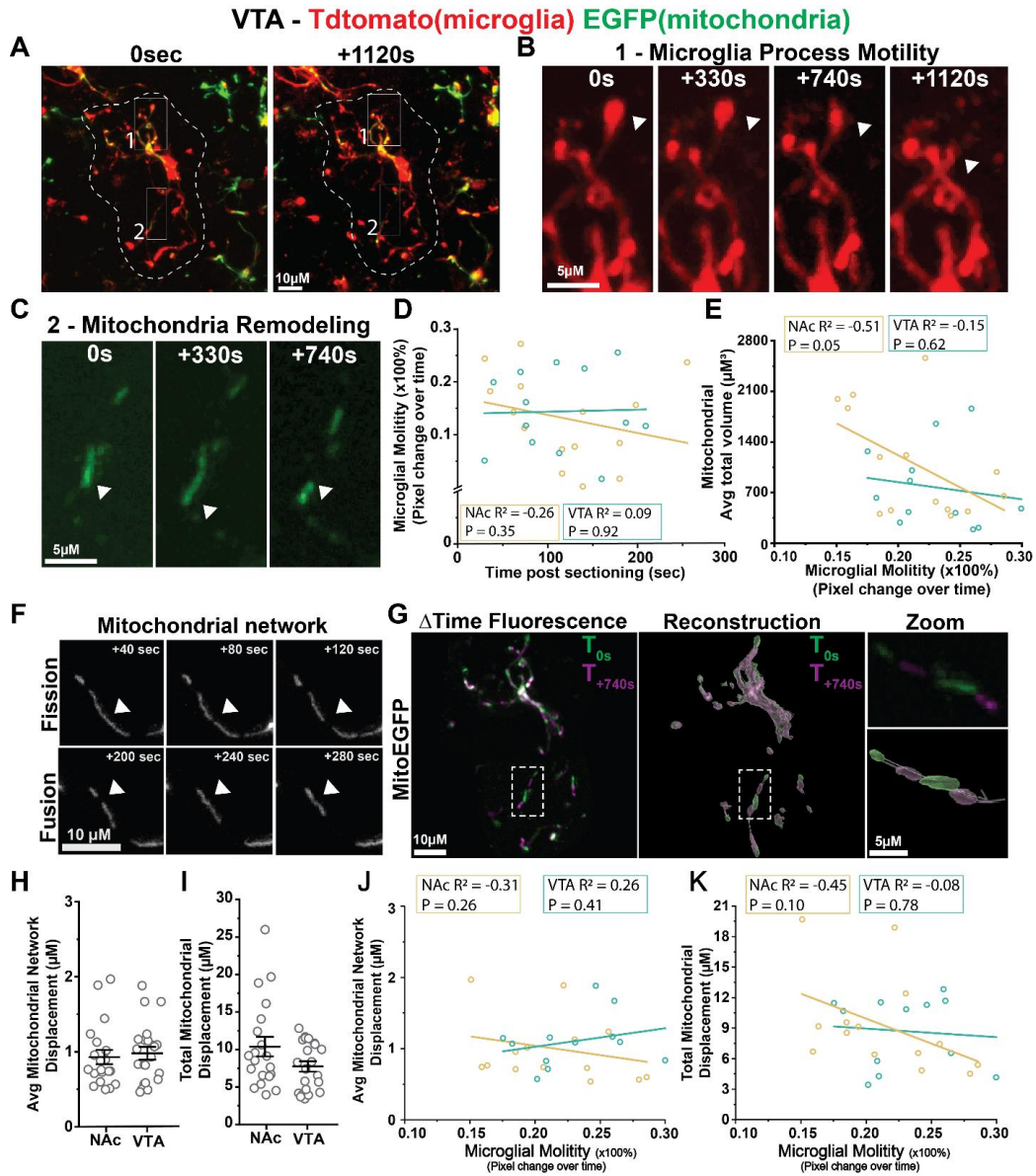


FIGURE 2: Mitochondrial number and mitochondrial motility are not aligned with microglial tissue surveillance. (A) Representative images of first frame and last frame of acute brain slice of VTA microglia (Td Tomato) and mitochondria (EGFP) at 1.5-2mos old mice. (B) Example of microglia process retraction indicated by white arrow at different timepoints. (C) Example of mitochondria motility, indicated by position change (white arrow). (D) Linear regression plots of microglial motility and time post sectioning. *D.* NAc R2 = -0.26 p=0.35 VTA R2 = -0.09 p=0.92. (E) Linear regression plots for showing relationships between mitochondrial avg. total volume and microglial motility. *E.* NAc R2 = -0.51 p=0.05, VTA R2 = -0.15 p=0.62. (F) Schematic representing mitochondrial ability to undergo fission and fusion. (G) 3D reconstructions of mitochondria (colored by time frame) and zoomed in panels (1 and 2) on right depicting fluorescence and respective surface reconstruction. (H-I) Quantification of microglial avg mitochondrial displacement and total displacement in both NAc and VTA. *G.* Two-sample t-test p=0.684 for microglial average mitochondrial displacement. *H.* Two-sample t-test p=0.07 for microglial mitochondrial total displacement. (J-K) Linear regression plots for showing relationships between average mitochondrial network displacement and total mitochondrial displacement versus microglial motility for both regions (NAc N=14 and VTA N=12). *J.* NAc R2 = -0.31 p=0.26, VTA R2 = 0.26 p=0.41. *K.* NAc R2 = -0.45 p=0.10, VTA R2 = -0.08 p=0.78.

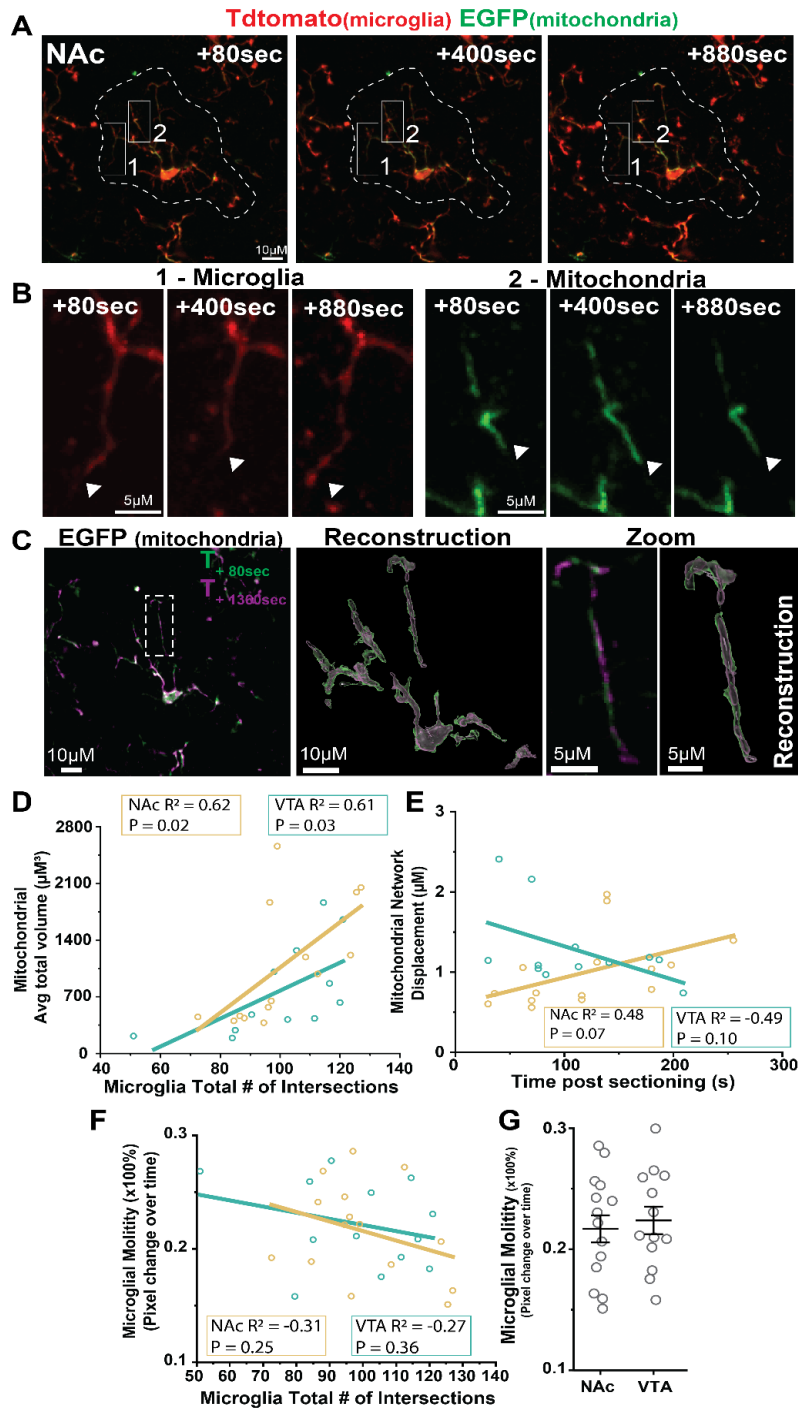


FIGURE S3: Microglial mitochondria present dynamic motility and network remodeling. (related to Fig.2). (A) Representative images of first frame and last frame of acute brain slice of NAc microglia (Td Tomato) and mitochondria (EGFP) at 1.5-2mos old mice. (B) Example of microglia process retraction/extension and mitochondrial displacement indicated by white arrow at different timepoints. (C) 3D reconstructions of mitochondria (colored by time frame) and zoomed in panels on right depicting fluorescence and respective surface reconstruction. (D) Linear regression plots for showing relationships between mitochondrial avg. total volume and microglial number of inters. NAc $R^2 = 0.62$ $p=0.02$, VTA $R^2 = 0.61$ $p=0.03$. (E) Linear regression plots of mitochondrial network displacement and time post sectioning. E. NAc $R^2 = -0.48$ $p=0.07$ VTA $R^2 = -0.49$ $p=0.10$. (F) Linear regression analysis of microglial motility and microglial total number of intersections (ImageJ sholl analysis). E. NAc R^2

= -0.31 p=0.25 VTA R2 = -0.27 p=0.36 for microglial motility vs microglial total number of inters. (G) Quantification of microglial motility in both NAc and VTA.

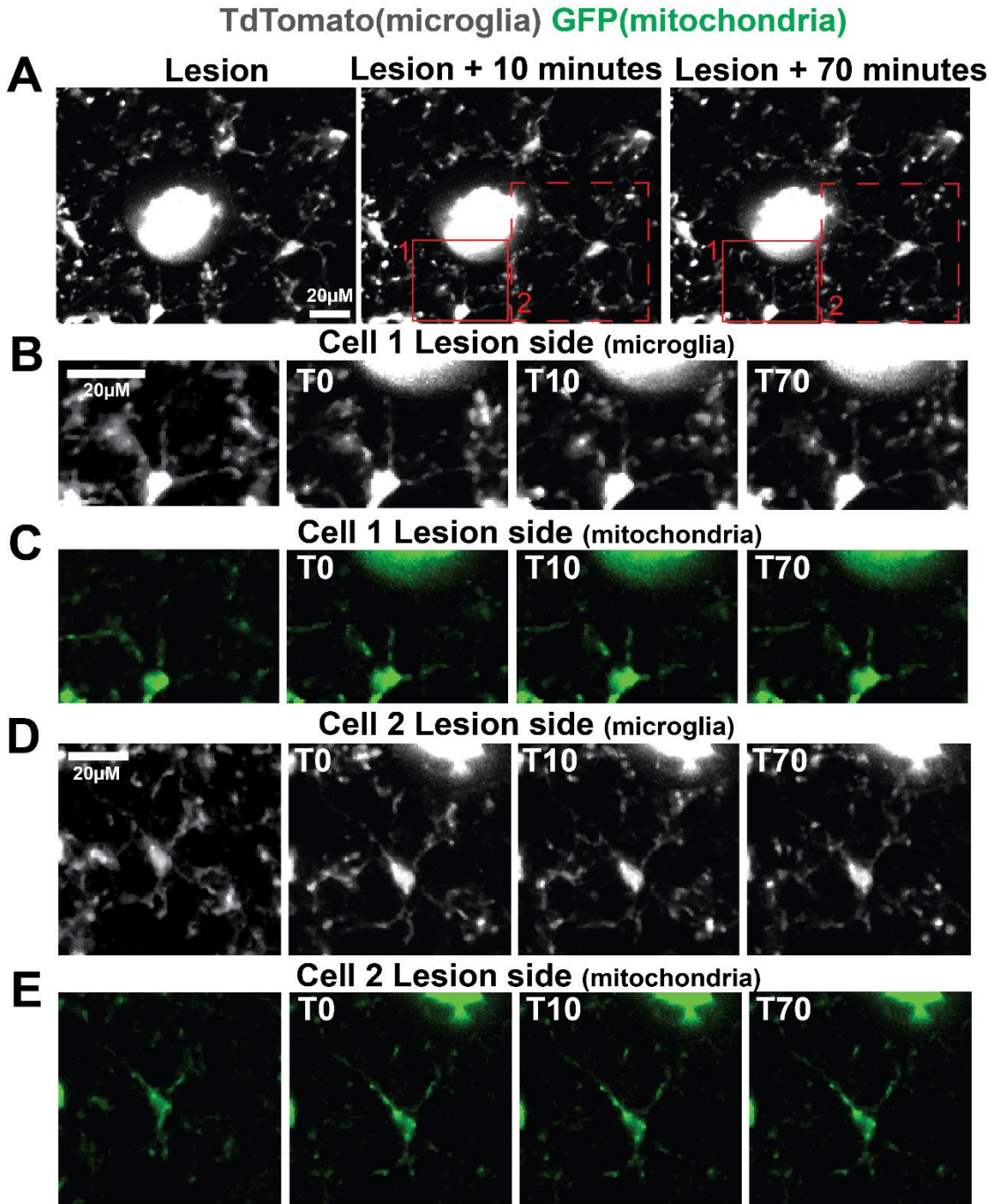


FIGURE 3: Mitochondrial distribution is stable during early phases of microglial response to focal injury. (A) Frames showing cells responding to laser lesion at 10 and 70 min post focal laser lesion. (B-E) Zoom represents microglia (td tomato) and its corresponding mitochondria (EGFP) responding to lesion.

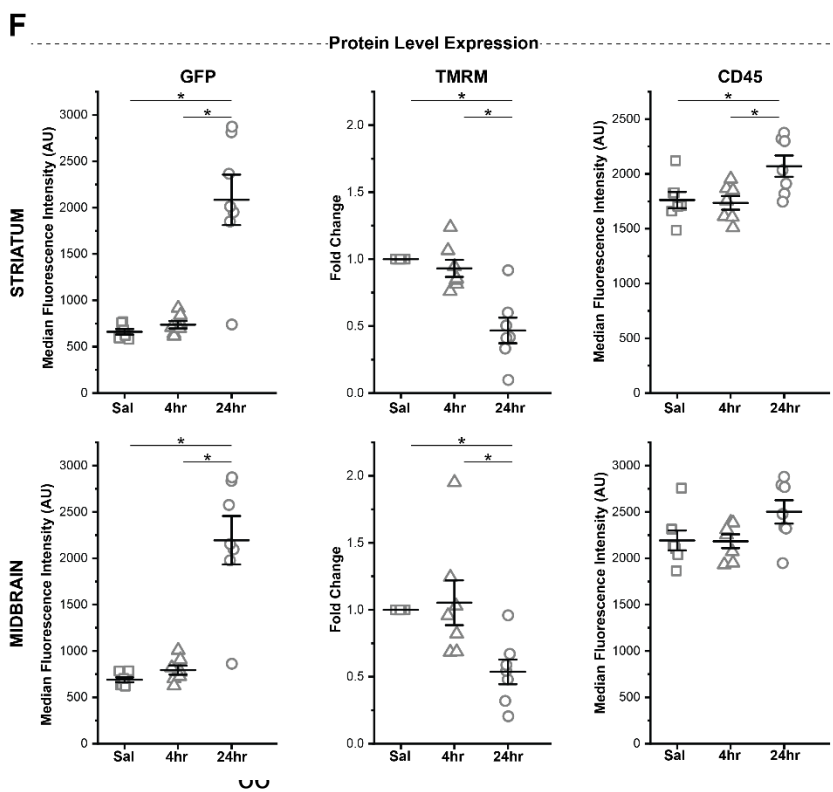
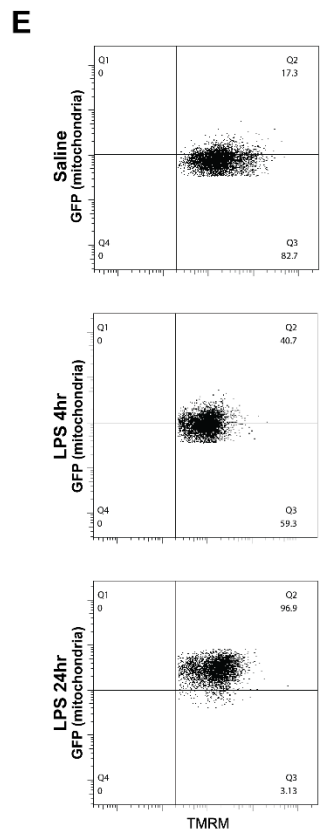
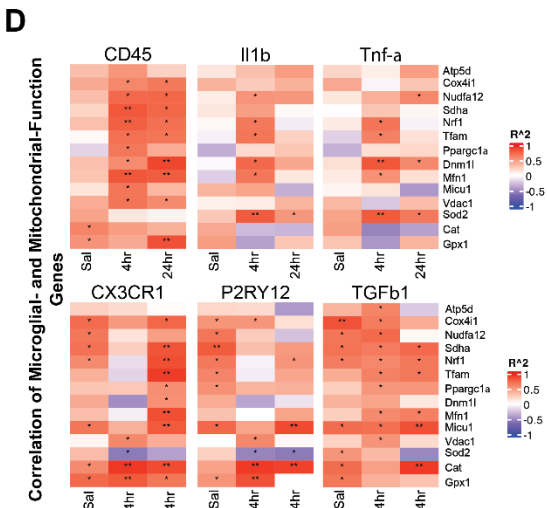
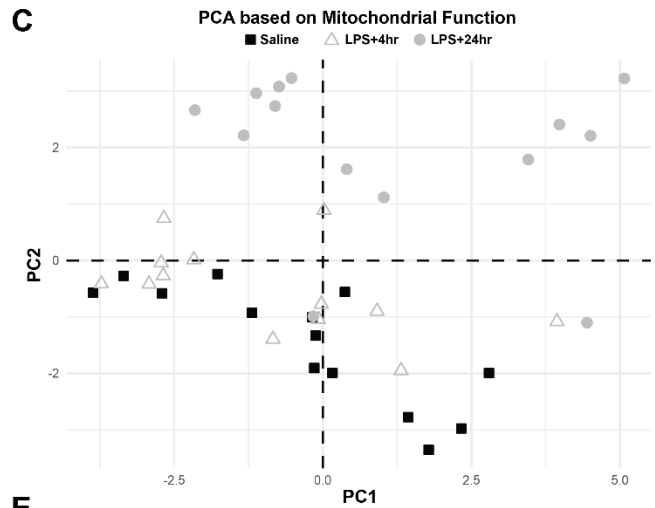
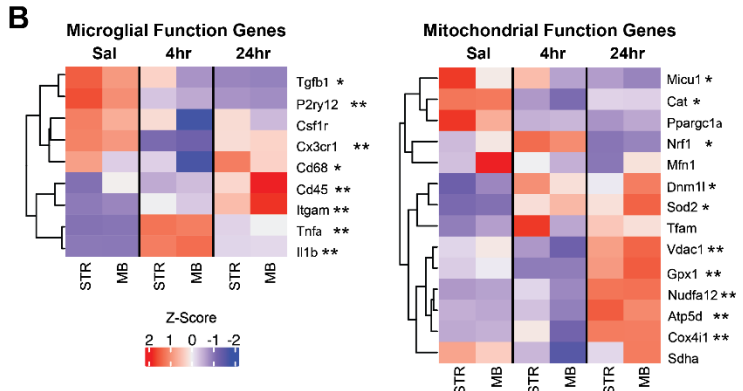
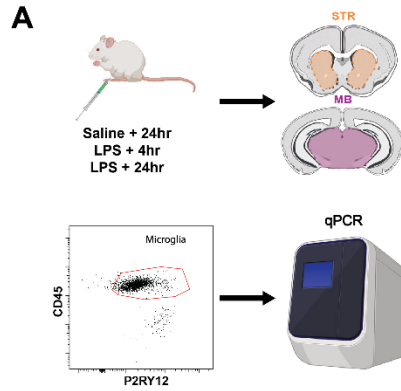


Figure 4: Response to inflammatory challenge (LPS) elicits mitochondrial changes in microglia. (A) 3-4mo *MG-MitoEGFP* mice were injected with saline 24hr prior to or LPS 4hr or 24hr prior FACS isolation of STR/MB microglia for downstream qPCR analysis. (B) Quantification of key microglial function and mitochondrial function genes in FACS isolated microglia show that shifts in key microglial genes in response to LPS treatment are accompanied by changes in microglial mitochondrial genes. Z-scores represent average gene expression across treatment groups and brain regions. See Table 1 for F- and P-values. (N = 7 Saline STR, N = 7 Saline MB, N = 7 LPS 4hr STR, N = 6 LPS 4hr MB, N = 7 LPS 24hr STR, N = 7 LPS MB). (C) Principal Component Analysis of samples based only on mitochondrial function genes along PC1 and PC2. (D) Heat maps depicting the correlation of microglial function genes associated with microglial inflammatory response (*Cd45*, *Il1b*, *Tnf-a*) and microglial homeostasis (*Cx3cr1*, *P2ry12*, *Tgfb1*) with mitochondrial function genes as analyzed by linear regression. See Table 2 for R²- and P-values. (E) Representative dot plots of FACS analyzed Saline, LPS 4hr, and LPS 24hr microglia comparing TMRM fluorescence intensity to GFP fluorescence intensity. (F) Quantification of Median Fluorescent Intensity of GFP, TMRM (individual cell TMRM signal was normalized to the same cell's GFP signal), and CD45 signal in the STR and MB of Saline (N = 7), LPS 4hr (N = 7), and LPS 24hr (N = 7) samples. One-way ANOVA: GFP STR, $F_{(2,18)} = 25.06735$, $p < 0.0001$; GFP MB, $F_{(2,18)} = 29,85264$, $p < 0.0001$; TMRM STR, $F_{(2,18)} = 19.2316$, $p < 0.0001$; TMRM MB, $F_{(2,18)} = 6.61021$, $p = 0.00704$; CD45 STR, $F_{(2,18)} = 5.52274$, $p = 0.01348$; CD45 MB, $F_{(2,18)} = 2.99003$, $p = 0.07565$.

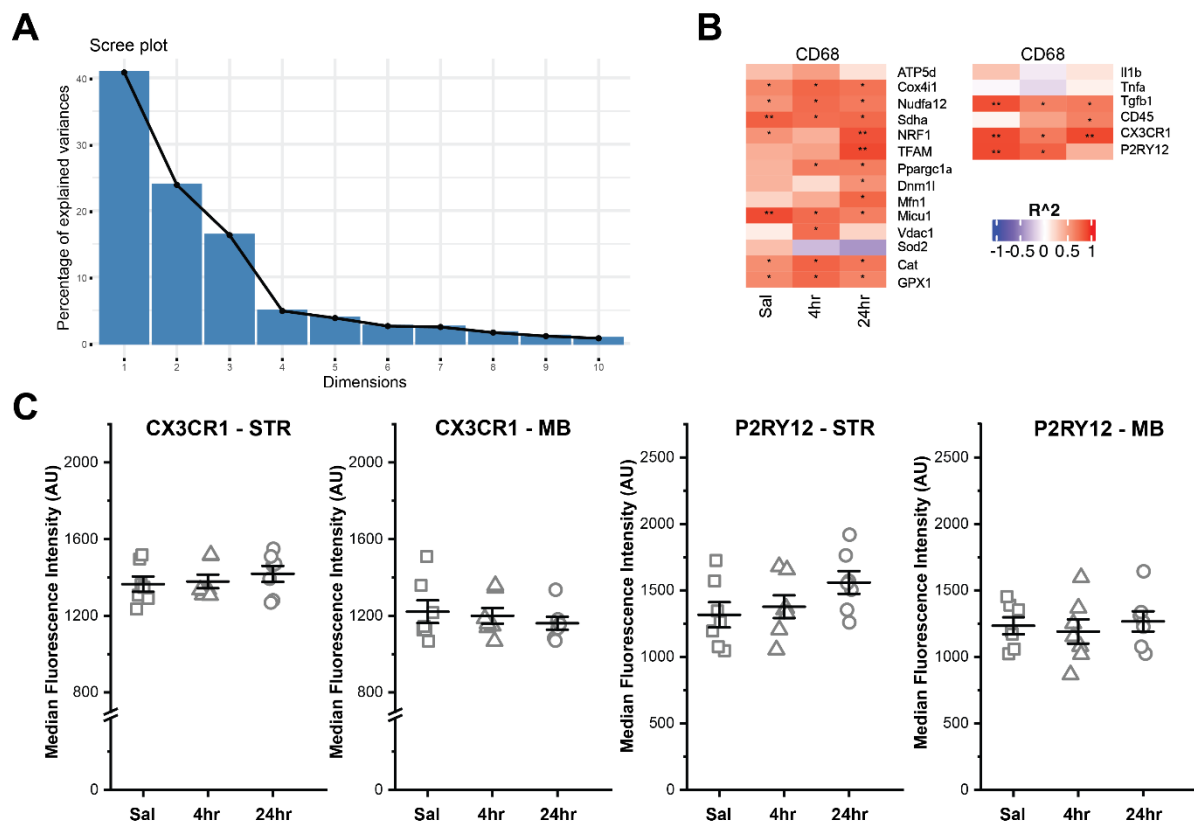


Figure S4: Microglial and mitochondrial responses to inflammatory challenge (LPS), related to Fig 4. (A) Scree plot describing the percentage of explained variance for the Principal Component Analysis of saline, LPS 4hr, and LPS 24hr samples based only on mitochondrial function genes. (B) Heat maps depicting the correlation of Cd68 with microglial function genes and mitochondrial function genes as analyzed by linear regression. See Supp Table 1 for R²- and P-values. (C) Quantification of Median Fluorescent Intensity of CX3CR1 and P2RY12 signal in the STR and MB of Saline (N =7), LPS 4hr (N=7), and LPS 24hr (N = 7) samples. Samples are not significantly different by treatment but were significantly different by region. Two-way ANOVA: CX3CR1 Treatment, $F(2,36) = 0.00442$, $p = 0.99559$, Region, $F(1,36) = 30.80804$, $p < 0.0001$; P2RY12 Treatment, $F(2,36) = 1.71502$, $p = 0.19514$, Region $F(1,36) = 7.52567$, $p = 0.00942$.

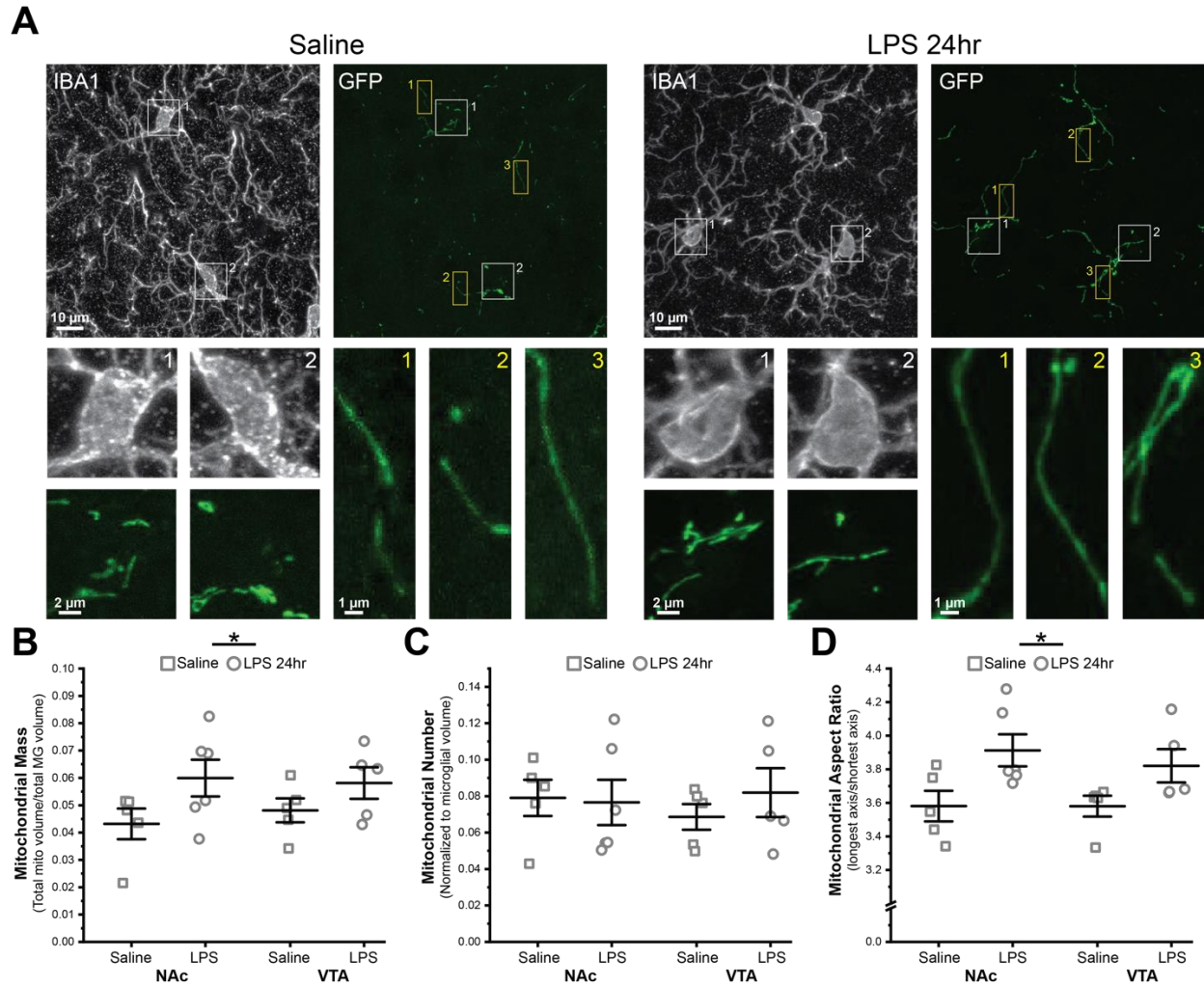


Figure 5: Inflammatory challenge (LPS) elicits changes in microglial mitochondrial morphology and increases mitochondrial mass. (A) Representative images of NAc microglia (IBA1) and microglial mitochondria (GFP) of 3-4mo *MG-MitoEGFP* mice injected with saline (left) or LPS 24hr (right) prior to euthanasia. Zoomed panels depict example somatic mitochondria (white frame) and cell process mitochondria (yellow frame). (B-D) Quantification of microglial mitochondrial changes in response to LPS. (B) Mitochondrial mass: Two-way ANOVA: main effect of treatment, $F_{(1,17)} = 5.19787$, p-value = 0.03579; main effect of region, $F_{(1,17)} = 0.0713$, p-value = 0.079266 (C) Mitochondrial number: Two-way ANOVA: main effect of treatment, $F_{(1,17)} = .23167$, p-value = 0.63642; main effect of region, $F_{(1,17)} = 0.05079$, p-value = 0.82438 (D) Mitochondrial Aspect Ratio: Two-way ANOVA: main effect of treatment, $F_{(1,17)} = 10.19319$, p-value = 0.00533; main effect of region, $F_{(1,17)} = 0.26571$, p-value = 0.61286.

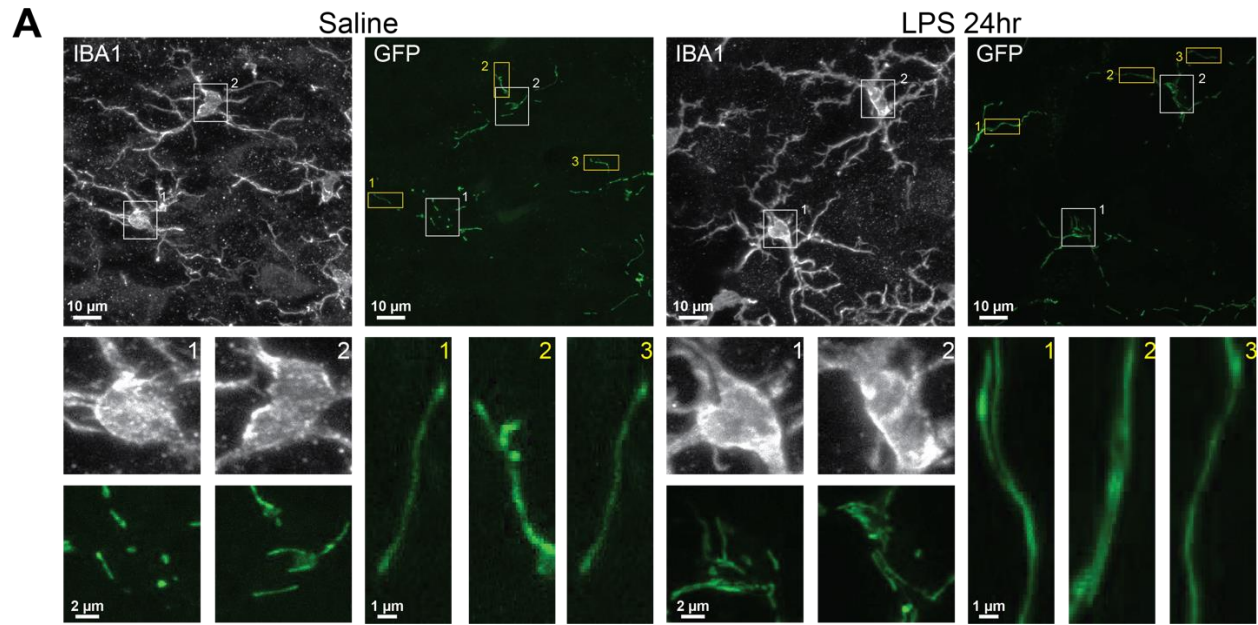


Figure S5: VTA microglial mitochondrial response to inflammatory challenge (LPS, related to Fig 5). (A) Representative images of VTA microglia (IBA1) and microglial mitochondria (GFP) of 3-4mo *MG-MitoEGFP* mice injected with saline (left) or LPS 24hr (right) prior to euthanasia. Zoomed panels depict example somatic mitochondria (white frame) and cell process mitochondria (yellow frame).

References Cited

1. Li Q, Barres BA. Microglia and macrophages in brain homeostasis and disease. *Nat Rev Immunol*. 2018 Apr;18(4):225–42.
2. Sierra A, Paolicelli RC, Kettenmann H. Cien Años de Microglía: Milestones in a Century of Microglial Research. *Trends Neurosci*. 2019 Nov;42(11):778–92.
3. Matsudaira T, Prinz M. Life and death of microglia: Mechanisms governing microglial states and fates. *Immunol Lett*. 2022 May;245:51–60.
4. Silvin A, Qian J, Ginhoux F. Brain macrophage development, diversity and dysregulation in health and disease. *Cell Mol Immunol*. 2023 Nov;20(11):1277–89.
5. Thion MS, Garel S. On place and time: microglia in embryonic and perinatal brain development. *Curr Opin Neurobiol*. 2017 Dec;47:121–30.
6. Frost JL, Schafer DP. Microglia: Architects of the Developing Nervous System. *Trends Cell Biol*. 2016 Aug;26(8):587–97.
7. Hammond TR, Dufort C, Dissing-Olesen L, Giera S, Young A, Wysoker A, et al. Single-Cell RNA Sequencing of Microglia throughout the Mouse Lifespan and in the Injured Brain Reveals Complex Cell-State Changes. *Immunity*. 2019 Jan 15;50(1):253-271.e6.
8. Bennett ML, Bennett FC, Liddel SA, Ajami B, Zamanian JL, Fernhoff NB, et al. New tools for studying microglia in the mouse and human CNS. *Proc Natl Acad Sci U S A*. 2016 Mar 22;113(12):E1738–46.
9. Matcovitch-Natan O, Winter DR, Giladi A, Vargas Aguilar S, Spinrad A, Sarrazin S, et al. Microglia development follows a stepwise program to regulate brain homeostasis. *Science*. 2016 Aug 19;353(6301):aad8670.
10. Grabert K, Michoel T, Karavolos MH, Clohisey S, Baillie JK, Stevens MP, et al. Microglial brain region-dependent diversity and selective regional sensitivities to aging. *Nat Neurosci*. 2016 Mar;19(3):504–16.
11. Stowell RD, Wong EL, Batchelor HN, Mendes MS, Lamantia CE, Whitelaw BS, et al. Cerebellar microglia are dynamically unique and survey Purkinje neurons in vivo. *Developmental Neurobiology*. 2018;78(6):627–44.
12. Paolicelli RC, Sierra A, Stevens B, Tremblay ME, Aguzzi A, Ajami B, et al. Microglia states and nomenclature: A field at its crossroads. *Neuron*. 2022 Nov 2;110(21):3458–83.
13. Böttcher C, Schlickeiser S, Sneeboer MAM, Kunkel D, Knop A, Paza E, et al. Human microglia regional heterogeneity and phenotypes determined by multiplexed single-cell mass cytometry. *Nat Neurosci*. 2019 Jan;22(1):78–90.

14. De Biase LM, Bonci A. Region-Specific Phenotypes of Microglia: The Role of Local Regulatory Cues. *Neuroscientist*. 2019 Aug 1;25(4):314–33.
15. Ayata P, Badimon A, Strasburger HJ, Duff MK, Montgomery SE, Loh YHE, et al. Epigenetic regulation of brain region-specific microglia clearance activity. *Nat Neurosci*. 2018 Aug;21(8):1049–60.
16. Hanamsagar R, Bilbo SD. Environment matters: microglia function and dysfunction in a changing world. *Curr Opin Neurobiol*. 2017 Dec;47:146–55.
17. Salter MW, Stevens B. Microglia emerge as central players in brain disease. *Nat Med*. 2017 Sep 8;23(9):1018–27.
18. Wolf SA, Boddeke HWGM, Kettenmann H. Microglia in Physiology and Disease. *Annu Rev Physiol*. 2017 Feb 10;79:619–43.
19. Gleichman AJ, Carmichael ST. Glia in neurodegeneration: Drivers of disease or along for the ride? *Neurobiol Dis*. 2020 Aug;142:104957.
20. Ceasrine AM, Bilbo SD. Dietary fat: a potent microglial influencer. *Trends Endocrinol Metab*. 2022 Mar;33(3):196–205.
21. Sequeira MK, Bolton JL. Stressed Microglia: Neuroendocrine-Neuroimmune Interactions in the Stress Response. *Endocrinology*. 2023 Jun 6;164(7):bqad088.
22. Wangler LM, Godbout JP. Microglia moonlighting after traumatic brain injury: aging and interferons influence chronic microglia reactivity. *Trends Neurosci*. 2023 Nov;46(11):926–40.
23. Hickman SE, Kingery ND, Ohsumi TK, Borowsky ML, Wang L chong, Means TK, et al. The microglial sensome revealed by direct RNA sequencing. *Nat Neurosci*. 2013 Dec;16(12):1896–905.
24. Madry C, Attwell D. Receptors, ion channels, and signaling mechanisms underlying microglial dynamics. *J Biol Chem*. 2015 May 15;290(20):12443–50.
25. Zengeler KE, Lukens JR. Microglia pack a toolbox for life. *Trends Immunol*. 2024 May;45(5):338–45.
26. Davalos D, Grutzendler J, Yang G, Kim JV, Zuo Y, Jung S, et al. ATP mediates rapid microglial response to local brain injury in vivo. *Nat Neurosci*. 2005 Jun;8(6):752–8.
27. Nimmerjahn A, Kirchhoff F, Helmchen F. Resting Microglial Cells Are Highly Dynamic Surveillants of Brain Parenchyma in Vivo. *Science*. 2005 May 27;308(5726):1314–8.
28. Eyo UB, Wu LJ. Microglia: Lifelong patrolling immune cells of the brain. *Prog Neurobiol*. 2019 Aug;179:101614.

29. Shen K, Pender CL, Bar-Ziv R, Zhang H, Wickham K, Willey E, et al. Mitochondria as Cellular and Organismal Signaling Hubs. *Annual Review of Cell and Developmental Biology*. 2022 Oct 6;38(Volume 38, 2022):179–218.
30. Collier JJ, Oláhová M, McWilliams TG, Taylor RW. Mitochondrial signalling and homeostasis: from cell biology to neurological disease. *Trends Neurosci*. 2023 Feb;46(2):137–52.
31. Picard M, Shirihai OS. Mitochondrial signal transduction. *Cell Metab*. 2022 Nov 1;34(11):1620–53.
32. Tan JX, Finkel T. Mitochondria as intracellular signaling platforms in health and disease. *J Cell Biol*. 2020 May 4;219(5):e202002179.
33. Kolliniati O, Ieronymaki E, Vergadi E, Tsatsanis C. Metabolic Regulation of Macrophage Activation. *J Innate Immun*. 2021 Jul 9;14(1):51–68.
34. Mills EL, O’Neill LA. Reprogramming mitochondrial metabolism in macrophages as an anti-inflammatory signal. *Eur J Immunol*. 2016 Jan;46(1):13–21.
35. Mills EL, Kelly B, Logan A, Costa ASH, Varma M, Bryant CE, et al. Succinate Dehydrogenase Supports Metabolic Repurposing of Mitochondria to Drive Inflammatory Macrophages. *Cell*. 2016 Oct 6;167(2):457-470.e13.
36. Diskin C, Pålsson-McDermott EM. Metabolic Modulation in Macrophage Effector Function. *Front Immunol*. 2018;9:270.
37. Ramond E, Jamet A, Coureuil M, Charbit A. Pivotal Role of Mitochondria in Macrophage Response to Bacterial Pathogens. *Front Immunol*. 2019;10:2461.
38. Wang Y, Li N, Zhang X, Horng T. Mitochondrial metabolism regulates macrophage biology. *J Biol Chem*. 2021 Jul;297(1):100904.
39. Afroz SF, Raven KD, Lawrence GMEP, Kapetanovic R, Schroder K, Sweet MJ. Mitochondrial dynamics in macrophages: divide to conquer or unite to survive? *Biochem Soc Trans*. 2023 Feb 27;51(1):41–56.
40. De Biase LM, Schuebel KE, Fusfeld ZH, Jair K, Hawes IA, Cimbri R, et al. Local Cues Establish and Maintain Region-Specific Phenotypes of Basal Ganglia Microglia. *Neuron*. 2017 Jul 19;95(2):341-356.e6.
41. Maes ME, Colombo G, Schoot Uiterkamp FE, Sternberg F, Venturino A, Pohl EE, et al. Mitochondrial network adaptations of microglia reveal sex-specific stress response after injury and UCP2 knockout. *iScience*. 2023 Oct 20;26(10):107780.
42. Bordt EA, Moya HA, Jo YC, Ravichandran CT, Bankowski IM, Ceasrine AM, et al. Gonadal hormones impart male-biased behavioral vulnerabilities to immune activation via microglial mitochondrial function. *Brain Behav Immun*. 2024 Jan;115:680–95.

43. Baik SH, Kang S, Lee W, Choi H, Chung S, Kim JI, et al. A Breakdown in Metabolic Reprogramming Causes Microglia Dysfunction in Alzheimer's Disease. *Cell Metabolism*. 2019 Sep 3;30(3):493-507.e6.
44. March-Diaz R, Lara-Ureña N, Romero-Molina C, Heras-Garvin A, Ortega-de San Luis C, Alvarez-Vergara MI, et al. Hypoxia compromises the mitochondrial metabolism of Alzheimer's disease microglia via HIF1. *Nat Aging*. 2021 Apr;1(4):385–99.
45. Fecher C, Trovò L, Müller SA, Snaidero N, Wettmarshausen J, Heink S, et al. Cell-type-specific profiling of brain mitochondria reveals functional and molecular diversity. *Nat Neurosci*. 2019 Oct;22(10):1731–42.
46. Agarwal A, Wu PH, Hughes EG, Fukaya M, Tischfield MA, Langseth AJ, et al. Transient Opening of the Mitochondrial Permeability Transition Pore Induces Microdomain Calcium Transients in Astrocyte Processes. *Neuron*. 2017 Feb 8;93(3):587-605.e7.
47. Yona S, Kim KW, Wolf Y, Mildner A, Varol D, Breker M, et al. Fate Mapping Reveals Origins and Dynamics of Monocytes and Tissue Macrophages under Homeostasis. *Immunity*. 2013 Jan 24;38(1):79–91.
48. Faust TE, Feinberg PA, O'Connor C, Kawaguchi R, Chan A, Strasburger H, et al. A comparative analysis of microglial inducible Cre lines. *Cell Rep*. 2023 Sep 26;42(9):113031.
49. Bedolla AM, McKinsey GL, Ware K, Santander N, Arnold TD, Luo Y. A comparative evaluation of the strengths and potential caveats of the microglial inducible CreER mouse models. *Cell Rep*. 2024 Jan 23;43(1):113660.
50. Madisen L, Zwingman TA, Sunkin SM, Oh SW, Zariwala HA, Gu H, et al. A robust and high-throughput Cre reporting and characterization system for the whole mouse brain. *Nat Neurosci*. 2010 Jan;13(1):133–40.
51. Dietrich MO, Liu ZW, Horvath TL. Mitochondrial Dynamics Controlled by Mitofusins Regulate Agrp Neuronal Activity and Diet-Induced Obesity. *Cell*. 2013 Sep 26;155(1):188–99.
52. Boldogh IR, Pon LA. Mitochondria on the move. *Trends Cell Biol*. 2007 Oct;17(10):502–10.
53. Lou N, Takano T, Pei Y, Xavier AL, Goldman SA, Nedergaard M. Purinergic receptor P2RY12-dependent microglial closure of the injured blood-brain barrier. *Proc Natl Acad Sci U S A*. 2016 Jan 26;113(4):1074–9.
54. Rock RB, Gekker G, Hu S, Sheng WS, Cheeran M, Lokensgard JR, et al. Role of Microglia in Central Nervous System Infections. *Clin Microbiol Rev*. 2004 Oct;17(4):942–64.

55. Rodríguez AM, Rodríguez J, Giambartolomei GH. Microglia at the Crossroads of Pathogen-Induced Neuroinflammation. *ASN Neuro*. 2022 May 29;14:17590914221104566.
56. Nair S, Sobotka KS, Joshi P, Gressens P, Fleiss B, Thornton C, et al. Lipopolysaccharide-induced alteration of mitochondrial morphology induces a metabolic shift in microglia modulating the inflammatory response in vitro and in vivo. *Glia*. 2019;67(6):1047–61.
57. Park J, Choi H, Min JS, Park SJ, Kim JH, Park HJ, et al. Mitochondrial dynamics modulate the expression of pro-inflammatory mediators in microglial cells. *J Neurochem*. 2013 Oct;127(2):221–32.
58. Orihuela R, McPherson CA, Harry GJ. Microglial M1/M2 polarization and metabolic states. *Br J Pharmacol*. 2016 Feb;173(4):649–65.
59. Hu Y, Mai W, Chen L, Cao K, Zhang B, Zhang Z, et al. mTOR-mediated metabolic reprogramming shapes distinct microglia functions in response to lipopolysaccharide and ATP. *Glia*. 2020 May;68(5):1031–45.
60. O'Neill LAJ, Kishton RJ, Rathmell J. A guide to immunometabolism for immunologists. *Nat Rev Immunol*. 2016 Sep;16(9):553–65.
61. Van den Bossche J, Baardman J, Otto NA, van der Velden S, Neele AE, van den Berg SM, et al. Mitochondrial Dysfunction Prevents Repolarization of Inflammatory Macrophages. *Cell Rep*. 2016 Oct 11;17(3):684–96.
62. Hoogland ICM, Houbolt C, van Westerloo DJ, van Gool WA, van de Beek D. Systemic inflammation and microglial activation: systematic review of animal experiments. *J Neuroinflammation*. 2015 Jun 6;12:114.
63. Noh H, Jeon J, Seo H. Systemic injection of LPS induces region-specific neuroinflammation and mitochondrial dysfunction in normal mouse brain. *Neurochem Int*. 2014 Apr;69:35–40.
64. Hoogland ICM, Westhoff D, Engelen-Lee JY, Melief J, Valls Serón M, Houben-Weerts JHMP, et al. Microglial Activation After Systemic Stimulation With Lipopolysaccharide and *Escherichia coli*. *Front Cell Neurosci*. 2018;12:110.
65. Su É, Villard C, Manneville JB. Mitochondria: At the crossroads between mechanobiology and cell metabolism. *Biology of the Cell*. 2023;115(9):e2300010.
66. Picard M, Shirihai OS, Gentil BJ, Burelle Y. Mitochondrial morphology transitions and functions: implications for retrograde signaling? *American Journal of Physiology-Regulatory, Integrative and Comparative Physiology*. 2013 Mar 15;304(6):R393–406.
67. Rangaraju V, Lewis TL, Hirabayashi Y, Bergami M, Motori E, Cartoni R, et al. Pleiotropic Mitochondria: The Influence of Mitochondria on Neuronal Development and Disease. *J Neurosci*. 2019 Oct 16;39(42):8200–8.

68. Weinberg SE, Sena LA, Chandel NS. Mitochondria in the Regulation of Innate and Adaptive Immunity. *Immunity*. 2015 Mar 17;42(3):406–17.
69. Zehnder T, Petrelli F, Romanos J, De Oliveira Figueiredo EC, Lewis TL, Déglon N, et al. Mitochondrial biogenesis in developing astrocytes regulates astrocyte maturation and synapse formation. *Cell Rep*. 2021 Apr 13;35(2):108952.
70. Alshial EE, Abdulghaney MI, Wadan AHS, Abdellatif MA, Ramadan NE, Suleiman AM, et al. Mitochondrial dysfunction and neurological disorders: A narrative review and treatment overview. *Life Sci*. 2023 Dec 1;334:122257.
71. Norat P, Soldozy S, Sokolowski JD, Gorick CM, Kumar JS, Chae Y, et al. Mitochondrial dysfunction in neurological disorders: Exploring mitochondrial transplantation. *NPJ Regen Med*. 2020 Nov 23;5(1):22.
72. Bernier LP, York EM, Kamyabi A, Choi HB, Weilinger NL, MacVicar BA. Microglial metabolic flexibility supports immune surveillance of the brain parenchyma. *Nat Commun*. 2020 Mar 25;11(1):1559.
73. Fairley LH, Lai KO, Wong JH, Chong WJ, Vincent AS, D’Agostino G, et al. Mitochondrial control of microglial phagocytosis by the translocator protein and hexokinase 2 in Alzheimer’s disease. *Proc Natl Acad Sci U S A*. 2023 Feb 21;120(8):e2209177120.
74. Hope KT, Hawes IA, Moca EN, Bonci A, De Biase LM. Maturation of the microglial population varies across mesolimbic nuclei. *Eur J Neurosci*. 2020 Oct;52(7):3689–709.
75. Madan S, Uttekar B, Chowdhary S, Rikhy R. Mitochondria Lead the Way: Mitochondrial Dynamics and Function in Cellular Movements in Development and Disease. *Front Cell Dev Biol*. 2021;9:781933.
76. Dou Y, Wu H jun, Li H quan, Qin S, Wang Y er, Li J, et al. Microglial migration mediated by ATP-induced ATP release from lysosomes. *Cell Res*. 2012 Jun;22(6):1022–33.
77. Chang YW, Tony Yang T, Chen MC, Liaw Y geh, Yin CF, Lin-Yan XQ, et al. Spatial and temporal dynamics of ATP synthase from mitochondria toward the cell surface. *Commun Biol*. 2023 Apr 18;6(1):1–19.
78. Norden DM, Trojanowski PJ, Villanueva E, Navarro E, Godbout JP. Sequential activation of microglia and astrocyte cytokine expression precedes increased Iba-1 or GFAP immunoreactivity following systemic immune challenge. *Glia*. 2016 Feb;64(2):300–16.
79. Hoogland ICM, Houbolt C, van Westerloo DJ, van Gool WA, van de Beek D. Systemic inflammation and microglial activation: systematic review of animal experiments. *J Neuroinflammation*. 2015 Jun 6;12:114.
80. Banks WA, Robinson SM. Minimal penetration of lipopolysaccharide across the murine blood-brain barrier. *Brain Behav Immun*. 2010 Jan;24(1):102–9.

81. Banks WA, Gray AM, Erickson MA, Salameh TS, Damodarasamy M, Sheibani N, et al. Lipopolysaccharide-induced blood-brain barrier disruption: roles of cyclooxygenase, oxidative stress, neuroinflammation, and elements of the neurovascular unit. *J Neuroinflammation*. 2015 Nov 25;12:223.
82. Hasegawa-Ishii S, Inaba M, Shimada A. Widespread time-dependent changes in tissue cytokine concentrations in brain regions during the acute phase of endotoxemia in mice. *Neurotoxicology*. 2020 Jan;76:67–74.

Chapter 3: Structural remodeling of microglial mitochondria across brain region and developmental stage

3.1 Abstract

Microglia undergo many structural and cellular changes across the rodent and human lifespan. This is particularly evident during early development when distinct microglial subtypes appear “tuned” to phagocytic activity. As professional phagocytes, they are involved in clearance of apoptotic cells that undergo programmed cell death as part of normal development. Recent evidence suggests they aid in synapse remodeling and clear newborn cells that are not actively undergoing apoptosis. Macrophages in other tissues are also professional phagocytes and mitochondrial state plays a key role in regulating the phagocytic profiles of these cells. Almost nothing is known about mitochondria in microglia during postnatal development and how these organelles may regulate critical phagocytic actions of these cells. This study examines mitochondrial structure in microglia during periods of postnatal development when microglial properties change dramatically as part of microglial maturation. Key features of mitochondrial morphology in early development differ from those found in young adulthood. Surprisingly, we also observed mitochondria localized to phagocytic cups in microglia, suggesting that specialized “cup mitochondria” play key roles in phagocytic function of microglia during development.

3.2 Introduction

Microglia play key roles in the progression of brain development during embryogenesis and early post-natal life. Microglial progenitors arise in the yolk sac and migrate into the rodent brain around embryonic day 8.5 and during early gestation in the human brain (1,2). Colonizing the brain before other cell types hints that microglia may be important in establishing conditions for neurogenesis and other cellular processes (3). Microglia seem well positioned to support cellular function during embryogenesis and early post-natal development. Microglia exhibit very distinct transcriptomic and morphological profiles during embryogenesis and early postnatal development compared to what is observed in adulthood. In particular, they show a more phagocytic profile during development (4) and they can engulf synapses as well as remove cell populations fail to integrate in local circuitry(5). Microglia with elevated phagocytic activity show prominent formation of structures called phagocytic cups, which frequently contain cells with pyknotic nuclei (6). Phagocytic cups can form on both the cell body as well as the cell processes of microglia. Microglial phagocytosis of newborn neurons and astrocytes plays a critical role in appropriate maturation of circuitry and impact adult behaviors such social play and mating (5,7). Microglial phagocytosis is also prominent during post-natal development of macaques, with microglia engulfing neural progenitor cells (5,8). Although microglial phagocytic cups have been observed in many contexts, the mechanisms by which these structures form and then resolve is not fully understood.

More information is available about mechanisms and dynamics of macrophage engulfment of debris or cells. Peripheral macrophages share a similar lineage to microglia and express many of the same cell surface receptors during development (9). Both are resident immune cells with robust phagocytic capacity. Macrophages in the periphery play key roles in

eliminating damaged cells through many phagocytic receptors (10), including complement pathway signaling(10). Changes in macrophage cell metabolism and mitochondrial state can potentially impact their engulfment of debris and dying cells (11). Indeed, mitochondrial membrane potential changes are associated with phagocytosis, where a lower membrane potential supports phagocyte engulfment of apoptotic cells (12,13). Aside from providing energy, mitochondria are also signaling hubs that can regulate nuclear transcription with key impacts on cell attributes and functions (14,15).

Mitochondrial function in regulation of microglial phagocytosis has not been studied. Recent evidence suggests that mitochondrial state can influence microglial phagocytosis of ab in the context of neurodegeneration, but nothing is known about whether these organelles can impact phagocytosis in development (16). Given our previous observation of abundant microglial phagocytic cups in microglia in the developing mesolimbic system, we felt this was an ideal context to explore how mitochondria may be linked to microglial maturation and microglial phagocytic function in these circuits.

3.3 Results

During these first two post-natal weeks in mice, microglia show rapid increases in cell density and morphological complexity in the nucleus accumbens (NAc) and ventral tegmental area (VTA)(6). To begin understanding the links between mitochondrial state and microglial morphological maturation or function during development, as described in chapter 1, we crossed mice that express inducible cre-recombinase in microglia (*CX3CRI^{CreER/+}*) with mice that express a mitochondrial-targeted GFP (*mitoGFP*) in Cre-dependent fashion (*MG-MitoGFP* mice). Qualitative observations show that microglia at P8 and P12 display more densely packed

mitochondrial networks in the soma and fewer in the microglial processes compared to what is observed in young adulthood (Fig. 1A).

To define the abundance and features of mitochondria in microglia as these cells undergo drastic changes in morphology and density during postnatal development, we used Imaris to reconstruct both cells and organelles in high magnification confocal images at post-natal day 8 and 12 in NAc and VTA. Between these two time points, microglia proliferate to achieve significant increases in cell density (6). They also develop a more complex, highly branched morphology and begin to establish regional differences in cell density and branching complexity (6). From Imaris reconstructions, we analyzed mitochondrial mass, number (relative to cell volume), and size of individual mitochondria (Fig. 2B, C, D). Mitochondrial mass in NAc microglia at P8 and P12 was like what was observed in microglia from young adult mice (Fig. 2B). Mitochondrial mass in VTA microglia was also comparable at P8 and P12 and then increased to the higher levels observed in young adults (Fig. 2B). We observed trends indicating mitochondrial number, and max volume in NAc microglia may increase in early development compared to what we observe in young adulthood. There were trends toward gradually decreasing mitochondrial number (relative to cell volume) in both regions from P8 to P12 to young adulthood (Fig. 1C). Finally, there were trends toward maximum volume of mitochondria within microglia being elevated at P8 and p12 compared to young adults (Fig. 2D). This is likely related to the observation of complex mitochondrial networks in somas of microglia at P8 and P12.

Analyses described so far were obtained from 3D reconstruction of GFP+ mitochondria and microglia within entire fields of view. To further investigate these apparent increases in maximum mitochondrial volume, we extracted measurements from individual microglia at

P8,12, and 60. A greater number of large volume mitochondria were observed in most microglia in both NAc and VTA at P8 and P12 compared to P60 (Fig. 2E). We also examined mitochondrial elongation via analysis of aspect ratio (the longest axis divided by shortest axis). There were trends toward elevated aspect ratio during early development, suggesting that elongation also contributes to larger max volumes observed during development (Fig. 2F).

Microglia in the developing mesolimbic circuitry frequently show phagocytic cups that contain condensed chromatin of dead cells (6). This was mainly observed in the first two weeks of post-natal development. Surprisingly, when mapping the features of mitochondria in microglia during postnatal development, we observed mitochondria localized to these phagocytic cups (Fig. 3A, B). During development, microglial cell processes have few mitochondria, particularly at their distal tips. Phagocytic cups are a key exception to this trend, where we see mitochondria in distal cell process phagocytic structures. How mitochondrial localization may be relevant to formation of such structures or fuel microglial phagocytic function has not been explored. To investigate this further we quantified mitochondrial mass and average mitochondrial volume within phagocytic cups instead of whole cell (Fig. 3C,D). Compared to values observed when analyzing mitochondria in the whole cell, mitochondria in the cups ranged from 0.1-1.2 μm^3 . We observed mitochondria in the cups show sphericity values closer to 1 in both scatter plot and cumulative percent plot, indicating most mitochondria exhibit punctate morphology in these structures (Fig. 3E,F). Not all microglia analyzed at these ages exhibited phagocytic cups. To probe whether there were differences in overall mitochondrial abundance in cells that do and or do not exhibit cups, we compared mean mitochondrial volume in both types of cells (Fig. 3G,F). No clear differences in mitochondrial volume were evident between cells with cups and cells without these structures.

3.4 Discussion

Among other functions, microglial functions during early development supports circuit maturation via refinement of synaptic connectivity, and clearance of dead cells, among other functions. What signaling mechanisms regulate how microglia engage in phagocytic behaviors? Microglia have an elaborate set of cell surface receptors, known as the microglial “sensome”(17,18). Signaling pathways downstream of these receptors are involved in immune responses, phagocytosis, and cell metabolism (17). A key set of receptors and downstream signaling pathways that can regulate microglial phagocytic behaviors are members of the classical complement pathway (CCP). This signaling pathway was initially defined as an innate immune pathway involved in host defense and phagocytic clearance of pathogens. Complement receptors (CRs) bind activated complement molecules deposited on pathogens or synaptic structures to initiate phagocytosis (19). In addition to detection of molecules that promote phagocytosis, there are also signals which can inhibit phagocytosis. CD47, a ligand for the receptor SIRP α (signal regulatory protein α), which is expressed on phagocytes, is one such molecule (47). This is considered a “don’t eat me” signal and activation of the SIRP α receptor can inhibit actin assembly which is needed for membrane remodeling and formation of a phagocytic cup (19,20). These are a few examples of signaling receptors that can shape phagocytic function in microglia and other immune cells.

In addition to these signaling pathways and markers, microglia, or other professional phagocytes such as macrophages can form larger phagocytic structures to engulf debris, pathogens and dying cells. Pathogens and apoptotic cells trigger initiation and activation of signaling pathways which lead to rearrangement of the actin cytoskeleton and cause the membrane to form phagocytic cup (21). Following the formation of the cup there are transient

membrane protrusions that extend and enclose around the foreign particle to develop a phagosome (21). Studies indicate that assembly of phagocytic actin cups rely on activity of proteins such as Arp2/3 complex (22). The rate of actin assembly and organization of actin networks forming the phagocytic cup depend on which phagocytic receptors are engaged (22).

There are types of phagocytosis attempts that result in full engulfment or engulfment of small portions of the target. In microglia partial phagocytosis has been called trogocytosis (23). This process is also observed in other phagocytes. This type of phagocytosis is associated with myosin II remodeling unlike other types are associated with actin remodeling (22). From these studies, various types of phagocytosis have been observed and are associated with different signaling cascades. While membrane remodeling to initiate formation of phagocytic cups has been detailed, it is unclear what signaling agents are mediating the uptake of targets and initiating phagocytosis.

Mitochondria have many functions(24), including potential roles in aiding phagocytosis (12,13). They are observed to modify their membrane potential to alter engulfment of targets during phagocytosis. There are also changes associated with morphology. To begin understanding mitochondria in contexts of phagocytosis we defined mitochondrial morphology within microglia during early development when microglia show heightened phagocytic action (25). The changes in mitochondrial morphology suggest that changes in mitochondrial properties across microglial development could be linked to microglia maturation. Microglia at these early developmental stages show more de ramified morphology and change in abundance. The differences observed in mitochondrial network morphology suggest mitochondria are closely following microglial state and future studies manipulating mitochondrial biogenesis may be

needed to understand how a large of role mitochondria play in microglial development during timepoints of higher phagocytosis events.

To understand the relevance of mitochondrial function and microglial formation of phagocytic cups during early development, we characterized mitochondrial morphology localized to microglial phagocytic cups during postnatal development. Mitochondria in the cups displayed smaller and more punctate morphology as shown by elevated sphericity compared to mitochondria in the rest of the cell. Mitochondria are known to establish varying morphologies across neuron sub compartments (26) and this is accompanied by distinct functional states of those mitochondria. Our current data implies mitochondria localization and morphology remodeling is correlated with microglial cup formation. Mitochondria in the phagocytic cup may generate energy required for digestion of engulfed targets. Mitochondrial fission, which can generate more spherical mitochondria, has been linked to heightened phagocytosis. Spherical mitochondria also show distinct membrane potential, indicating that these mitochondria are in a distinct functional state (12,13,27). Additionally, mitochondria in the cup display a more punctate morphology which such morphology has been associated with more effective trafficking along the cell membrane. This could be another reason why mitochondria in the cups display different morphologies than those observed in the rest of the cell. This could indicate the mitochondria morphology remodeling is relevant to processing of cell targets after initializing the membrane remodeling for phagocytic cup formation. Key future research directions could include manipulation of mitochondrial shape remodeling via inhibitors of mitochondrial fission to determine how these changes influence microglial phagocytosis. Additionally, live imaging of microglial phagocytic cup formation and mitochondria during early development could provide insight into how mitochondria morphology remodeling precedes or follows microglial formation

of cups. The localization of mitochondria in phagocytic cups which are located distally to microglial cell body suggests mitochondria are important in the digestion of targets but whether there are key signaling mechanisms occurring is unknown. Future experiments would help determine whether mitochondrial localization and morphology remodeling in distal processes occurs prior to formation of cup in microglia.

3.5 Materials and Methods

Transgenic Mice

CX3CR1^{CreER/+} mice were originally obtained from Jackson Labs (stock #025524) and subsequently maintained in our colony (28).

Rosa26-lsl-mito-EGFP mice (*mitoEGFP* mice) were obtained from Dr. Jeremy Nathans (Johns Hopkins University) and are available at Jackson Labs (stock #021429). These mice enable cre-dependent expression of GFP that is fused to an N-terminal signal derived from mouse cytochrome c oxidase, subunit VIIIa, enabling specific localization to mitochondria (29).

Mice used for experiments were heterozygous for all transgenes. In all experiments balanced numbers of male and female mice were used. Mice were housed in normal light/dark cycle and had ad libitum access to food and water. All experiments were performed in strict accordance with protocols approved by the Animal Care and Use Committees at UCLA.

Tissue collection and immunohistochemistry

CX3CR1^{CreER/+};mitoEGFP mice were deeply anesthetized via isoflurane inhalation and transcardially perfused with 1M phosphate buffered saline (PBS; pH 7.4) followed by ice-cold 4% paraformaldehyde (PFA) in 1M PBS. Brain tissue was isolated and postfixed PFS for ~4 h at

4°C and then stored in 1 M PBS with 0.1% sodium azide until sectioning. Coronal brain sections were prepared using a vibratome at 60 µm thickness. For immunostaining, free-floating brain sections were washed with 1M PBS (5 min) and then permeabilized and blocked in a solution of 2% bovine serum albumin (BSA) and 3% normal donkey serum (NDS) and 0.01% of Triton-X for 2 h with rotation at room temperature. Sections were then incubated overnight with primary antibodies prepared in 2% bovine serum albumin (BSA) and 3% normal donkey serum (NDS) at 4°C with rotation. Following primary antibody incubation, sections were washed 3x with 1M PBS and then incubated with secondary antibodies prepared in 2% bovine serum albumin (BSA) and 3% normal donkey serum (NDS) at room temperature for 2 h with rotation. This was followed by washes in 1M PBS (3x) with second wash containing 1:4000 dilution of DAPI in 1 M PBS. Sections were mounted using Aqua-Poly/Mount (Polysciences cat: 18606) and cover slipped (coverslips of #1.5 thickness) for confocal imaging. Primary antibodies used include rabbit anti- Iba1 (1:800; Wako, catalog #019-19741), chicken anti-TH (1:500; Aves, catalog #TYH). Secondary antibody combinations include rabbit AlexaFluor-647, chicken AlexaFluor-594, or chicken AlexaFluor-405 (used at 1:1000; all raised in donkey; Jackson ImmunoResearch Laboratories). For each set of analyses, three brain sections containing nucleus accumbens (NAc) and three brain sections containing ventral tegmental area (VTA) were chosen from each mouse.

Image acquisition and analysis

Fixed tissue slides were imaged using a Zeiss LSM880 confocal microscope or a Zeiss LSM700 confocal microscope. Within the NAc, images were acquired at the boundary between core and shell (identified anatomically) and include both subregions. In the VTA, images captured were medial to the medial lemniscus. To localize microglia with phagocytic cups we used the DAPI signal showing pyknotic nuclei.

For 3D reconstruction of microglia and mitochondria, confocal z stacks were acquired with a 63x objective and z interval of 0.3 μm and imported into Imaris (Bit plane) software for analysis. The surface reconstruction module was used for quantification of mitochondrial and microglial volumes and phagocytic cups in whole field of views. For all image analyses, two or three images from separate brain sections were analyzed per mouse to obtain an average value for that mouse. Two to 7 mice were analyzed per brain region, and per age. For individual cell analysis, 5-6 microglia from separate mice were isolated from the field of view surface reconstructions per brain region.

Statistics

Measurements were exported from Imaris (Bit plane). All measurements are described in the Imaris manual: volume, number of surfaces, sphericity, bounding box length for aspect ratio. Origin Lab was used for all graphs and statistical testing. No statistics shown due to low N.

3.6 Figures

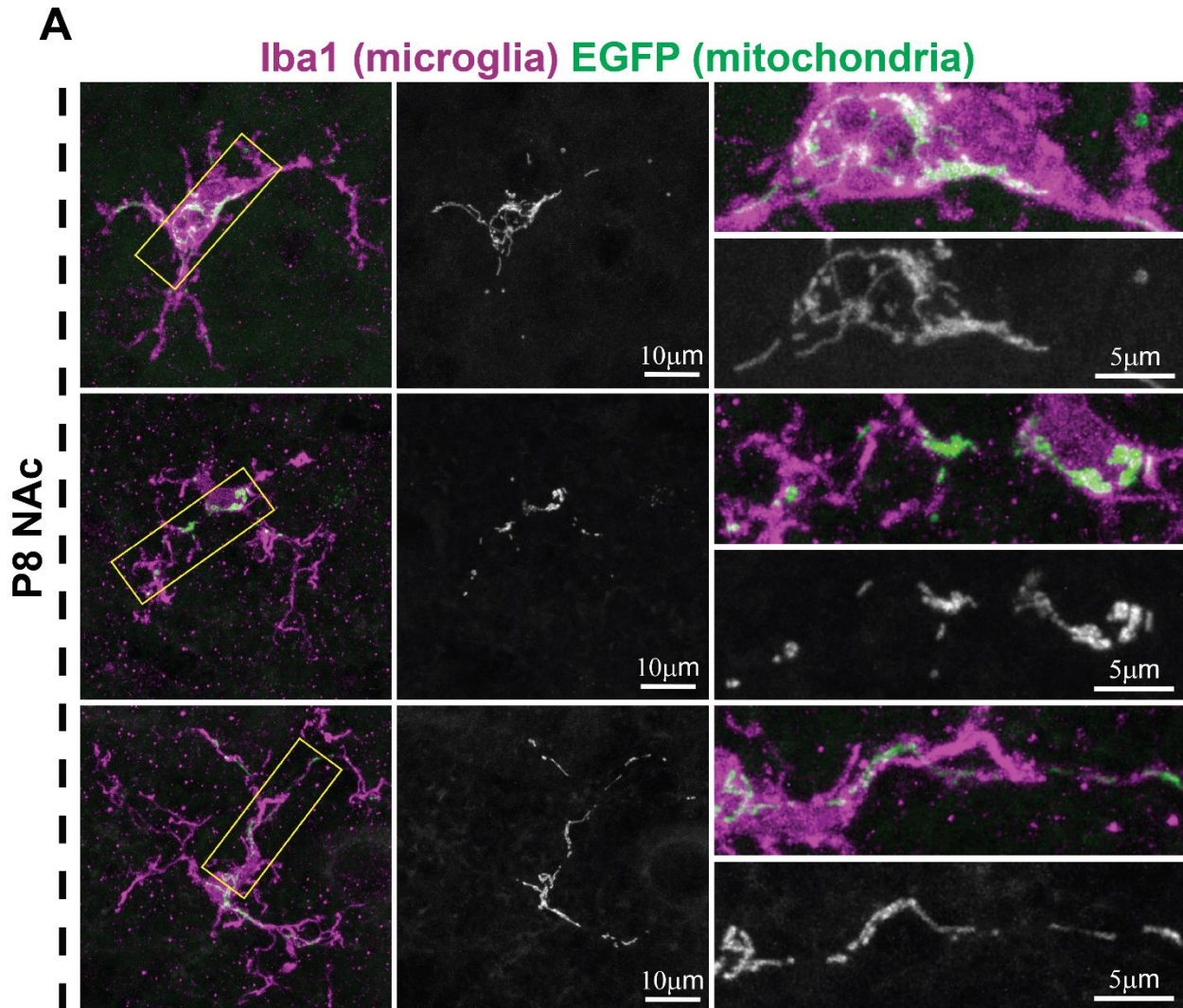


Figure 1: Microglia and mitochondrial networks in early development (A) Examples of MG-MitoEGFP+Iba1 staining. Regions in the *yellow* boxes are enlarged and show the high degree of variation in mitochondrial morphology observed during development.

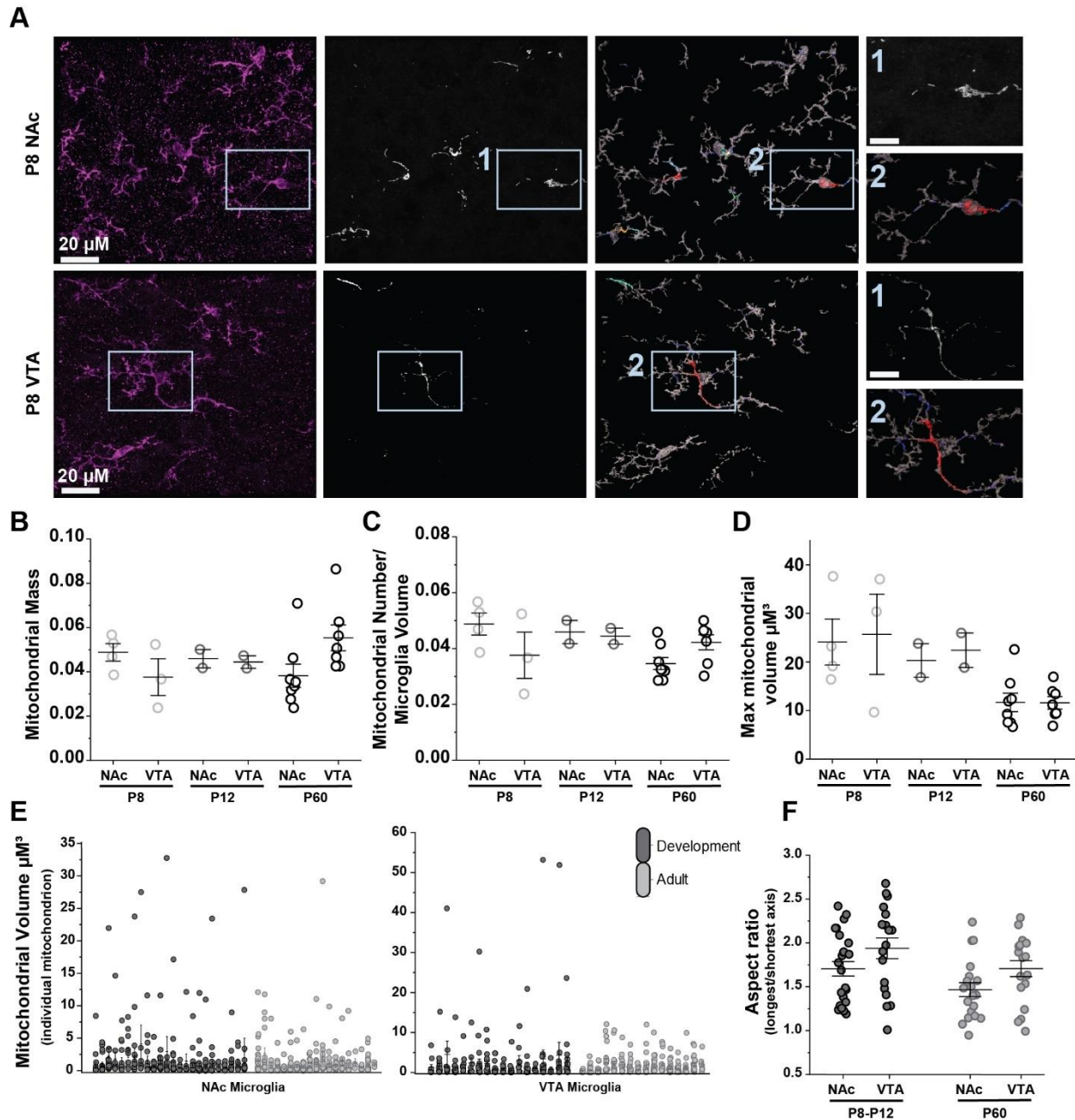


Figure 2: Mitochondrial network changes across developmental timepoints (A) Representative high-magnification images at P8 of microglia (Iba1), mitochondria (EGFP), and 3D reconstruction of mitochondria; color scale shows mitochondrial volumes, and reconstructions of microglia, with zoom of reconstructions (NAc and VTA). (B-D) Quantification of mitochondrial parameters across ages (P8, P12 and P60) and across regions (NAc, VTA). Within a given age, data points that come from the same mouse are identified by the same color. Mitochondrial mass (E) is quantified by calculating mitochondrial volume/microglial volume. (E) Quantification of mitochondrial volume for individual across ages (combined P8-P12 for development group and P60) and across regions (NAc, VTA). (F) Quantification of mitochondrial aspect ratio (longest and shortest axis of individual cells across combined P8-P12 for development group and P60) and across regions (NAc, VTA).

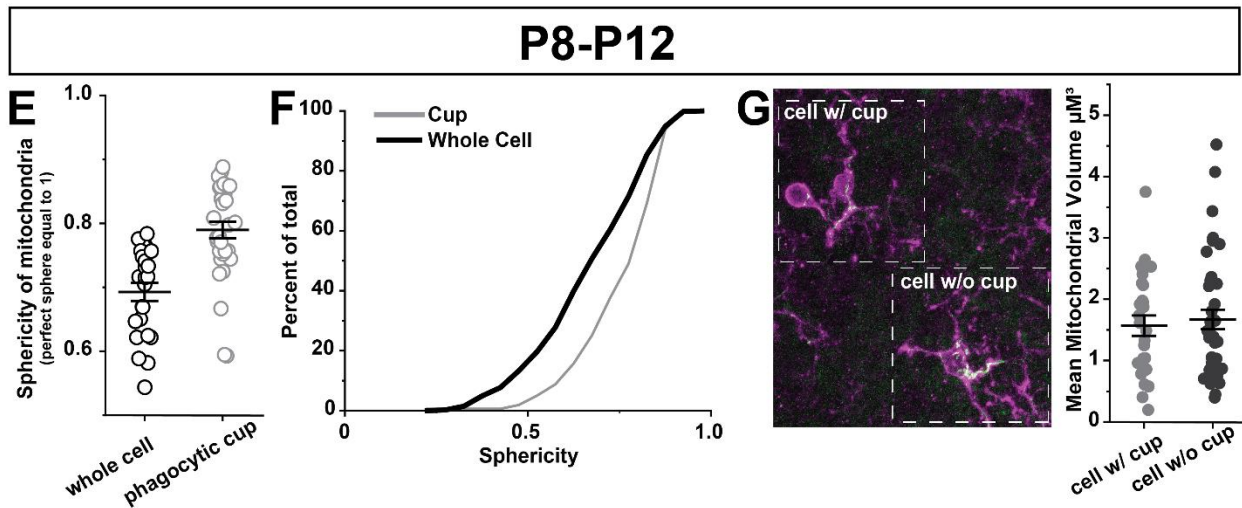
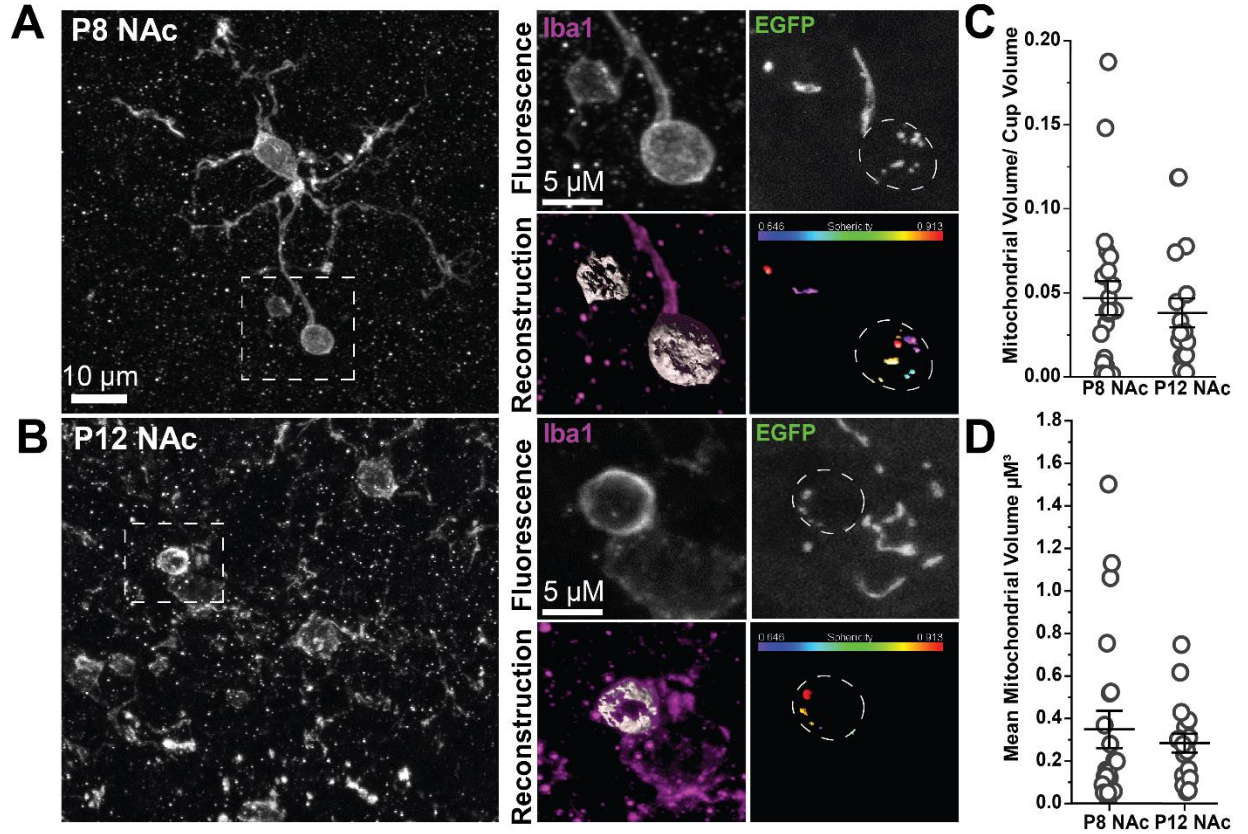


Figure 3: Microglial phagocytic cups display changes in mitochondrial network (A-B) Representative images of microglial cell with phagocytic cups at P8 and P12; Merge of all channels, 3D reconstruction of cup, and 3D reconstruction of EGFP mitochondria shown (left to right) as well as zoom of individual fluorescence channels. (C-D) Quantification of key morphological parameters of cup mitochondria; mitochondrial mass is calculated as mitochondrial volume/microglial volume; average mitochondrial volume. (E-F) Quantification of key morphological parameters of cup and whole cell mitochondria. Sphericity is a measure of roundness with 1.0 representing a perfect circle. Cumulative percent distribution of sphericity. (G) Average mitochondrial volume across cell with and without cups.

References Cited

1. Ginhoux F, Lim S, Hoeffel G, Low D, Huber T. Origin and differentiation of microglia. *Front Cell Neurosci* [Internet]. 2013 Apr 17 [cited 2024 Apr 19];7. Available from: <https://www.frontiersin.org/articles/10.3389/fncel.2013.00045>
2. Ginhoux F, Greter M, Leboeuf M, Nandi S, See P, Gokhan S, et al. Fate Mapping Analysis Reveals That Adult Microglia Derive from Primitive Macrophages. *Science*. 2010 Nov 5;330(6005):841–5.
3. Butovsky O, Ziv Y, Schwartz A, Landa G, Talpalar AE, Pluchino S, et al. Microglia activated by IL-4 or IFN- γ differentially induce neurogenesis and oligodendrogenesis from adult stem/progenitor cells. *Molecular and Cellular Neuroscience*. 2006 Jan 1;31(1):149–60.
4. Matcovitch-Natan O, Winter DR, Giladi A, Vargas Aguilar S, Spinrad A, Sarrazin S, et al. Microglia development follows a stepwise program to regulate brain homeostasis. *Science*. 2016 Aug 19;353(6301):aad8670.
5. VanRyzin JW, Marquardt AE, Argue KJ, Vecchiarelli HA, Ashton SE, Arambula SE, et al. Microglial Phagocytosis of Newborn Cells Is Induced by Endocannabinoids and Sculptures Sex Differences in Juvenile Rat Social Play. *Neuron*. 2019 Apr 17;102(2):435-449.e6.
6. Hope KT, Hawes IA, Moca EN, Bonci A, De Biase LM. Maturation of the microglial population varies across mesolimbic nuclei. *Eur J Neurosci*. 2020 Oct;52(7):3689–709.
7. Pickett LA, VanRyzin JW, Marquardt AE, McCarthy MM. Microglia phagocytosis mediates the volume and function of the rat sexually dimorphic nucleus of the preoptic area. *Proc Natl Acad Sci U S A*. 2023 Mar 7;120(10):e2212646120.
8. Cunningham CL, Martínez-Cerdeño V, Noctor SC. Microglia regulate the number of neural precursor cells in the developing cerebral cortex. *J Neurosci*. 2013 Mar 6;33(10):4216–33.
9. Grassivaro F, Menon R, Acquaviva M, Ottoboni L, Ruffini F, Bergamaschi A, et al. Convergence between Microglia and Peripheral Macrophages Phenotype during Development and Neuroinflammation. *J Neurosci*. 2020 Jan 22;40(4):784–95.
10. Hirayama D, Iida T, Nakase H. The Phagocytic Function of Macrophage-Enforcing Innate Immunity and Tissue Homeostasis. *Int J Mol Sci*. 2017 Dec 29;19(1):92.
11. Rambold AS, Kostelecky B, Elia N, Lippincott-Schwartz J. Tubular network formation protects mitochondria from autophagosomal degradation during nutrient starvation. *Proceedings of the National Academy of Sciences*. 2011 Jun 21;108(25):10190–5.
12. Cereghetti GM, Scorrano L. Phagocytosis: Coupling of Mitochondrial Uncoupling and Engulfment. *Current Biology*. 2011 Oct 25;21(20):R852–4.

13. Park D, Han C, Elliott MR, Kinchen JM, Trampont PC, Das S, et al. Continued clearance of apoptotic cells critically depends on the phagocyte Ucp2 protein. *Nature*. 2011 Aug 21;477(7363):220–4.
14. Weinberg SE, Sena LA, Chandel NS. Mitochondria in the Regulation of Innate and Adaptive Immunity. *Immunity*. 2015 Mar 17;42(3):406–17.
15. Shen K, Pender CL, Bar-Ziv R, Zhang H, Wickham K, Willey E, et al. Mitochondria as Cellular and Organismal Signaling Hubs. *Annual Review of Cell and Developmental Biology*. 2022 Oct 6;38(Volume 38, 2022):179–218.
16. Fairley LH, Lai KO, Wong JH, Chong WJ, Vincent AS, D’Agostino G, et al. Mitochondrial control of microglial phagocytosis by the translocator protein and hexokinase 2 in Alzheimer’s disease. *Proc Natl Acad Sci U S A*. 2023 Feb 21;120(8):e2209177120.
17. Hickman SE, Kingery ND, Ohsumi TK, Borowsky ML, Wang L chong, Means TK, et al. The microglial sensome revealed by direct RNA sequencing. *Nat Neurosci*. 2013 Dec;16(12):1896–905.
18. Healy LM, Zia S, Plemel JR. Towards a definition of microglia heterogeneity. *Commun Biol*. 2022 Oct 20;5(1):1–6.
19. Uribe-Querol E, Rosales C. Phagocytosis: Our Current Understanding of a Universal Biological Process. *Front Immunol* [Internet]. 2020 Jun 2 [cited 2024 May 8];11. Available from: <https://www.frontiersin.org/journals/immunology/articles/10.3389/fimmu.2020.01066/full>
20. Tsai RK, Discher DE. Inhibition of “self” engulfment through deactivation of myosin-II at the phagocytic synapse between human cells. *J Cell Biol*. 2008 Mar 10;180(5):989–1003.
21. Lee HJ, Woo Y, Hahn TW, Jung YM, Jung YJ. Formation and Maturation of the Phagosome: A Key Mechanism in Innate Immunity against Intracellular Bacterial Infection. *Microorganisms*. 2020 Aug 25;8(9):1298.
22. Krendel M, Gauthier NC. Building the phagocytic cup on an actin scaffold. *Current Opinion in Cell Biology*. 2022 Aug 1;77:102112.
23. Weinhard L, di Bartolomei G, Bolasco G, Machado P, Schieber NL, Neniskyte U, et al. Microglia remodel synapses by presynaptic trogocytosis and spine head filopodia induction. *Nat Commun*. 2018 Mar 26;9(1):1228.
24. Spinelli JB, Haigis MC. The Multifaceted Contributions of Mitochondria to Cellular Metabolism. *Nat Cell Biol*. 2018 Jul;20(7):745–54.
25. Hope KT, Hawes IA, Moca EN, Bonci A, De Biase LM. Maturation of the microglial population varies across mesolimbic nuclei. *Eur J Neurosci*. 2020 Oct;52(7):3689–709.

26. Faitg J, Lacefield C, Davey T, White K, Laws R, Kosmidis S, et al. 3D neuronal mitochondrial morphology in axons, dendrites, and somata of the aging mouse hippocampus. *Cell Reports* [Internet]. 2021 Aug 10 [cited 2024 May 2];36(6). Available from: [https://www.cell.com/cell-reports/abstract/S2211-1247\(21\)00939-6](https://www.cell.com/cell-reports/abstract/S2211-1247(21)00939-6)
27. Márquez-Ropero M, Benito E, Plaza-Zabala A, Sierra A. Microglial Corpse Clearance: Lessons From Macrophages. *Front Immunol*. 2020;11:506.
28. Yona S, Kim KW, Wolf Y, Mildner A, Varol D, Breker M, et al. Fate Mapping Reveals Origins and Dynamics of Monocytes and Tissue Macrophages under Homeostasis. *Immunity*. 2013 Jan 24;38(1):79–91.
29. Agarwal A, Wu PH, Hughes EG, Fukaya M, Tischfield MA, Langseth AJ, et al. Transient Opening of the Mitochondrial Permeability Transition Pore Induces Microdomain Calcium Transients in Astrocyte Processes. *Neuron*. 2017 Feb 8;93(3):587-605.e7.

Chapter 4: Conclusion

In this dissertation, I analyzed multiple mitochondrial properties such as morphology, motility and response to inflammation and explored how the status of these organelles relate to microglial function and phenotype. In chapter 1, I introduced various findings in the glial field that define key microglial functions and known mechanisms by which they carry out widely recognized cellular functions. I also introduced how microglial mitochondria are understudied and may play critical roles in regulating microglial function, which would be an important advance for the glial field. In chapter 2, I present evidence that mitochondrial morphology varies across NAc and VTA, where we previously observed different microglial properties. I also demonstrated cell process motility seemed not to be linked to mitochondrial localization, running counter to what the field would have expected. This was counter to what we expected but provides farther understanding in how mitochondria may support microglial motility or not. This data demonstrates that mitochondrial localization is not tightly linked to microglial process motility indicating microglia may rely on different transport of ATP across the cell that is not associated with location of mitochondria. Additionally, we still don't fully understand whether microglia may rely on mitochondrial localization for motility. We investigated one component of mitochondrial morphology but there may be tighter associations other components of mitochondrial localization such as fission and fusion.

I also present results from an extensive study revealing that mitochondrial properties are dynamic and may be linked to functional changes in microglia, particularly during inflammatory responses. This body of research suggests that changes in mitochondrial properties such as genes related to morphology and oxidative phosphorylation coincide with changes observed in microglia. There is no clear evidence that mitochondria are critical in supporting microglial

response to inflammation but there are correlations between these two components. Microglia respond to the LPS by shown increase in cytokines and these are associated with changes in mitochondrial genes. Furthermore, the change in mitochondrial mass and network size presents that mitochondrial morphology occurs with microglial response to LPS but it is still to be determined if such changes are required for microglial response.

In chapter 3, I present results from a study of microglial mitochondria during postnatal development. When microglia are more phagocytic, mitochondrial network remodeling in whole cell and phagocytic structures occurs. Such changes further imply that mitochondrial morphology and localization can occur in contexts where microglia undergo changes in function. How these changes are supporting or mediating microglial function remains to be understood. These data provide further hints that mitochondria may act as a regulatory organelle in contexts of microglial maturation and inflammation.

Upon beginning this project there were a lot of assumptions regarding relevance of mitochondrial function but this data indicates that mitochondria have subtle changes in contexts where microglia underwent phenotypic change. These data hint there are many correlative changes in mitochondria but how critical these changes are in supporting microglial function remain to be elucidated. Additionally, the work outlined above also presents novel tools for future work to evaluate mitochondria in microglia in other brain regions, ages or during pathological conditions. Visualizing mitochondria in many other contexts could discern how likely it is for this organelle to support microglial function. Future work may need to focus on other components of mitochondrial function such as calcium regulation and release of reactive oxygen species. This work also suggests that a promising new research frontier will be targeting

mitochondria to manipulate microglia in numerous contexts such as disease, CNS infection, and brain injury.

Next steps of this research question include manipulations of mitochondria to understand how critical these morphological and genetic changes are for microglial function. Various manipulations could include affecting expression of regulatory genes of mitochondrial oxidative phosphorylation or disrupting genes associated with mitochondrial biogenesis. Experiments looking at microglial response to acute injury and inflammation after mitochondrial manipulation would allow further understanding of how critical mitochondrial remodeling is in supporting microglial chemotaxis. Further probing of mitochondrial function will allow the field to determine if microglia rely on support of mitochondria or if microglia are flexible in energy supply. Such evidence would further our understanding of how microglia may be different from other CNS cells and how they are supporting cellular functions. Altogether, through a detailed examination of mitochondrial properties in multiple brain regions, developmental timepoints, and pathological challenges via novel visualization tools in vivo, this body of work lays the foundation for future studies to explore mitochondrial regulation of microglia via manipulation of discrete mitochondrial functions.